Zonguldak Karaelmas University
Department of Geodesy and Photogrammetry Engineering
Dr. Gürcan Büyüksalih

Universität Hannover
Institut für Photogrammetrie und GeoInformation

Dr.-Ing. K. Jacobsen

ACCURACY ASSESSMENT OF DIGITAL ELEVATION MODELS DERIVED FROM SHUTTLE RADAR TOPOGRAPHY MISSION (SRTM)

Master Thesis

Umut Güneş Sefercik

2006

Zonguldak Karaelmas University
Department of Geodesy and Photogrammetry Engineering
Dr. Gürcan Büyüksalih

Universität Hannover
Institut für Photogrammetrie und GeoInformation

Dr.–Ing. K. Jacobsen

ACCURACY ASSESSMENT OF DIGITAL ELEVATION MODELS DERIVED FROM SHUTTLE RADAR TOPOGRAPHY MISSION (SRTM)

Master Thesis

Umut Güneş Sefercik

2006

I assure that the present work was written independently and I have not used other than the stated sources and aids.

Hannover, 23rd of March 2006

Institut für Photogrammetrie und GeoInformation
Universität Hannover
Nienburger Str. 1
D-30167 Hannover
Tel.: ++49-511/762-2485
Fax: ++49-511/762-2483
e-mail: jacobsen@ipi.uni-hannover.de
http://www.ipi.uni-hannover.de

Dr.-Ing. Karsten Jacobsen

Hannover, October, 17th, 2005

master thesis
for Umut Güneş Sefercik

Accuracy Assessment of Digital Elevation Models Derived from Shuttle Radar Topography Mission (SRTM)

Digital elevation models are a basic component for any GeoInformation system (GIS), they are required for the generation of orthoimages and correct geometric handling of single images. The generation of height models can be based on stereo photogrammetry, laser scanning and interferometric synthetic aperture radar (InSAR). In any case it is time consuming and expensive. With the Shuttle Radar Topography Mission (SRTM) height models have been generated, covering the earth surface from 56° south to 60.25° north. With the exception of small gaps in steep parts, dry sand deserts and water surfaces the free available US C-band data are covering the area completely while the X-band data, distributed by the DLR, are covering it only partially. In the area of Zonguldak SRTM C-band and X-band height models are available together with reference data.

The accuracy and accuracy characteristics of the SRTM height models shall be investigated in the Zonguldak area. This shall include the dependency upon terrain coverage by forest, the dependency upon the terrain inclination and aspects. In addition the loss of accuracy by interpolation shall be analysed.

Handing out on: October, 17th, 2005
Handing in on: March, 23rd, 2005

CONTENTS

ABBREVIATIONS

ASCII	American Standard Code for Information Interchange
ASTER	Advanced Spaceborne Thermal Emission and Reflection Radiometer
CCD	Charge Coupled Device
CE90	Circular Error 90%
CNES	Centre National d'Etudes Spatials
DEM	Digital Elevation Model
DLR	German Aerospace Center
DSM	Digital Surface Model
GIS	Geographic Information System
HRV	High Resolution Visible
IMU	inertial measurement unit
INSAR	Interferometric Synthetic Aperture Radar
IPI	Institute of Photogrammetry and Geoinformation, University Hannover
IRS	Indian Remote Sensing
ISPRS	International Society for Photogrammetry and Remote Sensing
LIDAR	Light Detection And Ranging
NASA	National Aeronautics and Space Administration
NGA	National Geospatial-Intelligence Agency
PAN	Panchromatic
RMSE	Root-Mean-Square Error
SAR	Synthetic Aperture Radar
SRTM	Shuttle Radar Topographic Mission
TIN	Triangulated Irregular Network
USGS	US Geological Survey
WGS84	World Geodetic System 1984
3D	Three-Dimensional

INTRODUCTION

Digital elevation models (DEMs) are a basic component of any geo information system (GIS). The terrain can not only be described by the horizontal components; the height belongs to complete information. In addition height models are required for the generation of orthoimages – one of the most often used photogrammetric product. DEMs can be generated by laser scanning, photogrammetric methods or interferometric synthetic aperture radar (InSAR). In any case it is time consuming and expensive. The worldwide lack of qualified and accessible DEMs has been improved with the Shuttle Radar Topography Mission (SRTM) in February 2000. Based on InSAR height models have been generated covering the world from 56° southern up to 60.25° northern latitude. The DEMs based on the US C-band are available free of charge in the internet (http://edcsgs9.cr.usgs.gov/pub/data/srtm/) with a spacing of 3arcsec, corresponding to approximately 92m at the equator. Only for the USA the data with a spacing of arcsec (~30m at the equator) are also in the WEB. The DEMs based on the German / Italian X-band can be ordered from the DLR, Germany with a spacing of 1 arcsec. In the area of Zonguldak, Turkey, C-band and also X-band height models have been investigated.

1. DIGITAL ELEVATION MODELS (DEM)

1.1 What Is a Digital Elevation Model?

The term **D**igital **E**levation **M**odel (DEM) comprises the process of representing the elevation characteristics of the terrain in discreet form in a three-dimensional space of a surface. However, most often it is used to refer specifically to a raster or regular grid of spot heights. A **D**igital **T**errain **M**odel or DTM contains also information about object locations and actually be a more generic term for any digital representation of a topographic surface. A DEM is the simplest form of digital representation of topography and the most common.

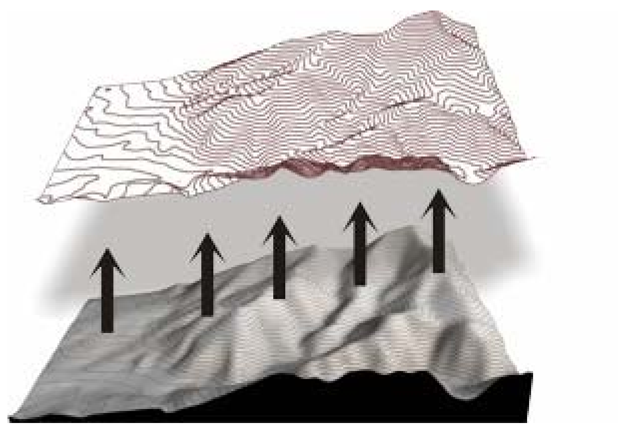

Figure 1.1: Example of Digital Elevation Model (DEM)

A DEM is a representation of Earth surface with X, Y horizontal coordinates and altitude Z. It describes the bare surface of the Earth. DSM is an acronym of **D**igital **S**urface **M**odel and describes the Earth's surface including vegetation, buildings, forests and etc. that means the visible surface of the Earth.

For the three dimensional data acquisition for higher resolution digital elevation models laser scanning is used. The measuring method for generating digital elevation models is based on active distance measurement and oriented by GPS positional determination and inertial measurement units (IMU). GPS/IMU-systems record the three dimensional position and attitude of the aircraft.

During the mission, by determining the traveling time of light pulse, laser scanning measures the distance between Earth's surface and aircraft. For every measurement, in addition, an opto-mechanical device deflects the laser beam laterally into a slightly different direction. In conjunction with the forward movement of the aircraft, a wide strip of terrain is scanned as a result. Figure 1.2 shows the laser scanning mode.

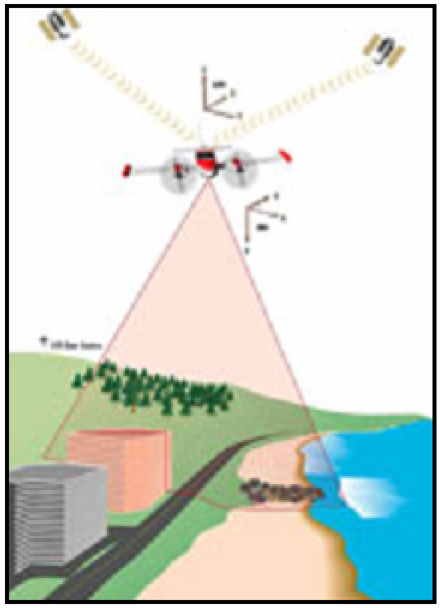

Figure 1.2: Laser scanning mode

For determining the position of each point on the Earth's surface accurately, the laser range, scan angle, GPS data and INS data are combined in post-flight processing.

The first pulse is reflected by the visible ground surface, the last pulse mostly by the land underneath. A Digital Surface Model is generated by the selection of the first pulse. The last pulses are the starting point for generating the Digital Terrain Model. Figure 1.3 shows the differences between first and last pulses.

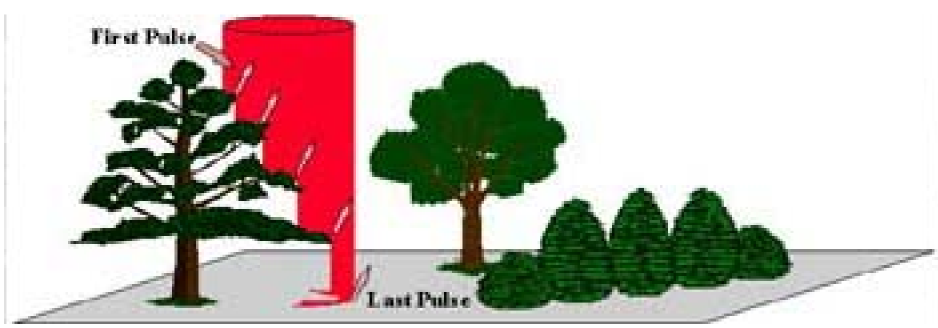

Figure 1.3: First pulse and last pulse

If the height model is determined by laser scanning, for each raster element in a DSM there are several measured values comprising different elevations (waterlines, ground, etc.). From the first pulse, the upper elevation is assigned to the height model, a surface *model is generated defining the visible surface (trees, buildings, forests, etc.).* Here, the figure 1.3 shows the first and the last pulse of a laser scanner height model. The first pulse describes the upper elevation level; that means a DSM. Buildings, vegetation, etc. are included in the DSM.

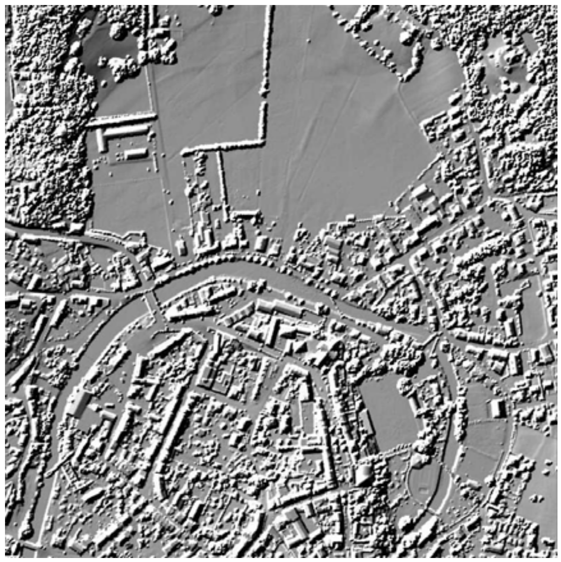

Figure 1.4: DSM (First pulse)

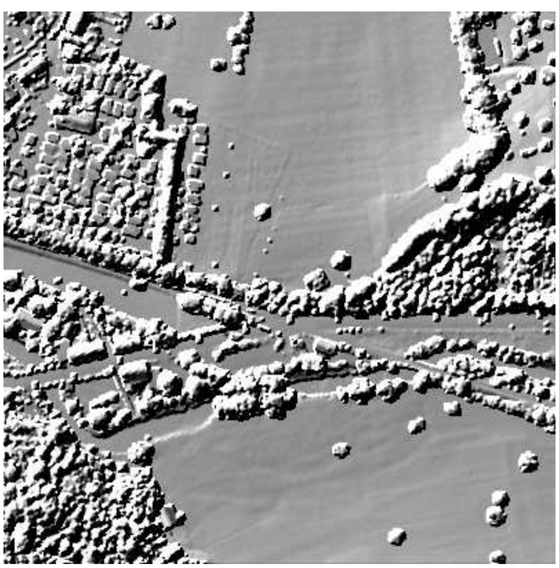

Figure 1.5: DSM first pulse (highest value)

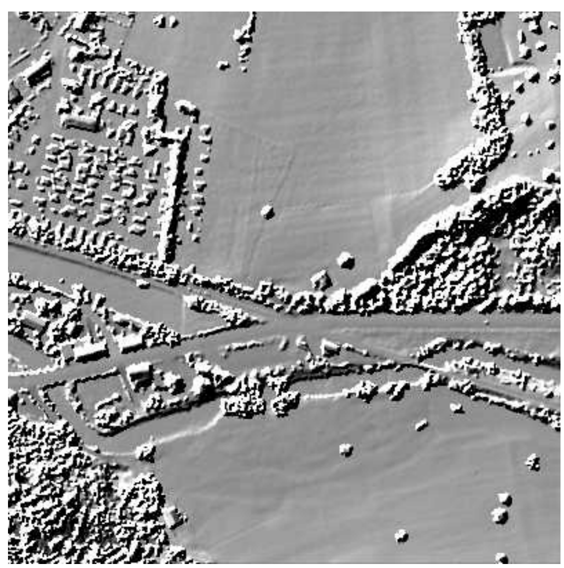

Figure 1.6: DSM first pulse (lowest value)

Here, the figures show the highest and lowest values of laser scanner height values.

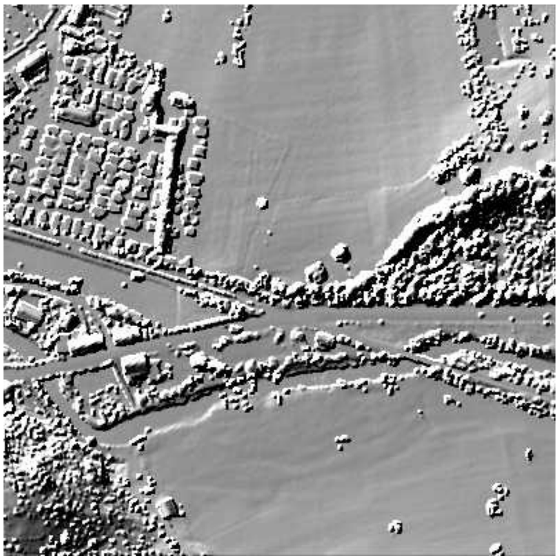

Figure 1.7: DSM last pulse – highest values

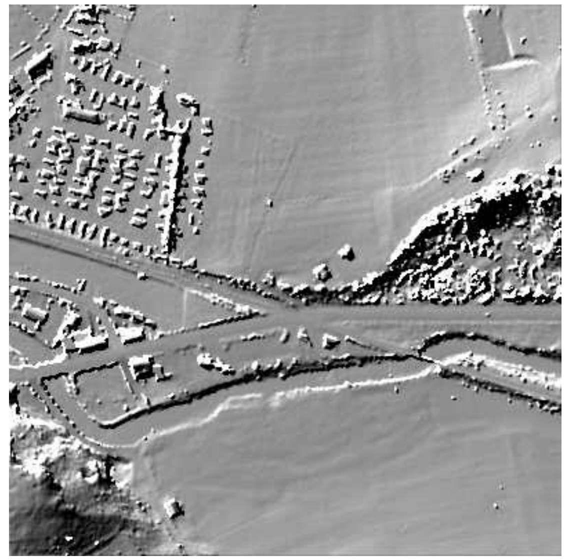

Figure 1.8: DSM last pulse – lowest values

Here, the figures show the highest and lowest values *of DSM last pulse*.

Figure 1.9: DEM (filtered last pulse)

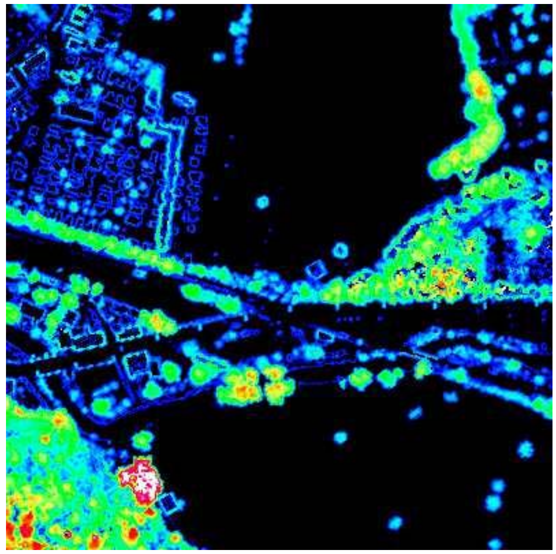

Figure 1.10: Difference model DSM first pulse – DSM last pulse with colour coded height values

A DSM describes the visible surface of objects; a DEM doesn't represent the object elevation except the bare ground. The DEM describes only the bare surface of the Earth and it is the most basic and interesting geographical data type. The DEM is a computer representation of the Earth's surface. It can be an ASCII or binary file and contains the spatial elevation data usually in a regular grided or not regular pattern. Terrain height in a DEM can be presented using following methods:

- Contour Lines

In a topographic map elevations are represented as contour lines

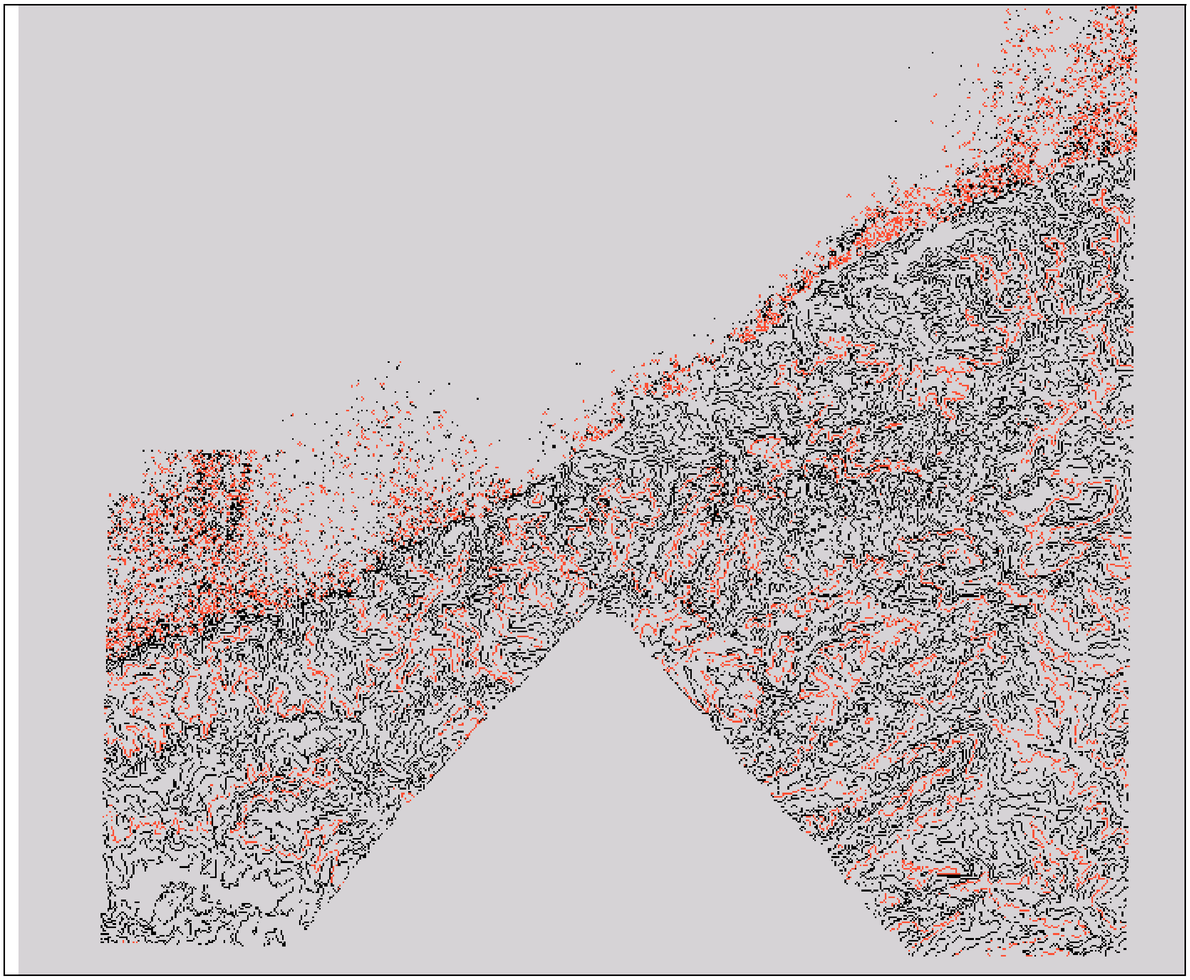

Figure 1.11: SRTM X-band DSM of Zonguldak test field presented as contour lines

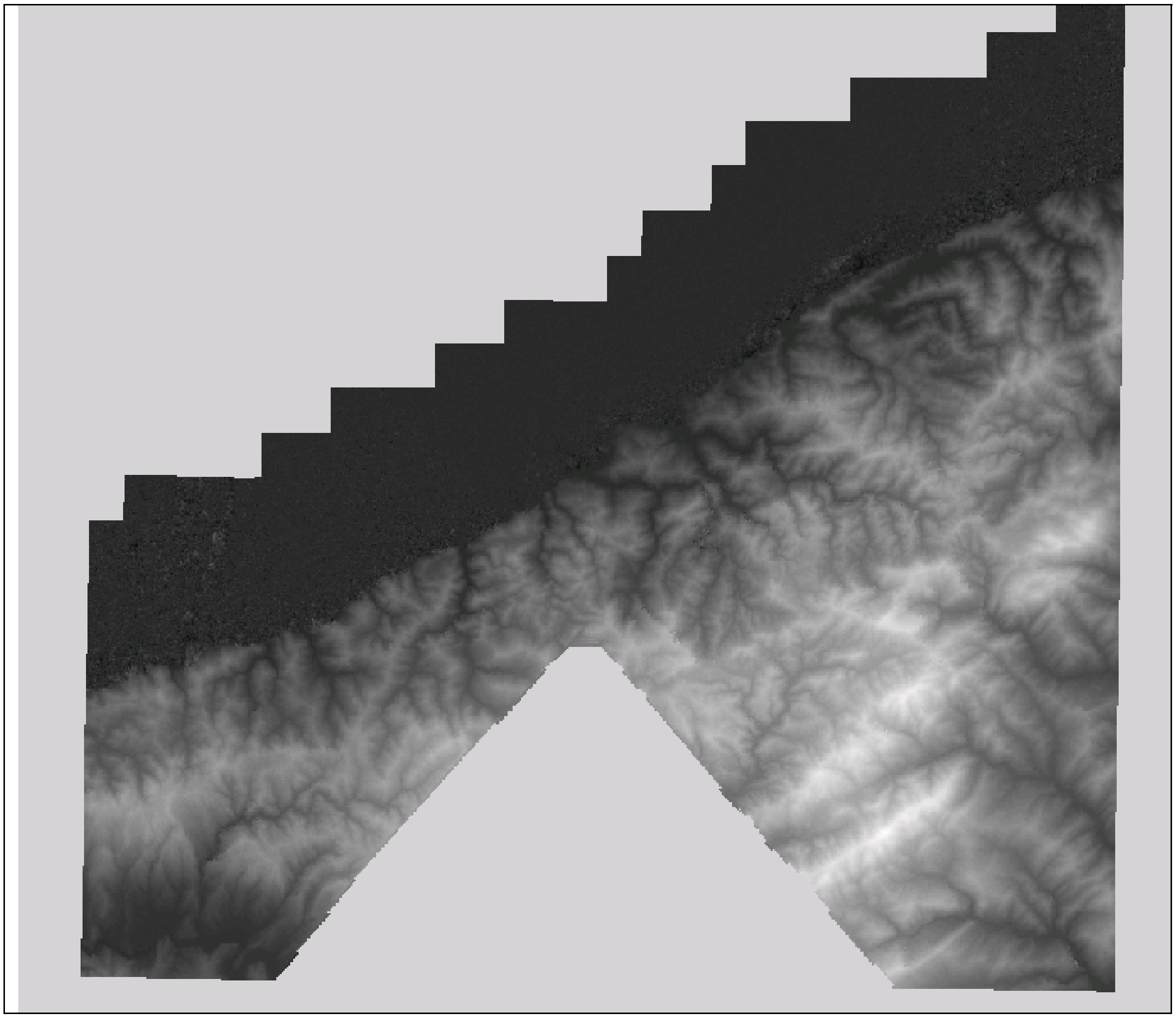

Figure 1.12: SRTM X-band DSM of Zonguldak test field as grey value coded presentation

- Grid Data

  Grid data can be derived from original data by means of aerial photographs, satellite stereo images, indirectly by digitizing contour lines or by InSAR. Figure 1.13 shows a 3D-presentation of grid data.

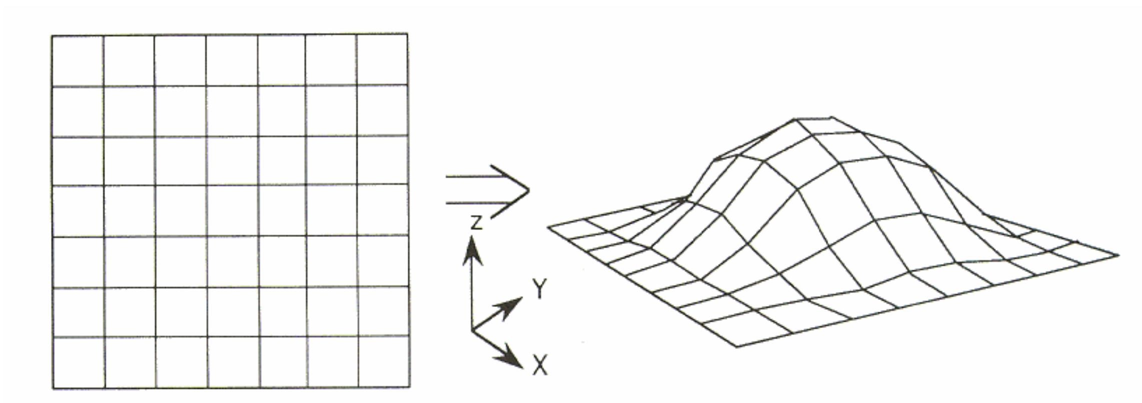

Figure 1.13: 3D-presentation of grid data

Terrain data other than the grid data are interpolated from the surrounding grid data.

- Random Point Data

Features of terrain are sometimes represented by a group of randomly located terrain data with three dimensional coordinates (X, Y, Z). For computer processing, random point data are used as **T**riangulated **I**rregular **N**etwork (TIN). The advantage of TIN is easy control of point density according to the terrain, though it has the disadvantage of being time consuming in the random search for the terrain point. Figure 1.14 shows the TIN type.

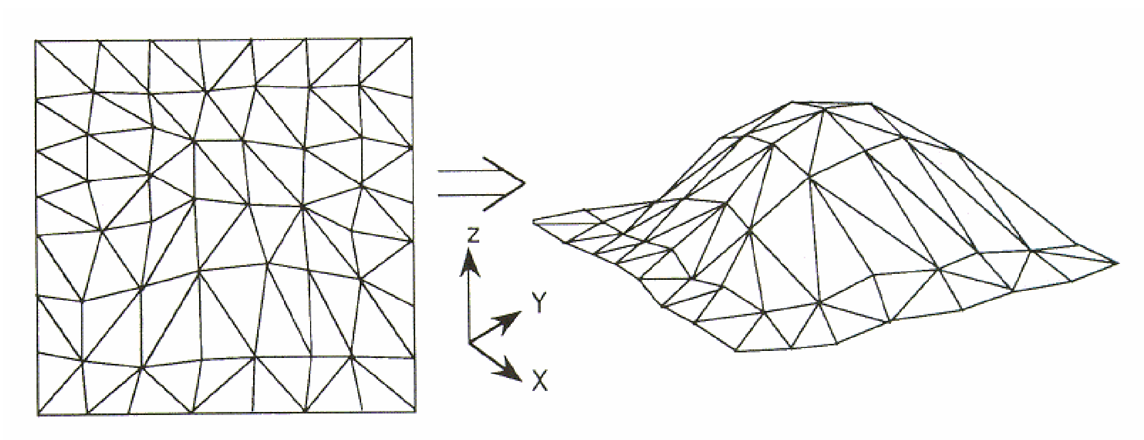

Figure 1.14: TIN type

A TIN represents a surface as a set of non-overlapping contiguous triangular facets, of irregular size and shape (Chen, 1987). TIN uses the data on the irregularly spaced samples as the basis of a system of triangulation (Burrough, 1986).

The most popular TIN model, used in commercial software, is the Delaunay TIN. This triangulation is the straight-line dual of the Voronoi diagram and is constructed by connecting the points whose associated Voronoi polygons share a common edge. The Delaunay TIN has the following properties:

- It must be unique and
- It maximizes the minimum internal angles of each triangle

The circumference that passes through the three vertices of a Delaunay triangle does not contain any other sample point. This property is known as the empty circle criterion (Tsai 1993). This property is used to construct the TIN model directly from the sample set. Figure 1.15 shows the empty circle criterion to create a Delaunay TIN.

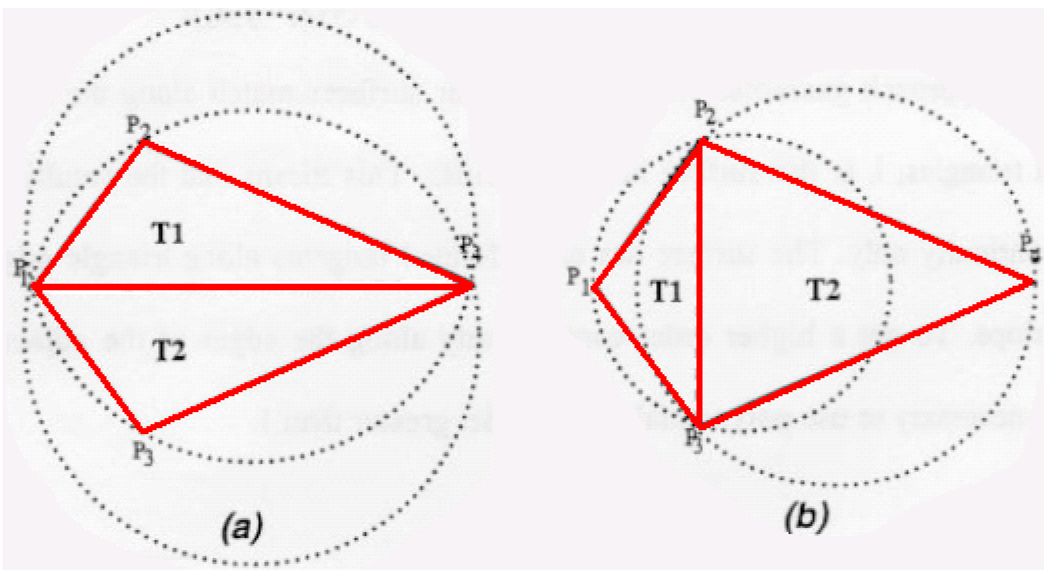

Figure 1.15: Empty circle criterion to create a Delaunay TIN

(a) T1 and T2 are not Delaunay triangles, only (b) T1 and T2 are Delaunay triangles

- Surface Function

  Based on the TIN other points or a more dense regular grid can be interpolated linear or with a higher degree.

Reference DEMs of Test Field

Two different reference DEMs were used for analysis of the SRTM X-band and C-band DEMs in this investigation. The first is the old reference DEM based on digitized contour lines of 1:25000 scale topographic map of test field, named DEM25000 and the second is the new reference DEM produced in 2005 based on large scale photogrammetry, named DEM2005. Figure 1.16 shows the old reference DEM derived from 1:25000 standard topographic map as grey value coded presentation. This DEM has 40m point spacing.

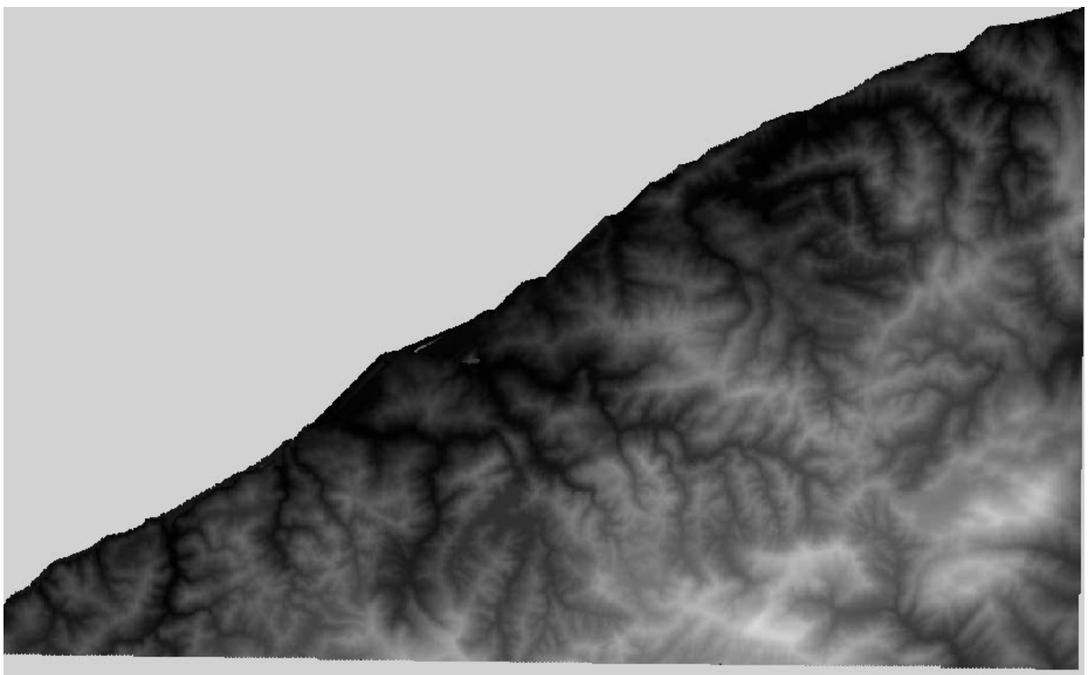

Figure 1.16: Old Reference DEM of Zonguldak test field based on topographic map 1 : 25 000 (DEM25000)

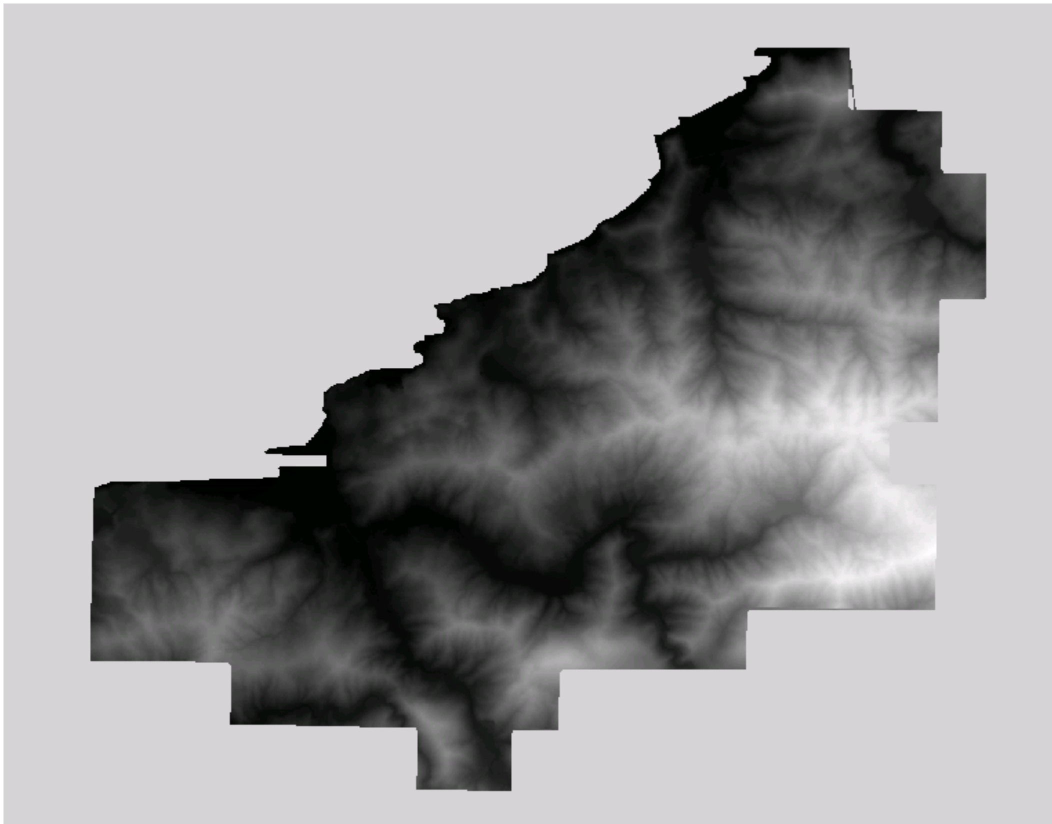

Figure 1.17: New Reference DEM of Zonguldak City (Turkey) based on large scale photogrammetry (DEM2005)

The figure 1.17 shows the new reference DEM of Zonguldak test field produced in 2005 as grey value coded presentation. This DEM has 10m grid size and produced by large scale photogrammetric techniques.

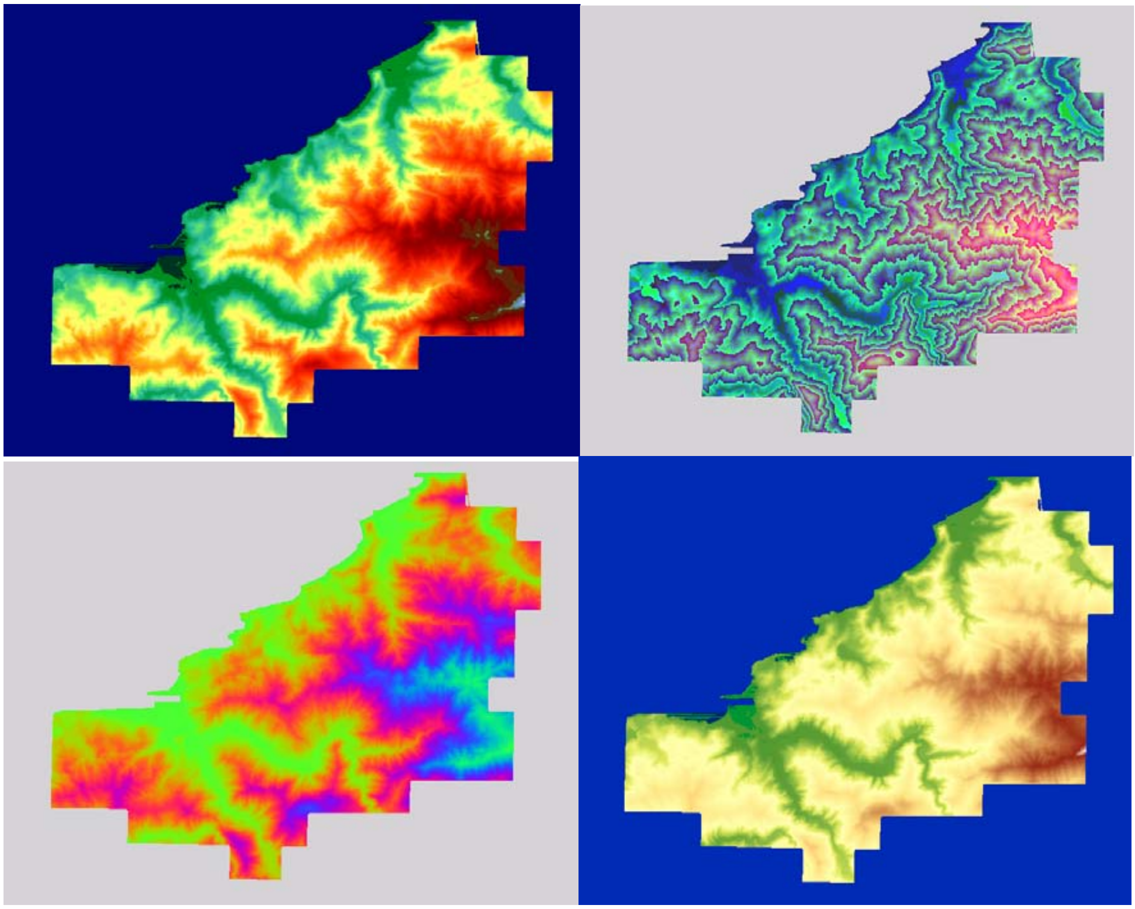

Figure 1.18: Reference DEM shown with different colour coding (DEM2005)

1.2 DEM Generation

In the process of DEM generation, a wide variety of methods can be used. Most often stereo photogrammetry based on aerial photos or space images are used.

When using optical images with conventional photogrammetry for a DEM generation, it is inevitable to use at least two images for the same area taken from different projection centres. The DEM generation by aerial photos is accurate, but time consuming. With space images it may be more economic.

When using stereo-pairs for a DEM generation, the standard deviation of the height SZ depends on the parameters of base-height ratio (B/H) and the standard deviation of the x-parallax expressed in the unit of the ground sampling distance.

$$SZ = H/B * Spx \qquad Spx \text{ [ground sampling distance]}$$

Other techniques for a DEM generation are airborne or space-borne Interferometric SAR (InSAR) and airborne laser scanning (LIDAR).

In interferometric SAR technique, two SAR images are acquired from two slightly different positions with both the images covering the same area. SAR images consist of information about back-scattered energy and phase of the signals. In this technique, the two SAR images are registered to the sub-pixel accuracy to generate the interferogram, which consists of the combined phases of the two images. This phase information at each pixel in the interferogram will be in accordance with the topography of the terrain at the respective pixel positions. These phases are then unwrapped to get the heights of the points: InSAR technique has accurate and detailed information.

Laser scanning is also called Laser Radar or Lidar (**LI**ght **D**etection **A**nd **R**anging). LIDAR has become a very prominent tool to collect accurate high-resolution topographic data. It has many advantages over the conventional techniques of DEM generation. It has an accuracy of up to 10 - 15 cm in the vertical and 50 - 100 cm in the horizontal component. It produces detailed information.

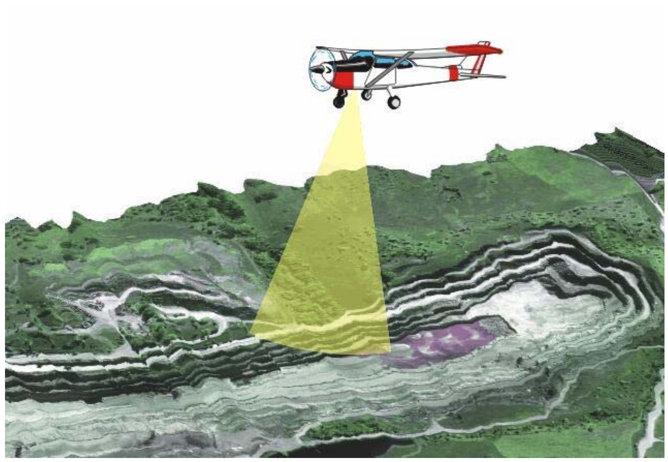

Figure 1.19: Airborne laser scanning

1.3. Accuracy of a DEM

The accuracy of a DEM is generally represented by spatial resolution and height accuracy. The accuracy of a DEM can be evaluated according to spatial resolution. The accuracy of a DEM can be determined against reference data.

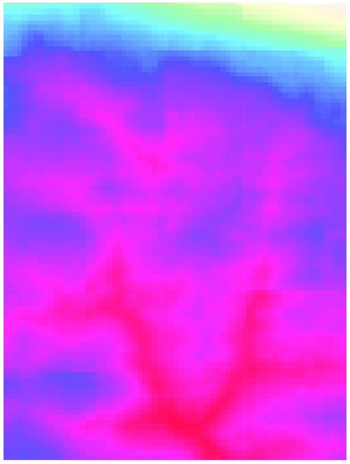

Figure 1.20: USGS Standard 7.5′ DEM

30 by 30m data resolution

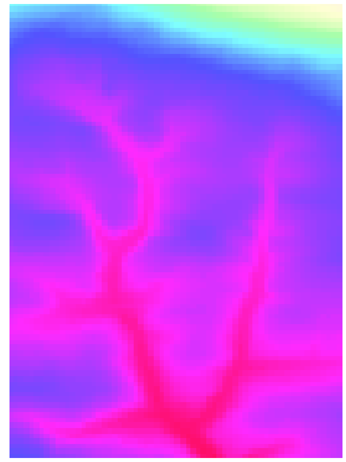

Figure 1.21: High Resolution DEM

fractal resampled from 5 to 30m

A lot of techniques can be used for DEM acquisition. On the following table 1.1 is a summary of techniques and accuracies.

DEM acquisition technique	**Coverage**	**Accuracy**
Terrestrial survey	Local, large scale mapping	1cm…10cm
Photogrammetry	Regional	10cm…1m
Laser profiling	Regional	0.15m…2m
space borne SAR interferometry	Regional to global	0.5m…20m
airborne SAR interferometry	Regional	10cm…5m
Digitizing from map	Depends on mapping coverage	Depends on maps

Table 1.1: Overview of DEM acquisition techniques

For cartographic mapping, height accuracy requirements are defined by U.S National Map Accuracy Standards and these are shown in following table 1.2.

Map Scale	horizontal accuracy RMS (m)	vertical accuracy RMS (m)	Cartographic Image Map Resolution (m)	Thematic Image Map Resolution (m)
1:250000	75	15-30	14	≤75
1:100000	30	6-15	6	≤30
1:50000	15	6	3	≤15
1:25000	7.5	3	1.5	≤7.5

Table 1.2: US requirement for mapping

For other countries such rules usually not exists because it is depending upon the area and the requirements.

1.4. Application Areas

The DEM can be used for generation of digital orthoimage maps, 3-D views as well and for terrain analysis.

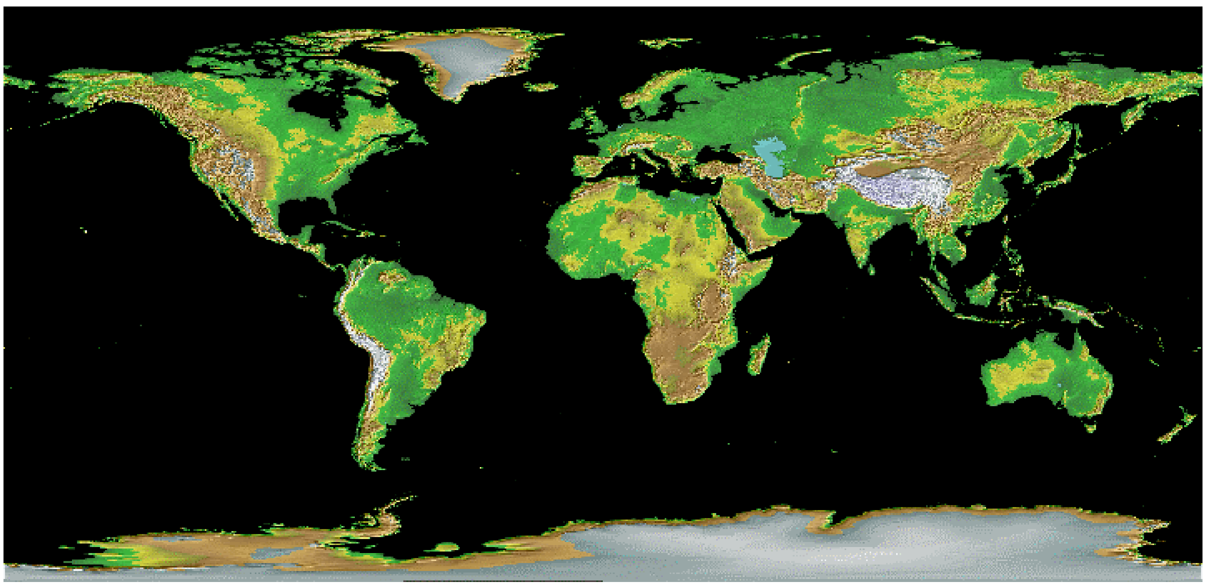

Figure 1.22: Overview to the World

- Terrain determination, such as point elevation, slope, distance, aspect
- Environmental analysis
- Modeling of hydrologic functions
- Cartography
- Civil applications
- Geographical Information System (GIS)
- Urban planning
- Disaster management
- Forest fires
- Agriculture
- Erosion control
- Flood management
- Earthquake analysis
- Contour line generation

- Modeling of telecommunication
- Military applications
- Engineering fields (Fill for roads/canals, site selection for dams and tunnels, etc.)

2. RADAR SYSTEM THEORY and INTERFEROMETRIC PROCESSING

2.1. What is RADAR?

· Radar

Word of Radar is an acronym obtained from the phrase **RA**dio **D**etection **A**nd **R**anging. The aim of this instrument is detecting and tracking targets at considerable distances. Radar has electronic equipment and using them for transmitting short burst of radio energy which is going on light speed and reflected off a target and returned as an echo.

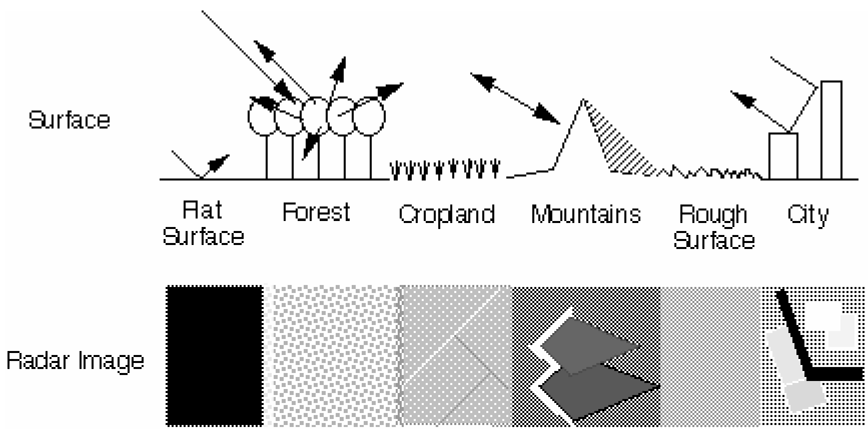

Figure 2.1: Radar images for different surface features

2.2. Radar history and developments

Radar was invented during World War II and it has been used for detection and tracking of targets like as ships and comprehensively at nighttime bombing.

After World War II, firstly Side Looking Aperture Radar (SLAR) was improved and used for imagery at resolutions in the 10-20 meter range. With this instrument, cloud-covered tropic regions were mapped. SLAR technique was very useful for the radar imaging but for obtaining a high azimuth resolution in the image, the antenna on the system must be impracticably long. Because of this unrealistic antenna length, a new radar technology was invented by the researchers and the name of this new technology was Synthetic Aperture Radar (SAR).

Firstly SAR technique was used for military purposes too. Than it was started to use on non-military aims and airborne SAR was designed which later became space-borne SAR systems for many planetary discoveries.

SAR systems have been developed step by step for many years and the latest SAR technology is Interferometric SAR (InSAR). SAR and InSAR techniques will be described separately in the other special parts.

2.3. Basic principles of Radar technique

The Radar instrument emits electromagnetic pulses in the radio and microwave regime and detects the reflections of these pulses from objects in its line of sight. The radar technique uses the two-way travel time of the pulse to determine the range to the detected object and its backscatter intensity to infer physical quantities such as size of surface roughness. A mono-static radar uses only one antenna, both for transmitting and receiving, where as in a so-called bi-static radar, the transmitting and receiving antennas are physically separated (Skolnik, 1962). A basic radar system is shown on figure 2.1.

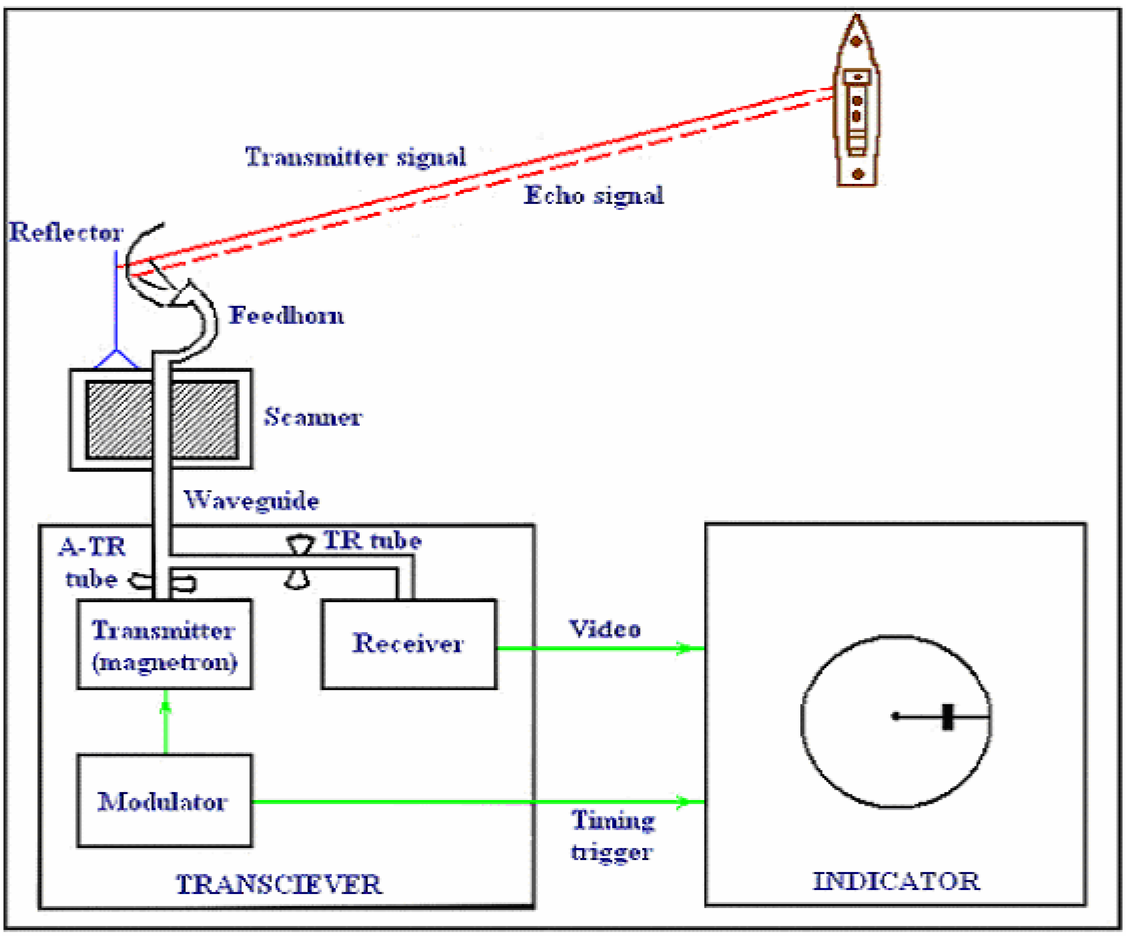

Figure 2.2: Principle of radar system

As seen in figure 2.2, basic radar system has components for processing signal and radar images.

Modulator

The function of the modulator is to insure that all circuits connected with the radar system operate in a definite time relationship with each other and that the time interval between pulses is of the proper length. Modulator simultaneously sends a synchronizing signal to trigger the transmitter and the indicator sweep. This establishes a control for the pulse repetition rate (PRR) and provides a reference for the timing of the travel of a transmitted pulse to a target and its return as an echo.

Transmitter

The transmitter generates radio-frequency energy in the form of short powerful pulses as a result of being turned on and off by triggering signals from the modulator.

Transmitting and Receiving antenna System

The function of the antenna system is to take the radio frequency energy from the transmitter, radiate this energy in a highly directional beam, receive any echoes or reflections of transmitted pulses from targets, and pass these echoes to the receiver.

In carrying out this function the radio frequency pulses generated in the transmitter are conducted to a FEEDHORN at the focal point of a directional reflector, from which the energy is radiated in a highly directional pattern. The transmitted and reflected energy are conducted by a common path.

This common path is an electrical conductor known as a WAVEGUIDE. A waveguide is hollow copper tubing, usually rectangular in cross section, having dimensions according to the wavelength or the carrier frequency, i.e., the frequency of the oscillations within the transmitted pulse or echo.

Because of this use of a common waveguide, an electronic switch, a TRANSMIT-RECEIVE (TR) TUBE capable of rapidly switching from transmit to receive functions, and vice versa, must be utilized to protect the receiver from damage by the potent energy generated by the transmitter. The TR tube, as shown in figure 2.1 blocks the transmitter pulses from the receiver. During the relatively long periods when the transmitter is inactive, the TR tube permits the returning echoes to pass to the receiver. To prevent any of the very weak echoes from being absorbed by the transmitter, another device known as an ANTI-TR (A-TR) TUBE is used to block the passage of these echoes to the transmitter.

Receiver

The function of the receiver is to amplify or increase the strength of the weak radio frequency echoes and reproduce them as video signals to be passed to the indicator. The receiver contains a crystal mixer and intermediate frequency amplification stages required for producing video signals used by the indicator.

Indicator

The primary function of indicator is to provide a visual display of the ranges and bearings of radar targets from which echoes are received. The secondary function of the indicator is to provide the means for operating various controls of the radar system.

2.4. Applications of Radar

Imaging radar has several geo-science applications listed in table 2.1 below.

Table 2.1
Operational Geo-science Applications of Imaging Radar

- **Reconnaissance type original mapping of cloud-infested remote areas for the purpose of**
  - Geology
  - Geomorphology
  - Forestry
  - Land use
  - Cartography

- **Regional geological fracture patterns**
  - Dam site selection
  - Nuclear power plant site selection
  - Petroleum exploration
  - Mineral exploration

- **Meso- and macroscale stream network analysis**
- **Monitoring of catastrophic damages due to**
  - Floods
  - Hurricanes
  - Earthquakes

- **Maritime traffic**
- **Ice distribution on lakes, sea ice**
- **Monitoring icebergs**

2.5. Applications of Side-Looking Radar

SLR also has other geo-science applications listed in table 2.2 below.

Table 2.2

Examples of Other Geo-science Applications of Side-Looking Radar

- **Lakes and oceans**
  - Lake levels
  - Oil spills
  - Ocean waves and sea state
  - Internal waves
  - Polar ice motion
  - Polar ice thickness, age
  - Monitoring of hurricanes

- **Coasts**
  - Shoreline erosion
  - Wetlands mapping
  - Coastal wave diffraction

- **Water management**
  - Drainage basin geometry
  - Planting patterns
  - Soil moisture
  - Snow cover
  - Frozen and unfrozen ground
  - Ground water through vegetation and fracture analysis
  - Glacier subsurface sounding

- **Vegetation**
  - Crop species
  - Soil moisture
  - Range species, spread of woody weeds

- **Soils**
  - Soil type in arid, arctic, and cloud-infested areas
  - Micro-relief (surface roughness)
  - Subsurface sounding

- **Geology and Geomorphology**
  - Regional geomorphology
  - Subsurface sounding

- **Mapping**
  - Land use assessment at meso- and macro-scale
  - Urban meso-scale change detection
  - Revision of small-scale maps
  - Monitoring of large construction

2.6. Advantages of Radar

Radar imaging has some advantages and possibilities listed in table 2.3 below.

Table 2.3
Advantages of Radar Imaging Over Other Imaging Systems

- **Primary Advantages**
  - It can penetrate clouds and serve as all-weather sensor
  - It can (from aircraft) produce synoptic views of large areas, typically for mapping at scale 1:50,000 to 1:400,000
  - Coverage can be obtained quickly at specific times
  - It permits imaging at very shallow look angles, and thus results in dramatically different perspectives than common vertical photographs

- **Secondary Advantages**
  - Long wavelength Radar has the potential to penetrate vegetation, surface layers of snow
  - It provides its own illumination, and thus control over the illumination angle
  - It employs wavelengths different from photographic sensor, and thus provides different information (on surface roughness, dielectric properties, moisture)
  - It enables resolution to be independent of distance to the object
  - It can use polarization effects
  - It can operate simultaneously in several wavelengths, and thus has a multispectral potential
  - It can image ocean waves, even from orbital distances

2.7. What are SAR and InSAR?

- SAR

SAR is an acronym of **S**ynthetic **A**perture **R**adar and a specific class of radar systems like **S**ide **L**ooking **R**adar (SLR). In SAR technique, the radar operation is based on a "Synthetic Aperture". Whether a SAR is operated on an aircraft or spacecraft has no effect on the resolution in the range direction.

SAR is an active system and provides its own illumination source by transmitting microwaves and recording their backscattering signals. And sophisticated SAR signal processing system converts these signals to high resolution image using the time delay of backscattered energy.

Figure 2.3 shows the space-borne SAR imaging geometry.

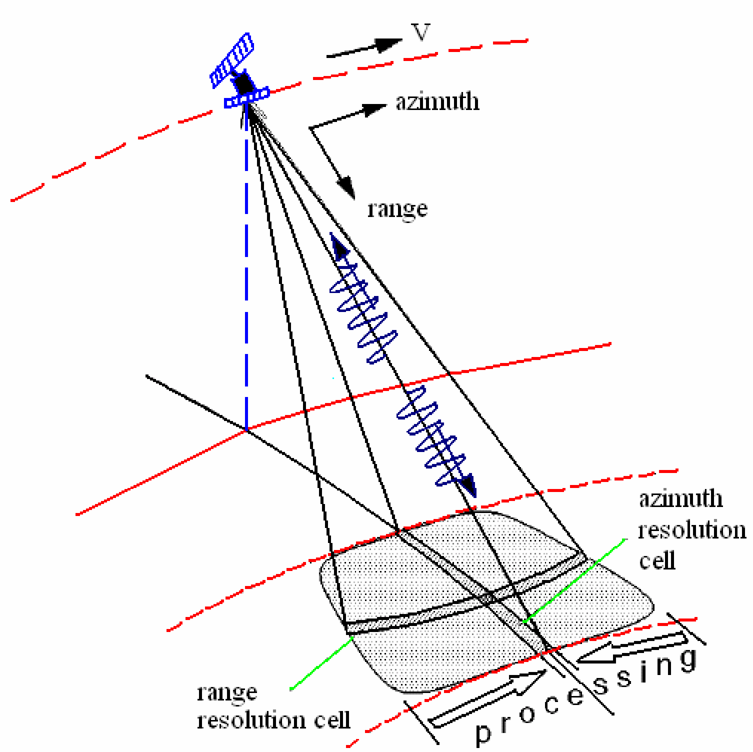

Figure 2.3: Space-borne SAR imaging geometry

Synthetic aperture radar is different from **R**eal **A**perture **R**adar (RAR) and synthetically increases the antenna's size or aperture to increase the azimuth resolution though the same pulse compression technique as adopted for range direction. In Synthetic aperture processing signals and phases are received from targets by a small antenna than this effect is converted to effect of a large antenna with synthetic aperture length. Figure 2.4 shows the relation between real aperture and synthetic aperture radar.

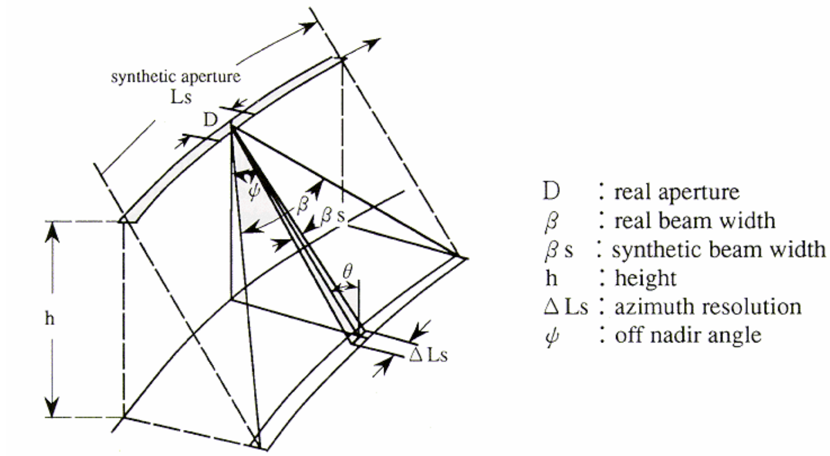

Figure 2.4: Relation between real aperture and synthetic aperture radar

The resolution in the azimuth direction is given by half of real aperture radar as shown as follows.

Real beam width : $\beta=\lambda/D$
Real resolution: $\Delta L= \beta R=Ls$ (synthetic aperture length)
Synthetic beam width : $\beta s =\lambda / 2Ls= D / 2R$
Synthetic resolution : $\Delta Ls = \beta sR = D / 2$

λ = wavelength
D = aperture of radar
R = slant range

By this reason regardless of very high altitude of a satellite and the slant range, SAR has a high azimuth resolution with a small size of antenna.

The data acquisition by Synthetic Aperture Radar (SAR) is based on the direction perpendicular to the orbit and the distance. The determination of the location based on distances is causing some problems in steep terrain. If the terrain inclination is exceeding the incidence angle, the position of a higher elevated point is shown before the position of a lower point even if this is reverse in the object space (point 4 in figure 2.5 is located in the slant range image before point 3). This so called *layover* is mixing the radar signals and there is no possibility of a correct reconstruction in such steep parts. Caused by the higher incidence angle of SAR the shadows (areas with no information) are larger like usually in optical images. The compression of the information by the *foreshortening* is reducing the information in these parts.

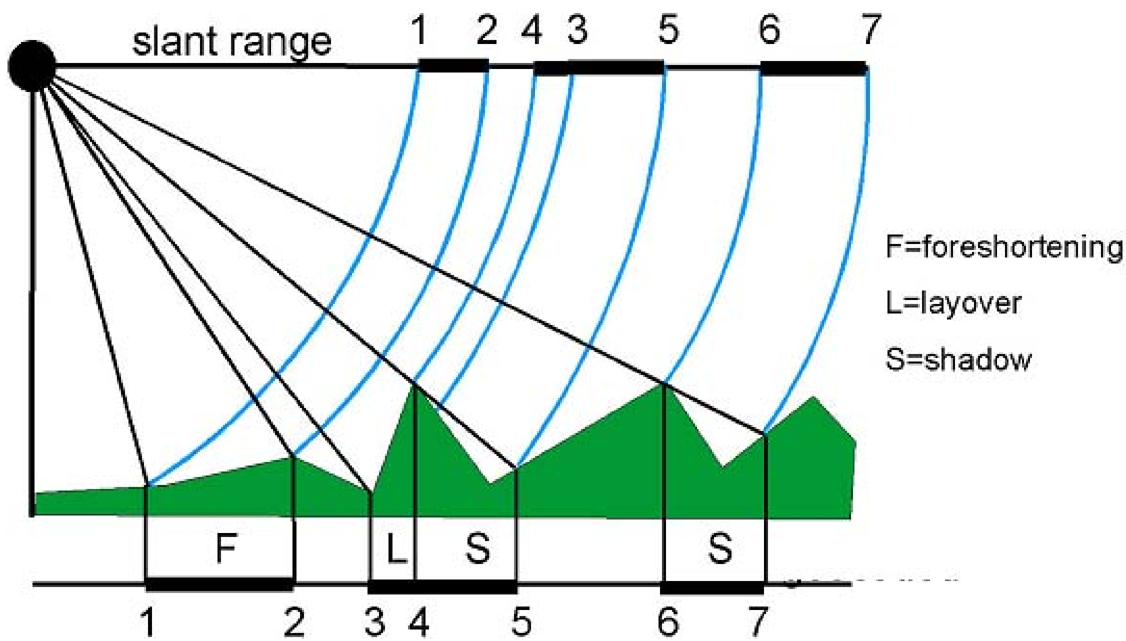

Figure 2.5: Location determination by SAR

- InSAR

InSAR is a nested acronym of **In**terferometric **S**ynthetic **A**perture **R**adar. For DEM generation, two SAR images are achieved for produce three dimensions from different view angles to same area. Following figure 2.6 shows the geometry of SAR interferometry.

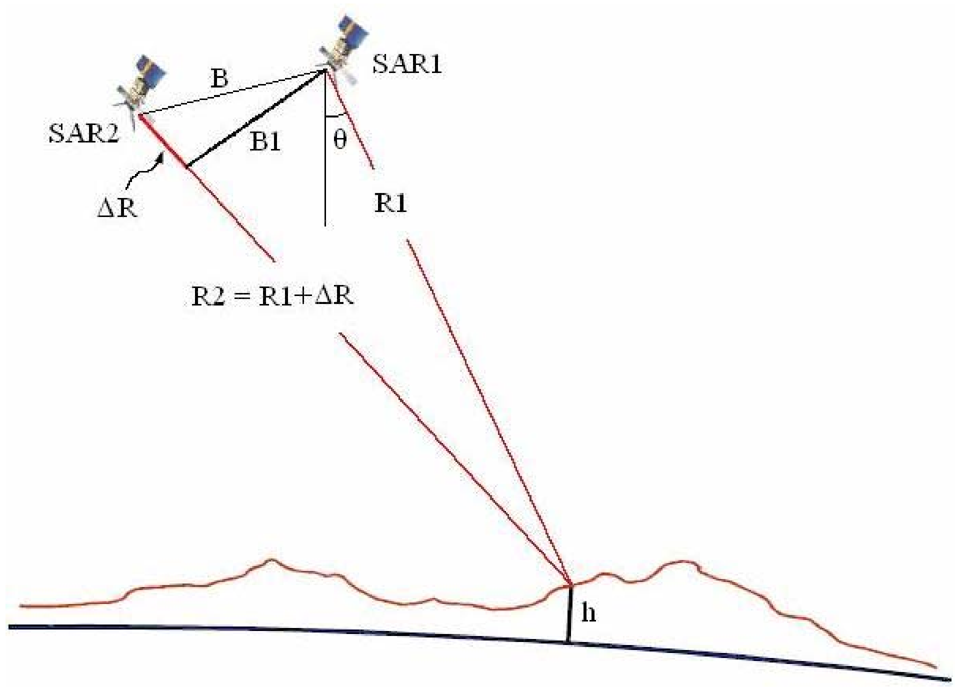

B: Baseline of the interferometer
R: Distance between satellite and object
ΔR: Difference of distances between SAR1 and SAR2 to object
h: Altitude of object

Figure 2.6: Geometry of SAR interferometry (satellite flight passes into the plane)

SAR interferometry exploits the phase of SAR to measure stereo parallaxes to an accuracy of a fraction of a wavelength. Phase differences of two complex-valued SAR images of the same interest area are computed on a pixel-by-pixel basis. In figure 2.6 phase difference is found as:

$$\Delta\phi = \phi_2 - \phi_1 = (4\pi : \lambda)(\mathbf{R_2} - \mathbf{R_1})$$

Obviously, the range parallax $\Delta R = (R_2 - R_1)$ is a measure for the look angle θ which, in turn, depends on terrain height h.

When using this process, interferometric SAR becomes very useful in two different major groups.

The first group is 'single-pass interferometer' and second one is 'double-pass interferometer'. In single-pass interferometer, on the same aircraft or spacecraft, two different antennas are used and also these antennas have different view angles, they look to the same interest area and produce three-dimension for the objects for generate a digital elevation model (DEM). In this system, signal is transmitted by a single antenna and received by two antennas. As example **S**huttle **R**adar **T**opography **M**ission (SRTM) used this single-pass interferometry technique. This study is about accuracy assessment of digital elevation models derived from shuttle radar topography mission (SRTM).

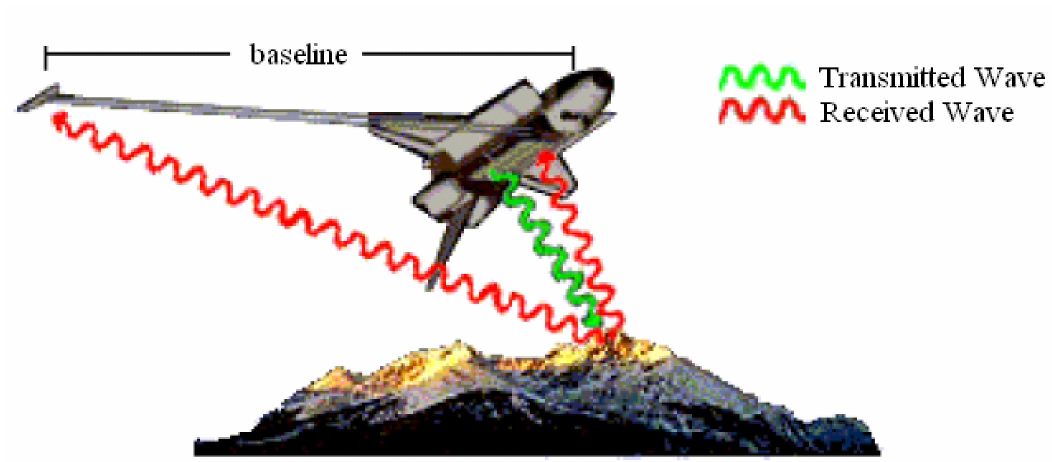

Figure 2.7: SRTM single-pass InSAR configuration (not in scale: baseline exaggerated)

The second group interferometer is ‘double-pass interferometer’. In double-pass interferometer, only single antenna is used. Over the same area, aircraft or a satellite flies twice with slightly displaced orbits at two different epochs. On these epochs, the distance to previous visit must be kept small to fulfill the interferometric condition. The backscattered signals from these two epochs for the same area are used for interferometric processing.

3. SHUTTLE RADAR TOPOGRAPHY MISSION (SRTM)

3.1 What is SRTM?

Shuttle **R**adar **T**opography **M**ission (SRTM) was flown on board the space shuttle Endeavour in February 2000 and its duration was 11 days in space. It was a joint project between the National Aeronautics Space Administration (NASA) the National Imagery and Mapping Agency (NIMA) and the Deutsches Zentrum für Luft und Raumfahrt (DLR). The Italian Space Agency was cooperating with DLR.

The aim of SRTM was to produce digital elevation data for 80% of the Earth’s land surface between 60° northern and 56° southern latitude. Based on the mission, height values with a spacing of 1- arc-second (approximately 30 meters) have been generated. Endeavour (SRTM) was placed on a 233km orbit height with an inclination of 57°.

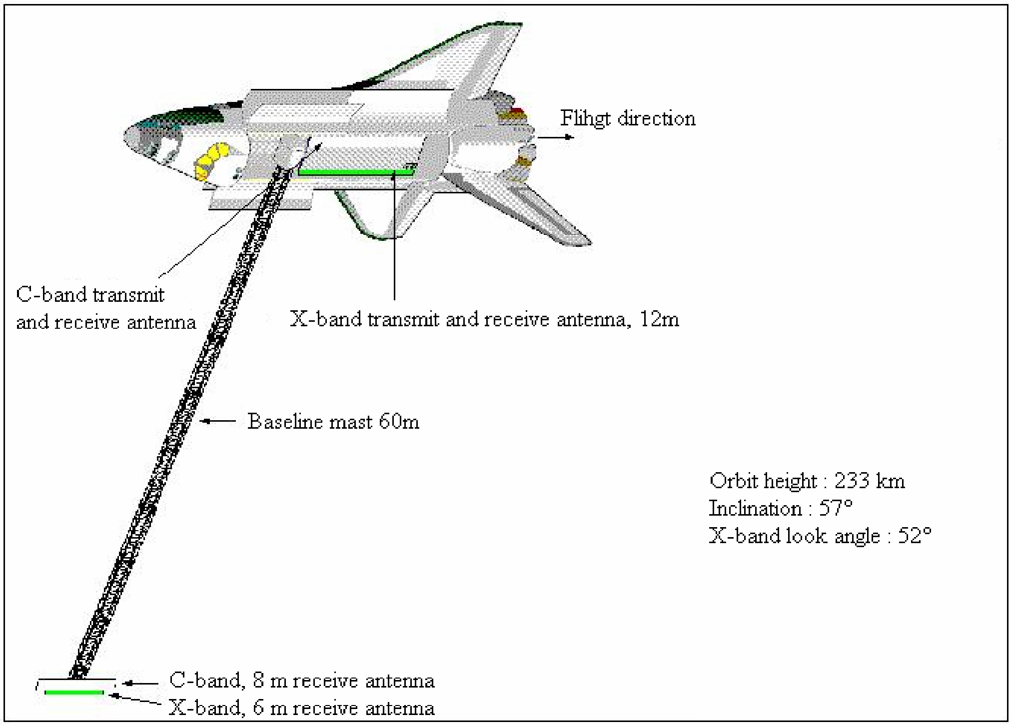

Figure 3.1: SRTM configuration with the secondary antennas mounted on the mast

During the mission, two different antennas were installed on board the shuttle. The main antenna length was 12m and located in cargo bay and it acted as transmitter and receiver. The second one was an outboard antenna or slave antenna fixed at the end of 60m long mast and was only receiver. The US used the C-band and Germany/Italian the X-band.

- C-band

The US American C-band operated with a wave length of λ= 5.6cm. It had capability for ScanSAR mode, in this mode, the antenna beam is electronically steered towards different elevation angles in a repeated stepwise fashion. Thus, four narrow but overlapping sub-swath were imaged quasi simultaneously to form a 225km wide swath (Bamler, 1999) (figure 3.2). With C-band 119.51 million square km were imaged corresponding to 99.97% of the target area. The 8.6 Terabytes of C-band data were recorded on 208 high density digital data tapes and stored on the shuttle. Figure 3.3 shows the coverage by the SRTM C-band.

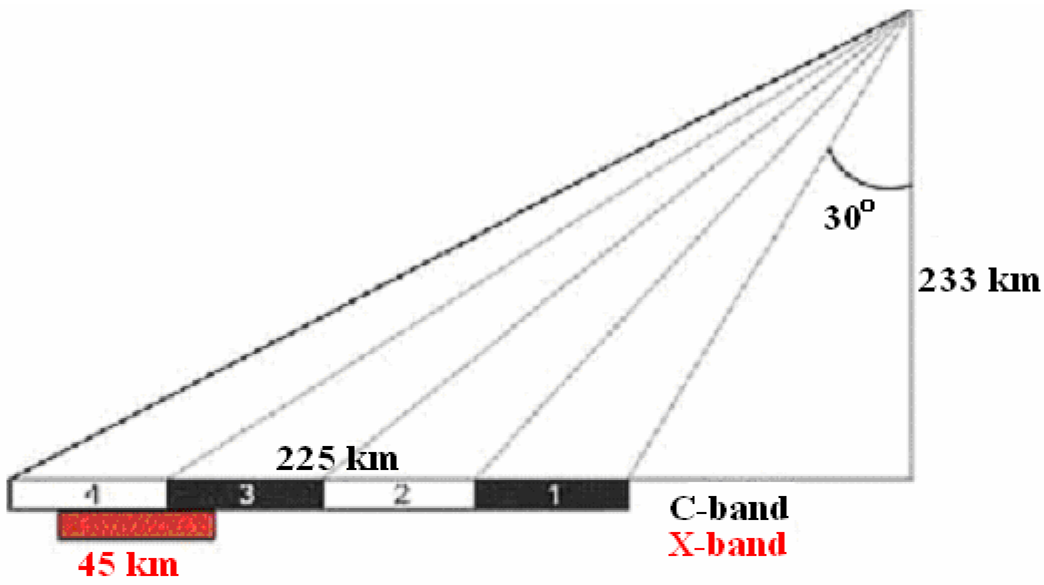

Figure 3.2: Swath width of SRTM C-band and X-band

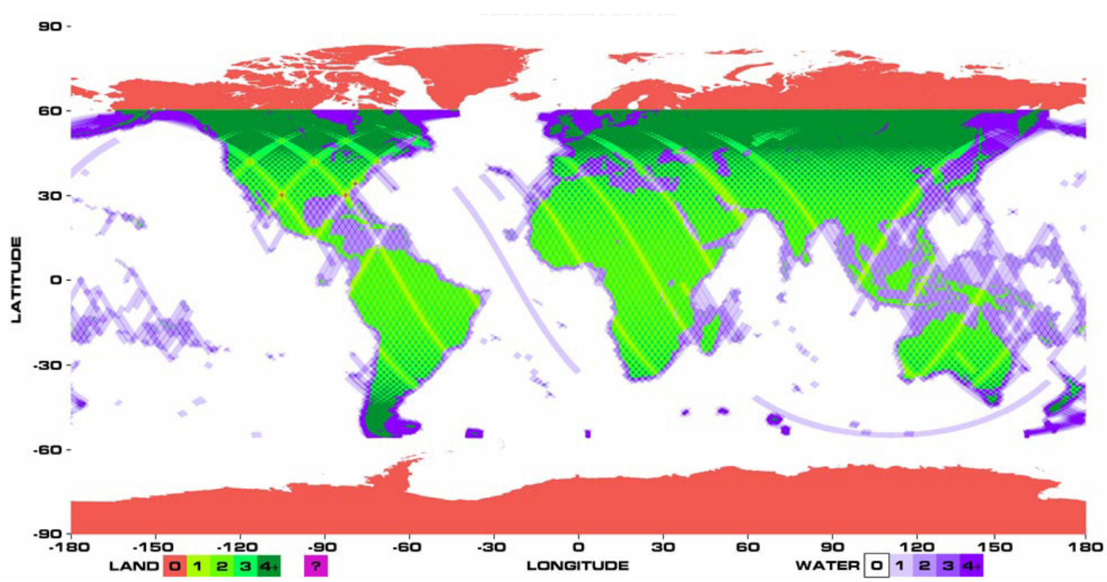

Figure 3.3: SRTM C-band coverage

The C-band has nearly a complete coverage and 94.6% of the mapped area is covered at least twice and approximately 50% at least three times. Because of the radar layover, in very steep areas gaps of in total 0.15%. The C-band height model is available free of charge in the internet with a limited point spacing of 3 arcsec corresponding to 92m at the equator.

- X-band

The German/Italian X-band had no capability for ScanSAR mode and was limited to a swath width of 45km (see figure 3.2). Because of this, the X-band data do have large gaps between the strips.

The X-band has some advantages its wavelength is λ= 3cm and depend on this shorter wavelength its relative vertical accuracy by theory is higher than for the C-band. The X-band data can be bought from the DLR with a point spacing of 1 arcsec, corresponding to 31m at the equator.

The X-band has 52° incidence angle. In the coverage, there are gaps between the swaths which become smaller with growing latitude. Figure 3.4 shows the coverage of SRTM X-band for parts of Asia.

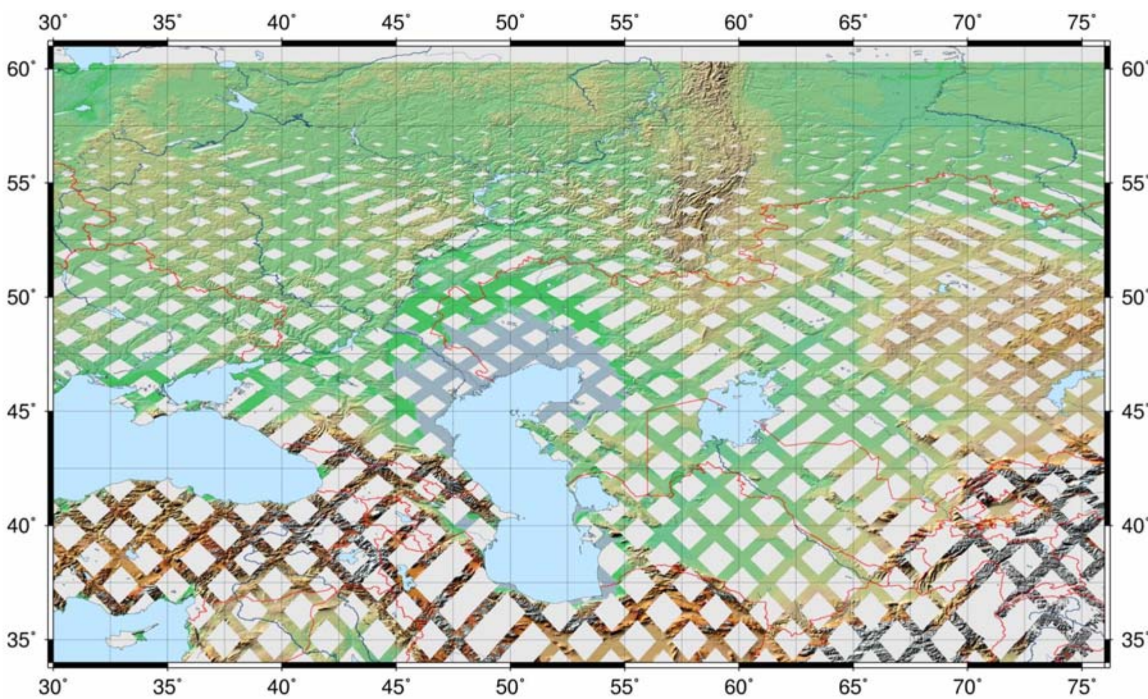

Figure 3.4: Example of SRTM X-band coverage

In this study, the test field is Zonguldak, located at the Black Sea in Turkey. Figure 3.5 shows the coverage of test field by the X-band. The test field is located in the red circle and the white part shows the gaps of the X-band height model.

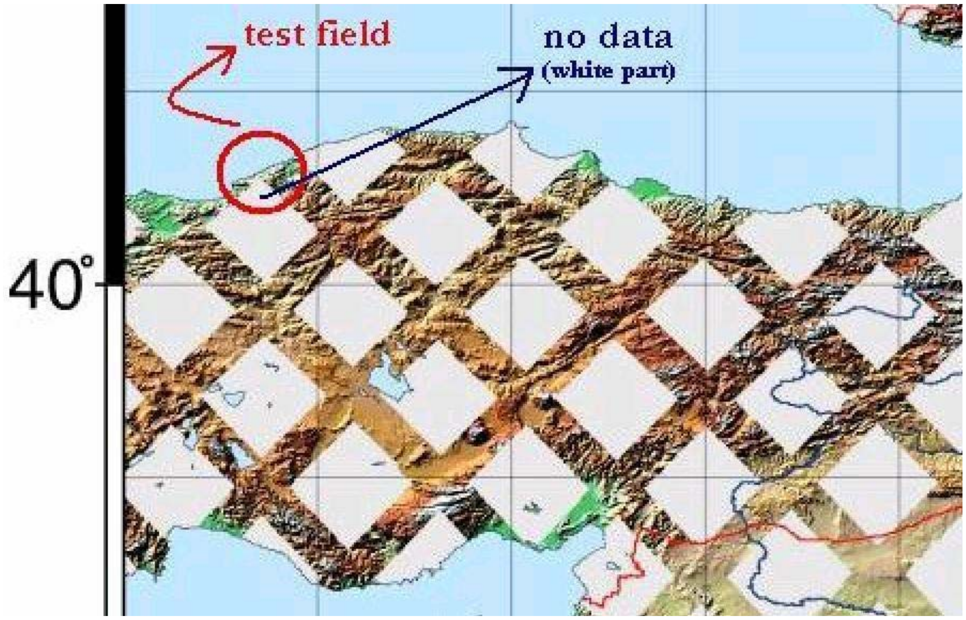

Figure 3.5: SRTM X-band coverage of area around test field

3.2 Imaging Technique of SRTM

SRTM used the first space-borne single-pass interferometric SAR (InSAR), it produced the first near-global, homogenous, high resolution digital elevation model.

A suite of sensors is responsible for measuring and controlling the proper alignment of the secondary antenna with respect to the main antenna and the attitude and position of the interferometric system in orbit.

A star tracker measured the orientation of the interferometric system in orbit, which was supported by an inertial reference unit consisting of three 2axis gyros. An optical tracker of the secondary antenna which is a video camera and LED targets, allowed a relative 3-axis measurement of the boom antennas. Additionally, two GPS antennas, one on the main antenna structure the other one on the secondary, provided 0.8m orbital position accuracy determination and furthermore, a time reference for the radar with an accuracy of 100 microseconds.

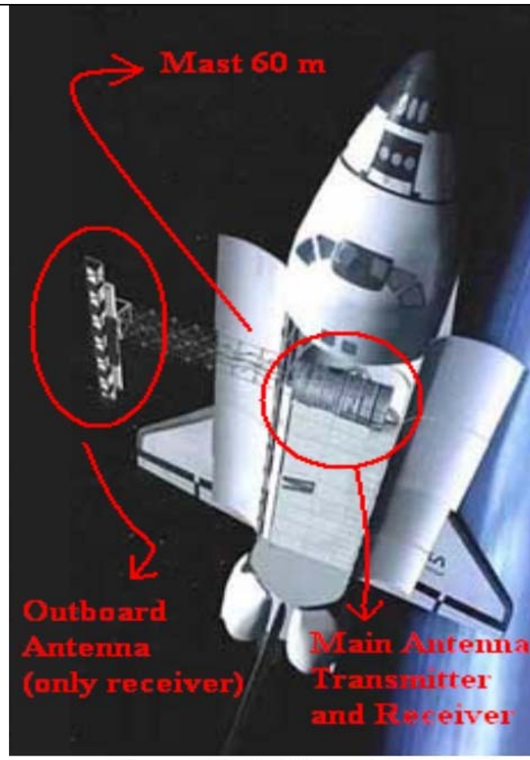

Figure 3.6: SRTM antenna

Figure 3.7: SRTM single-pass InSAR

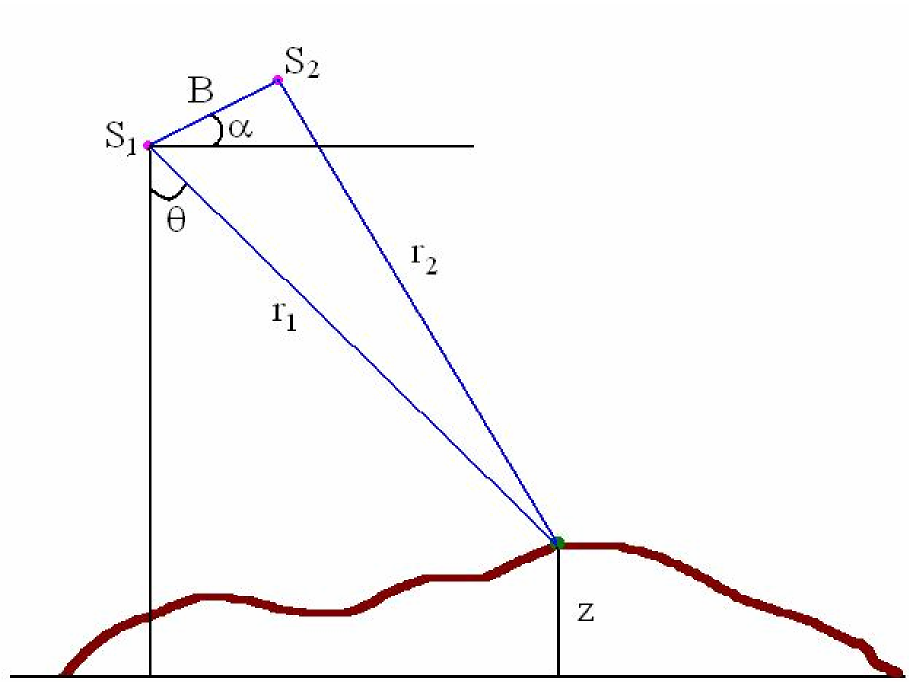

Figure 3.8: A single-pass interferometer uses two antennas at different locations to measure the difference in range to the surface

Depend on this figure, the phase difference between two different antennas can be written

$$\Delta\phi = -(\alpha 2\pi / \lambda)(r_1 - r_2)$$

In this equation,

λ is the radar wavelength
r_1 and r_2 are the radar ranges between antennas and the observing object
$\alpha = 2$ for standard repeat-track interferometry and $\alpha = 1$ when the signal is transmitted out of one antenna and simultaneously received through two different antennas separated in elevation, such as in the case of SRTM.

The phase difference can be written with these terms

$$\Delta\phi = -(\alpha 2\pi / \lambda)(B\sin(\theta - \alpha))$$

B is the baseline separating the antennas
θ is the radar look angle

- Interferogram

Radar interferometry is a technique that can be used for the generation of three dimensional images of the Earth's surface. Interferometry is the study of interference patterns accomplished by combining two sets of signals. The result of this combination is called an interferogram or a fringe map (figure 3.9)

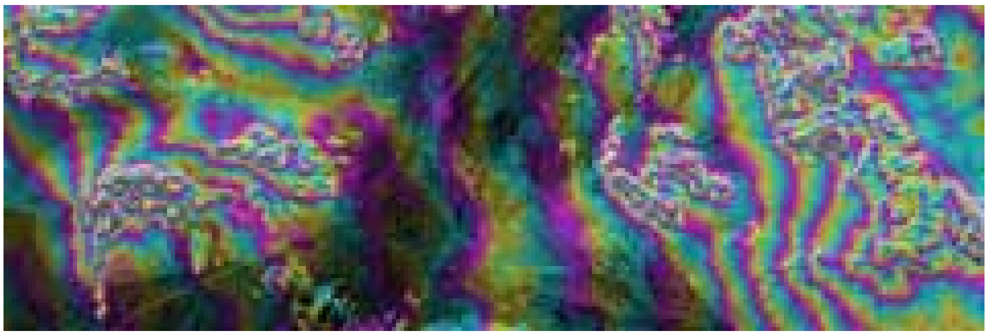

Figure 3.9: Interferogram (fringe map)

3.3 Advantages of Using SRTM data and Application areas

SRTM data has some advantages like:

- Near-global coverage
- Good resolution
- Homogeneity
- Wide Overlap from ascending and descending paths
- Extensive availability
- Low cost

The Products of SRTM have an impact that digital elevation models are utilized. The usage areas of SRTM can be separated into 3 different groups.

- **Science Community**
    - Climate impact
    - Water and wildlife management
    - Geological and hydrological modeling
    - Geographic information systems (GIS)
    - Mapping purposes
    - Educational programs

- **Commercial Providers**
  - Telecommunications
  - Air traffic routing and navigation
  - Planning and construction
  - Hydrological and meteorological services
  - Geocoding of remote sensing data and the market of multimedia applications

- **Operational Users**
  - Generating and updating geo-information for governmental issues
  - Administrating assistance in areas inflicted by catastrophes
  - Airline operation safety

4. TEST AREA

4.1. General Description of the Test Area Zonguldak

Test area Zonguldak is located in north-west part of Turkey. Figure 4.1 shows the test area's location on the world map.

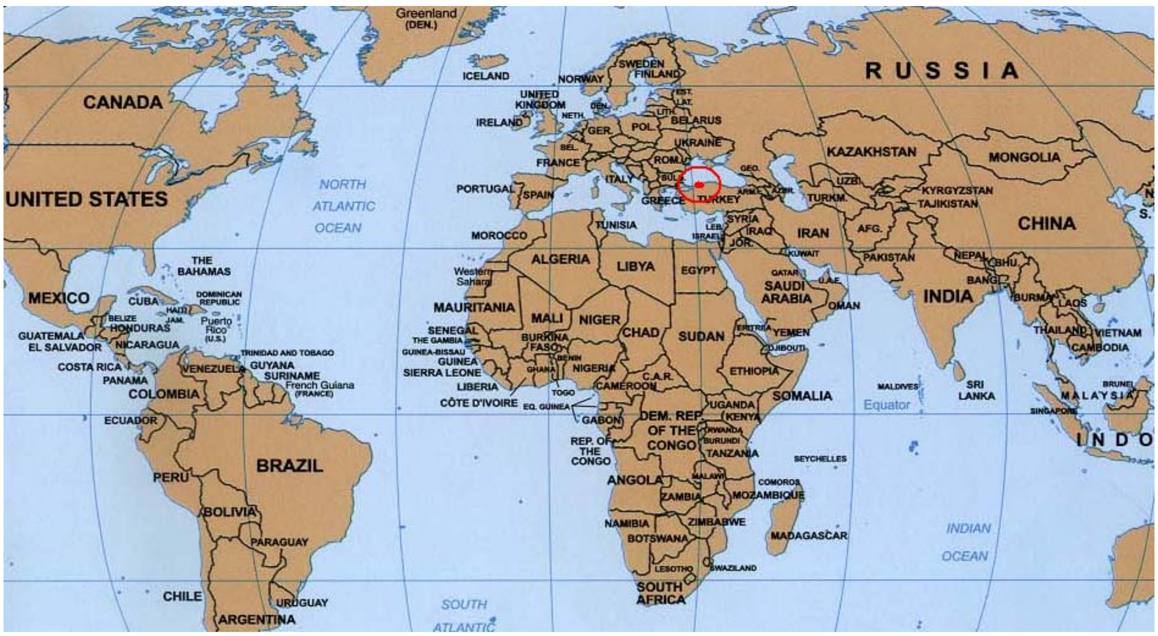

Figure 4.1: Rough location of test area

In the central part of the test area, the city of Zonguldak is located, which is in the West Black Sea region of Turkey.

Figure 4.2: Map of Turkey

4.2. Characteristic of Test Area

Zonguldak has very rough and mountainous topography that's why terrain inclination has a big influence on the accuracy of the results. Figure 4.3 shows the OrbView-3 space image of test field. The mountainous topography is obvious.

Figure 4.3: OrbView-3 image of test field Zonguldak

At the upper side of the image, the city centre and harbour can be seen, the reservoir of Zonguldak can be seen in the lower part.

The colour coded slope map of the new reference height model of the city is shown in figure 4.4. Blue represents flat areas and red represents large inclinations.

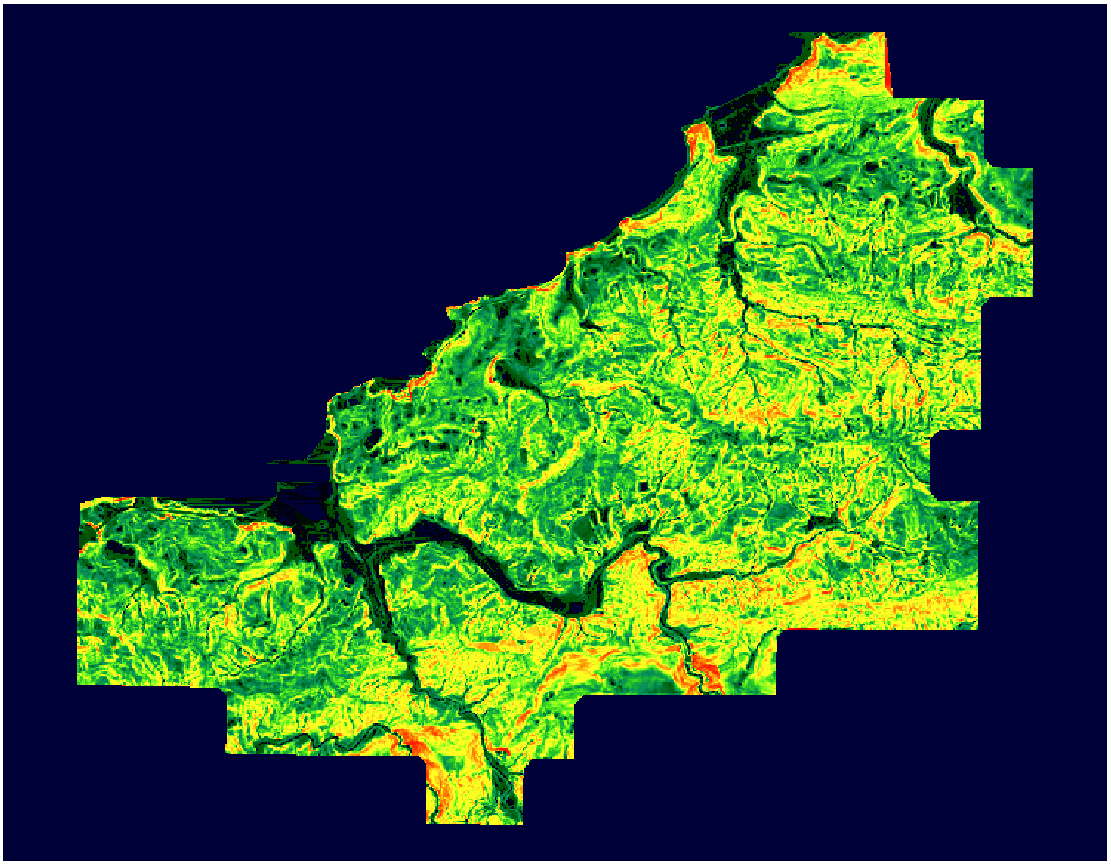

Figure 4.4: Colour coded slope map of DEM2005

The frequency distribution of the terrain inclination is represented in figure 4.5.

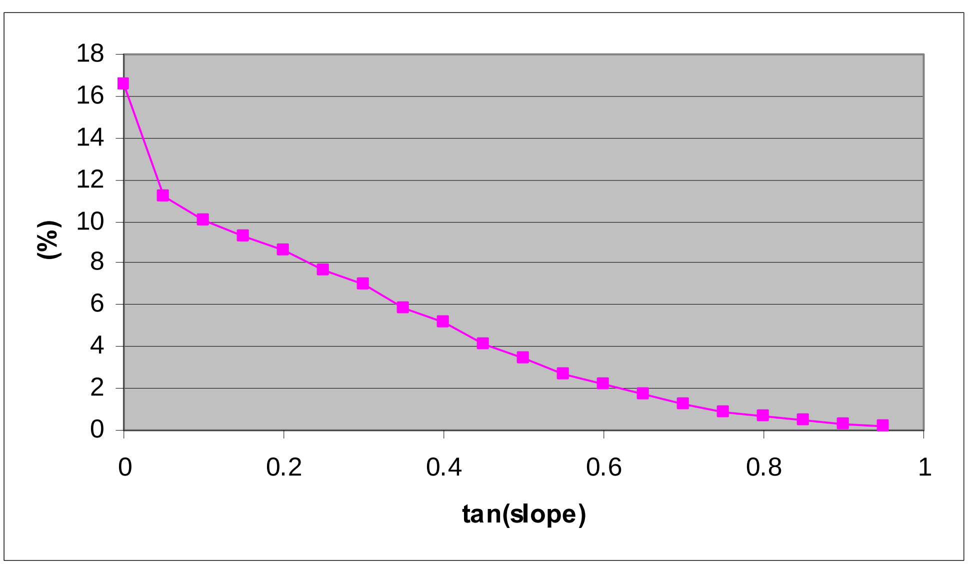

Figure 4.5: Frequency distribution of terrain inclination

5. STRATEGY

5.1 Used Programs

In order to asses the accuracy of digital elevation models derived from SRTM for the test area Zonguldak several programs were used. With the exception of LISA, these programs are components of program system BLUH, developed by Dr. Karsten Jacobsen, Institute of Photogrammetry and Geoinformation (IPI), University of Hannover, Germany. Following programs have been used:

Programs	**Function**
DIGDEM	Conversion binary to ASCII DEM
BLTRA	Transformation of national net, geographic and geocentric Coordinates or Image Orientation
DEMSHIFT	Shift of a DEM to another in X, Y, Z and Scaling in Z
DEMANAL	Analysis of DEM against a reference DEM
RASCOR	Analysis, Correction and Plot of a DEM
LISA	Interpolation and visualization of a DEM
DEMINT	Computation of Z-value for points with given X and Y by interpolation of a raster-digital elevation model
MANI	Manipulation of Object Coordinates, Image Orientations, IMU-data and Pixel Addresses
ZANAL	Analysis of a DEM
ZPROF	Plot profiles
BLCON	Conversion of Ground Coordinates Window Function, Reduction to Equal Distributed Points, change of spacing

Table 5.1: Used programs and their functions

In order to achieve the DEM in the national coordinate system the SRTM DEMs in binary format have been converted by DIGDEM into ASCII and then transformed to national, geographic or geocentric coordinates with program BLTRA.

5.2 DEMSHIFT

The SRTM height models may have a horizontal shift, in addition the reference DEM in the national coordinate system may be influenced by a local datum effect. By this reason the program DEMSHIFT is used to shift a digital elevation model to another by adjustment. In program DEMSHIFT, one DEM is selected as a reference and it must be

available as ASCII-file in raster arrangement (equal point spacing); it may have some data gaps. If the reference DEM is not available in raster form, with suitable programs this can be generated for example by LISA-BASIC. Some differences of last digits in the X- and Y-coordinates of the reference file may cause problems with the determination of the grid spacing. This can be avoided by the rounding function – see input dialog of DEMSHIFT. The DEM which shall be shifted and scaled has to be in ASCII-form, it may have a random point distribution, but it may be also available in ASCII-raster form with a different spacing like the reference. The points are interpolated in the reference file for analysis by bilinear interpolation.
Capacity: the reference DEM may have a size up to 5001 x 5001 points. For the file for analysis no capacity limit exists.
The shift and the possible scaling are determined by adjustment. Depending upon the terrain inclination, a different number of iterations is required. Independent upon the specified number of iterations in the input, the iteration stops if there is no more improvement of the sigma0. If the scale of the Z-component also shall be determined, the last iteration will be made without scaling. The convergence radius of the DEM shifting may be limited depending upon the terrain inclination – in this case the DEM for shifting should be roughly shifted in advance by program BLCON or MANI.
Only the first 10 000 000 points of the file for shifting are respected in the adjustment, but all points are used for the output file (Jacobsen, 2005).

5.3 MANI

If large RMSZ values are achieved with DEMSHIFT, this indicates large shifts of the height model with a size outside the convergence radius. In this case a pre-correction of the height model with program MANI is possible. The values for pre-correction can be achieved by a visual inspection of the height models like shown in figure 5.1. For example a point located in a river junction can be measured in both DEMs and the difference in location can be used as a pre-correction.

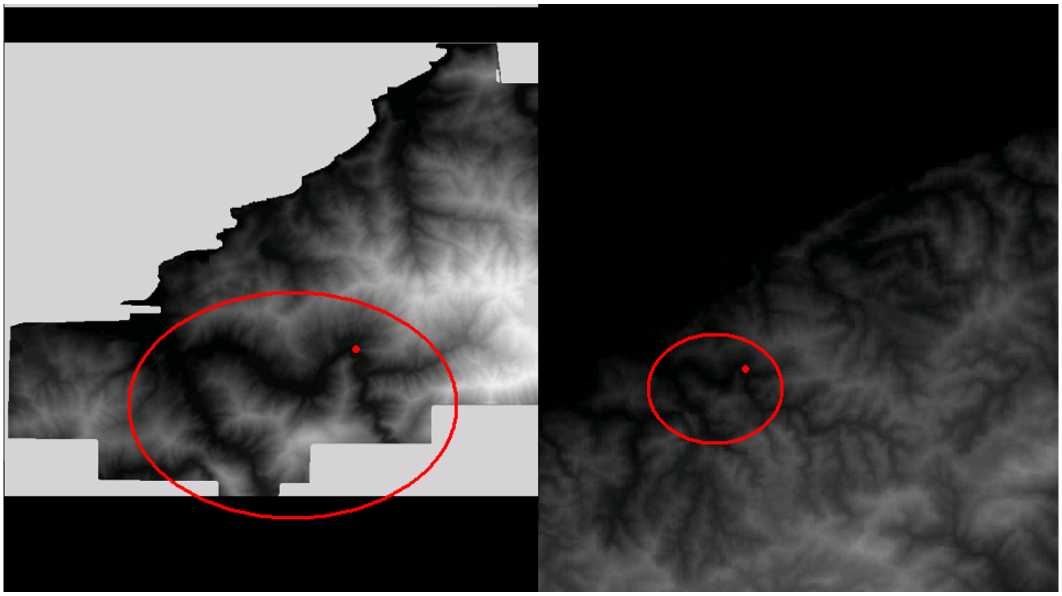

Figure 5.1: Selection of points for pre-correction with program MANI

5.4 DEM Analysis: DEMANAL

DEMANAL is a program that analyse the accuracy and accuracy characteristic of a DEM against a reference DEM. In program DEMANAL, different classes of objects can be analyzed separately - for example the forest and open areas. Each area can be analyzed separately because different types of objects can reflect their own accuracy characteristics and the results achieved for these different land classes may be different. In DEMANAL, the discrepancies between the both DEMs will be analyzed in detail including the analysis for a dependency against the terrain inclination and the height level. The influence of a vertical scale difference can be respected iteratively. The reference DEM must be available as ASCII-file in raster arrangement (equal point spacing); it may have some data gaps. If it is not available in raster form, it can be generated for example by a program LISA-BASIC. The DEM for analysis has to be in ASCII-form, it may have a random point distribution, but it may be also available in ASCII-raster form with a different spacing and reference. The reference points corresponding to the file for analysis are determined by bilinear interpolation (Jacobsen, 2005).
Capacity: the reference DEM may have a size up to 5001 x 5001 points. For the file for analysis no capacity limit exists (Jacobsen, 2005).

In this study, two different height models were used as reference for the analysis. One of them is based on the topographic map 1: 25000 (old) (DEM25000) the other is from a large scale photogrammetric measurement (new) (DEM2005).

In the study, SRTM C-band and X-band data accuracies are analyzed using the old and the new reference height models. DEMANAL shows the distribution of the point heights, the frequency distribution of slope on the terrain, the frequency distribution of DZ and others. Figure 5.2 shows the frequency distribution of DZ of the new reference DEM.

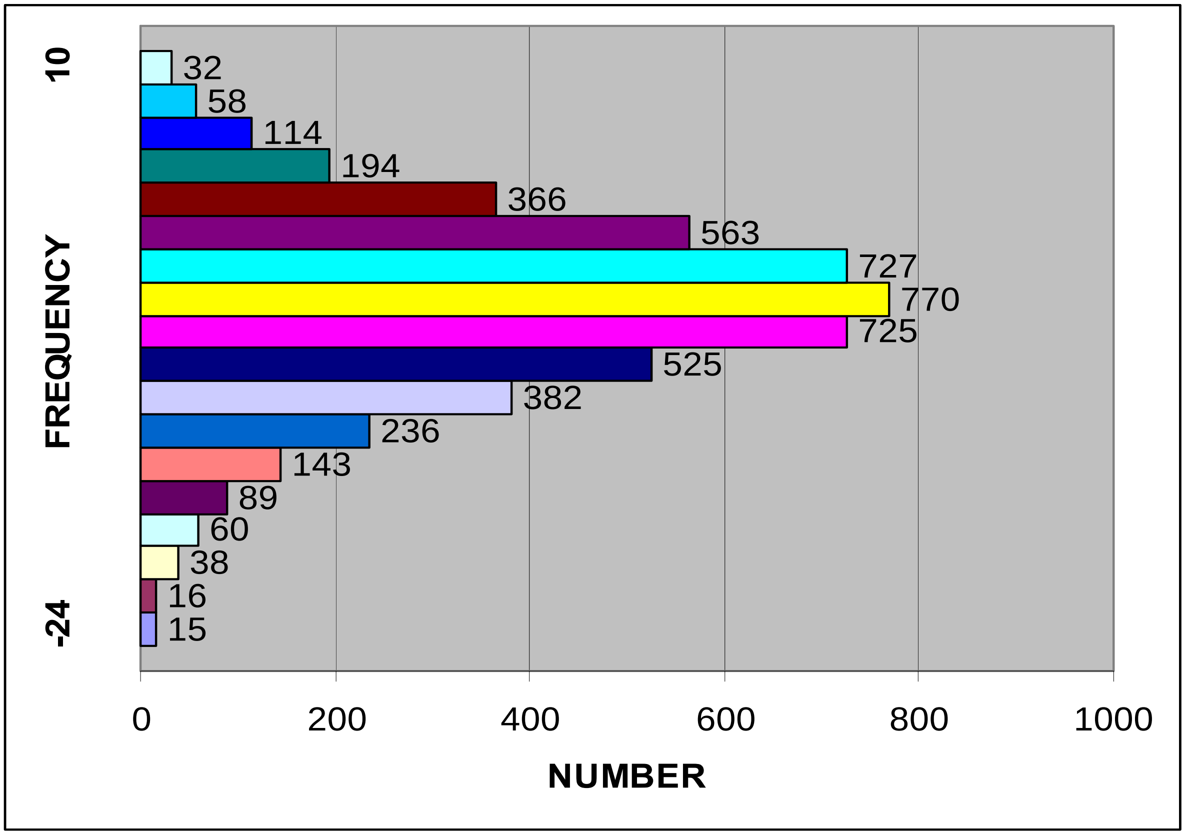

Figure 5.2: Frequency distribution of DZ of SRTM C-band against DEM2005 – negative values = SRTM height model located above reference DEM

5.5 LISA

The program LISA is used for interpolation and visualization of a digital elevation models. With LISA, after generation of a digital elevation model the results can be visualised. As example figure 5.3 shows a colour coded three dimensional representation of the test field Zonguldak.

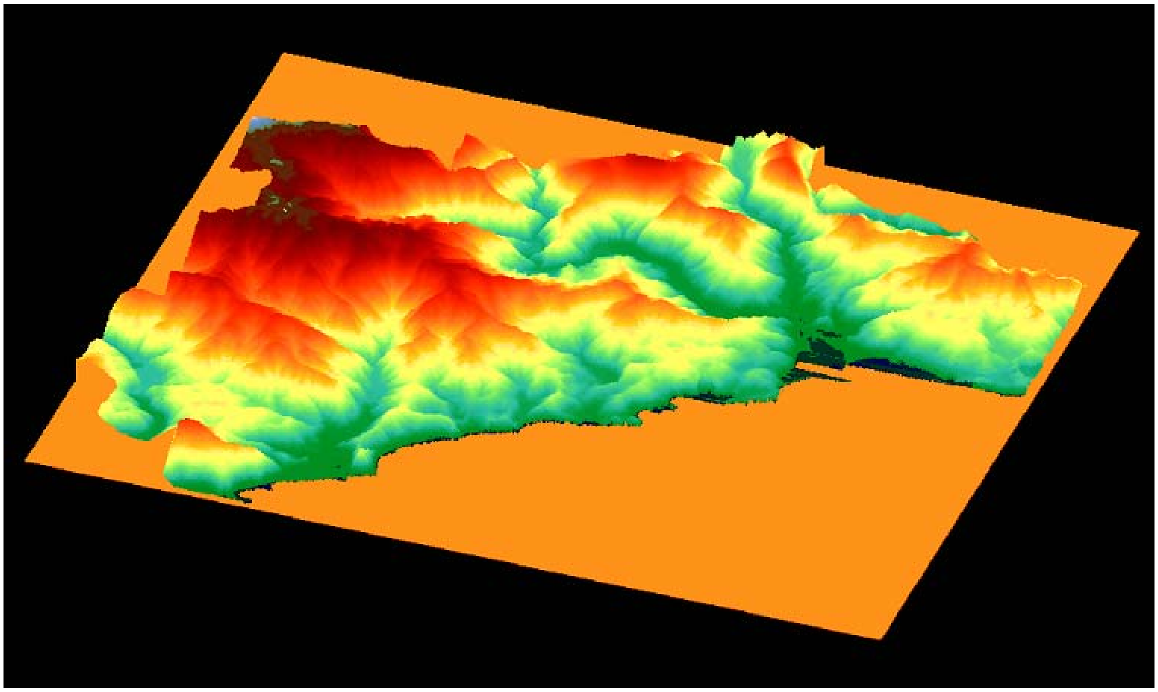

Figure 5.3: Colour coded three dimensional presentation of test field Zonguldak generated by LISA

In Figure 5.4 the grey value coded SRTM C-band height model of test field Zonguldak can be seen.

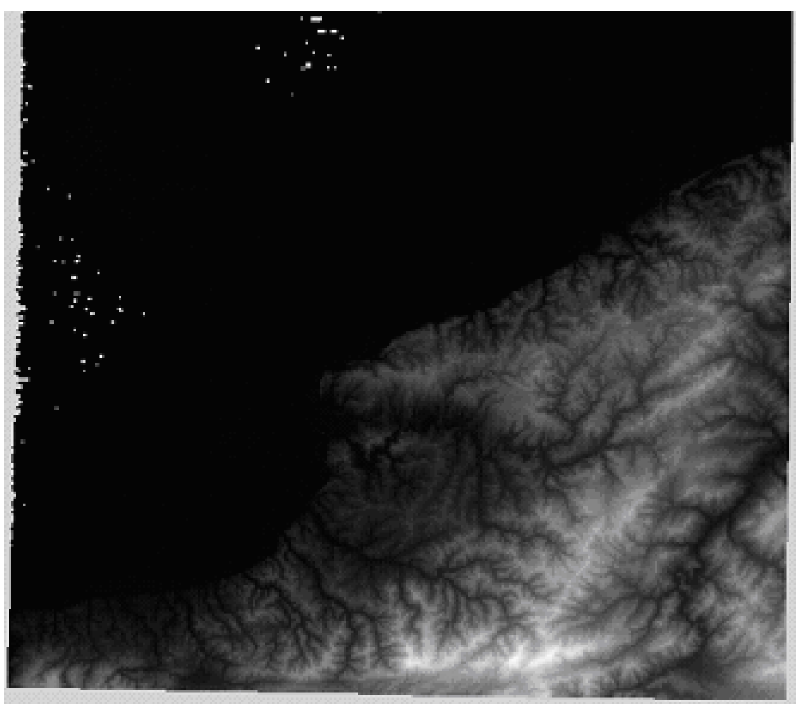

Figure 5.4: SRTM C-band DSM of the test field Zonguldak

In LISA, a DEM can be presented with different colour palettes. This allows a more detailed presentation of DEM details. Figure 5.5 shows the SRTM C-band DEM of the test field Zonguldak colour coded with different palettes.

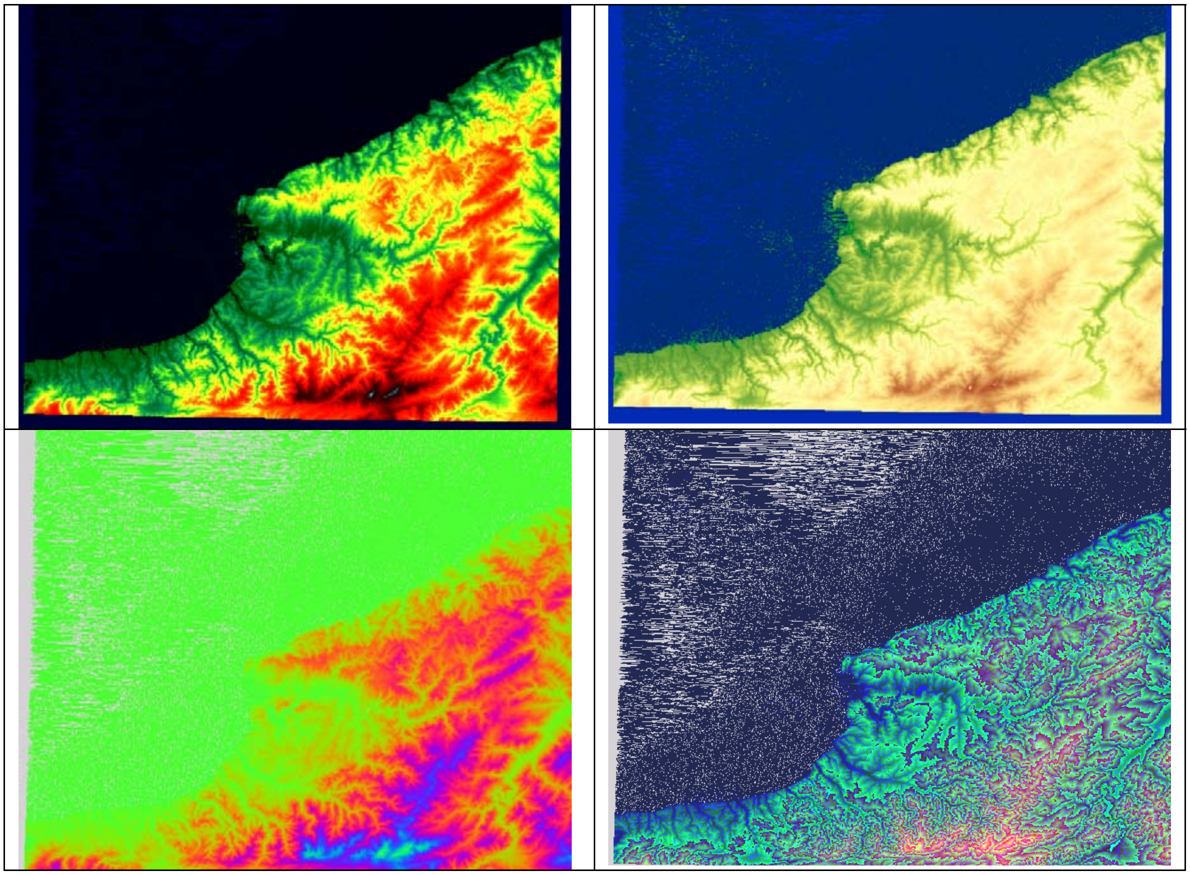

Figure 5.5: SRTM C-band DSM of the test field Zonguldak colour coded with different colour tables

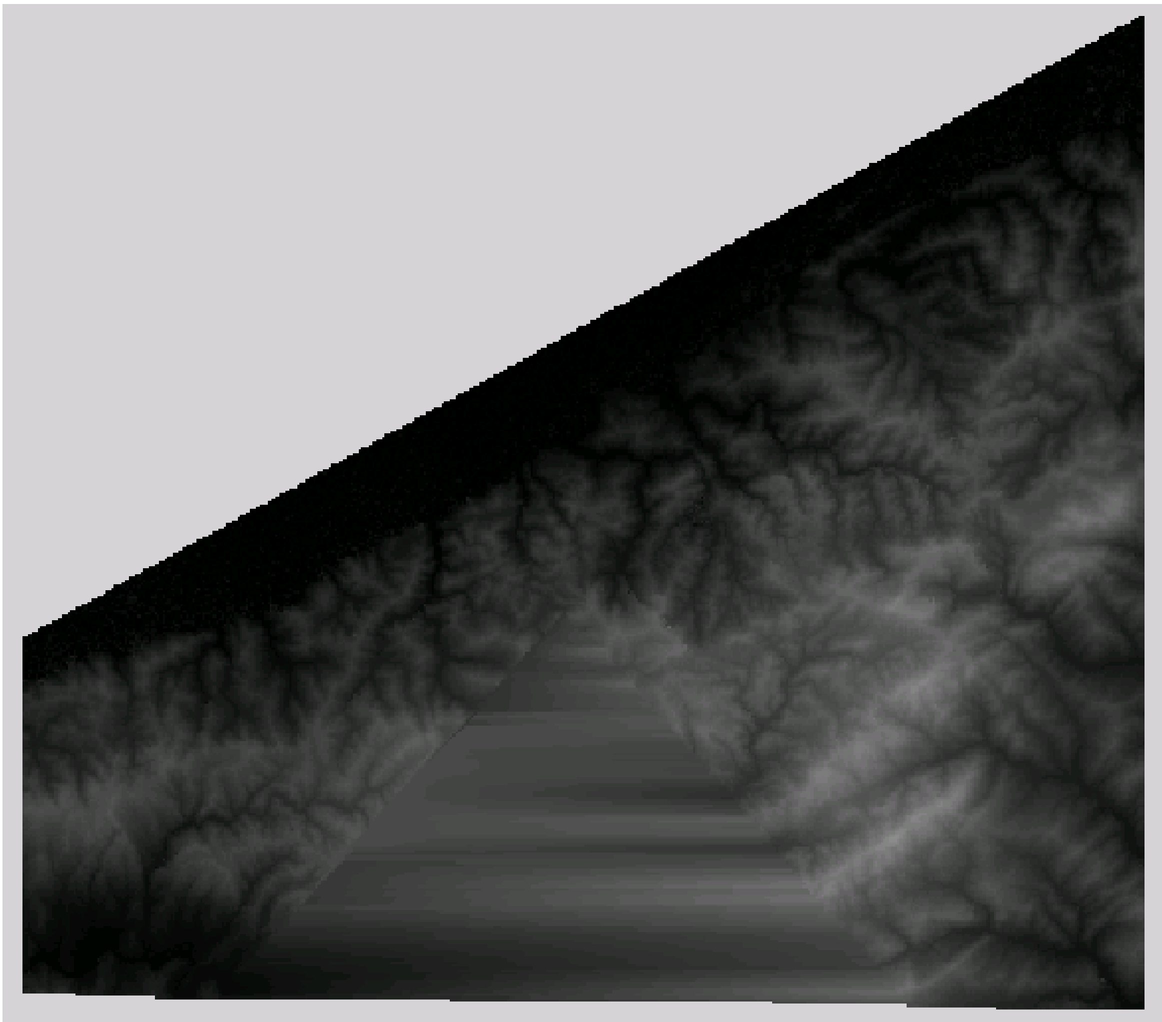

Figure 5.6: Grey value coded SRTM X-band DSM of test field Zonguldak

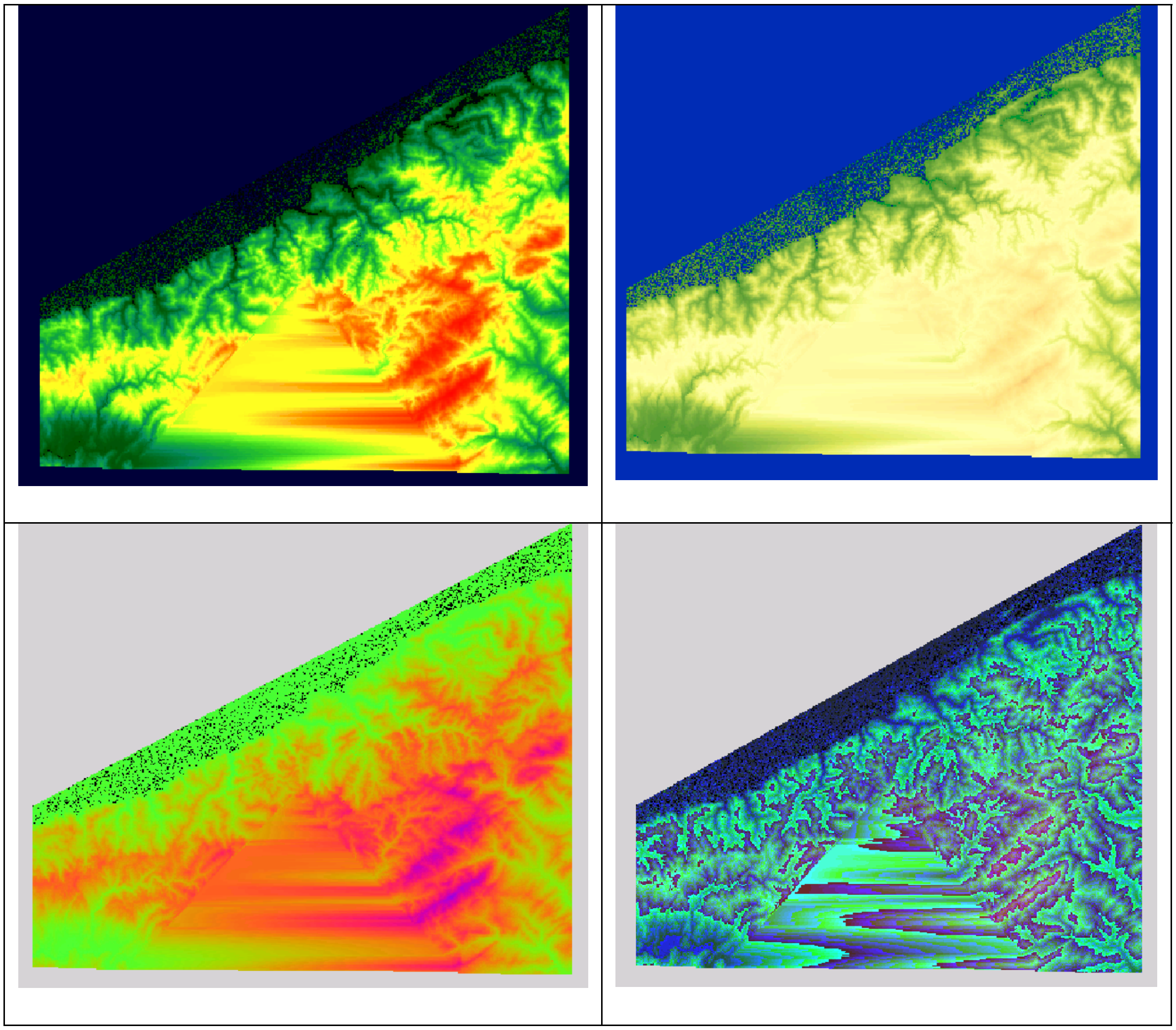

Figure 5.7: SRTM X-band DSM with different colour tables

For SRTM X-band data the estimated height accuracy is available from the DLR as height error map (HEM).

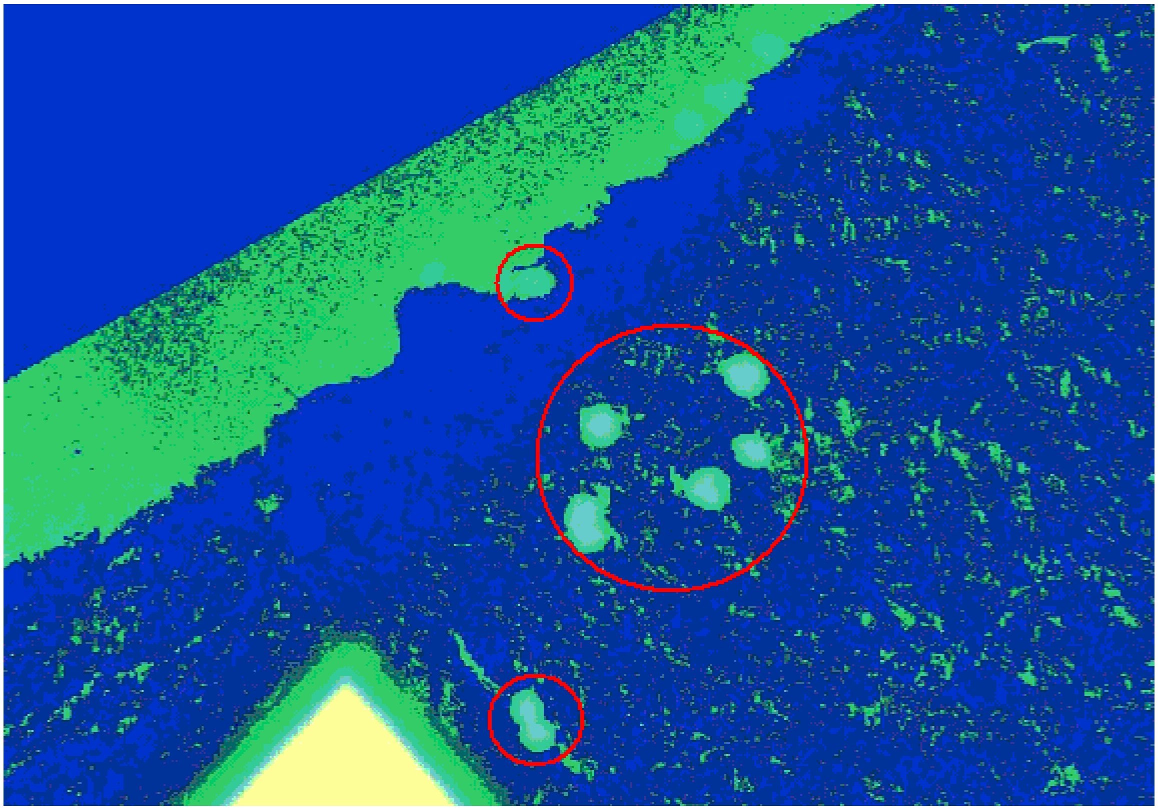

Figure 5.8: SRTM X-band height error map (HEM) (colour coded)

The upper circle is the harbour of Zonguldak. Because of flat water surface there is a mirror effect, so no energy is going back to the antenna causing not accurate height values. Other circles are corresponding to steep areas but the HEM is not so detailed like for example the slope map.

5.6 Other Programs

Program BLTRA was used to transform coordinates from one map projection to another. For example, the SRTM heights models had to be transformed from geographic coordinates to national coordinates. Table 5.2 shows the transformation steps of this process.

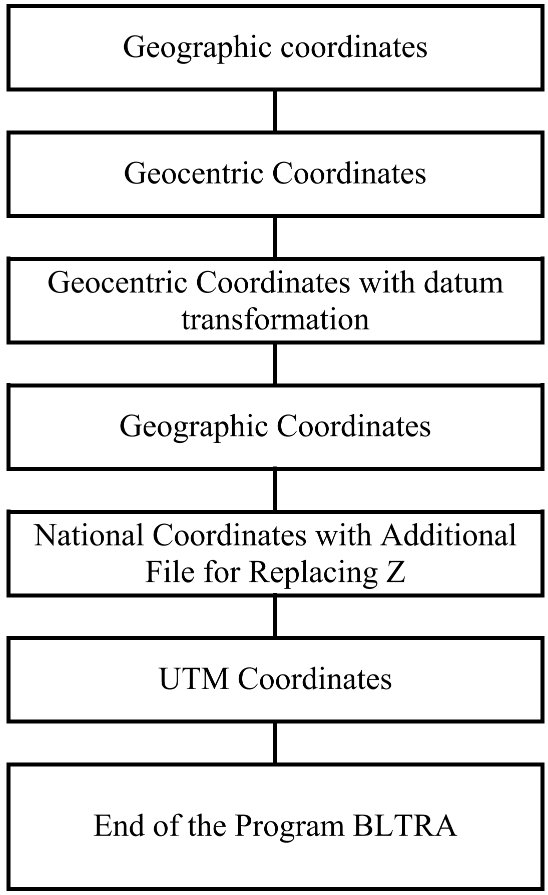

Table 5.2: Used processing steps with BLTRA

In program BLTRA, as additional file for replacing Z the original file, generated by DIGDEM has to be used because the height values don't have to be transformed. Listing of program DIGDEM

```
DATE 31.10.2005   14:56:06

 INPUT  IMAGE    N41E031.hgt
 OUTPUT DEM      N41E031.geo
 SPACING  3 ARC SECONDS

 HGT-FILE   (SRTM  C-BAND)

 END OF DIALOG 14:56:43

 OUTPUT WITHOUT POINTS WITH Z=0.

 AVERAGE HEIGHT:    229.12   MIN:      1.00   MAX:    1630.00
     794440. VALUES  = 55.08 % NOT EQUAL 0.

 END OF PROGRAM DIGDEM 31.10.2005   14:56:51
```

* For this example, additional file for replacing Z is *N41E031.geo*.

5.7 Used Reference DEMs

In this project, two different digital elevation models were used as references for the analysis and they are explained separately below.

5.7.1 Old Reference DEM - from topographic map 1:25000 (DEM25000)

The old reference digital elevation model of the test field Zonguldak was produced from scanned contour lines of 1:25,000 scale topographic maps. It is named in this thesis as DEM25000. It has 40m grid spacing.

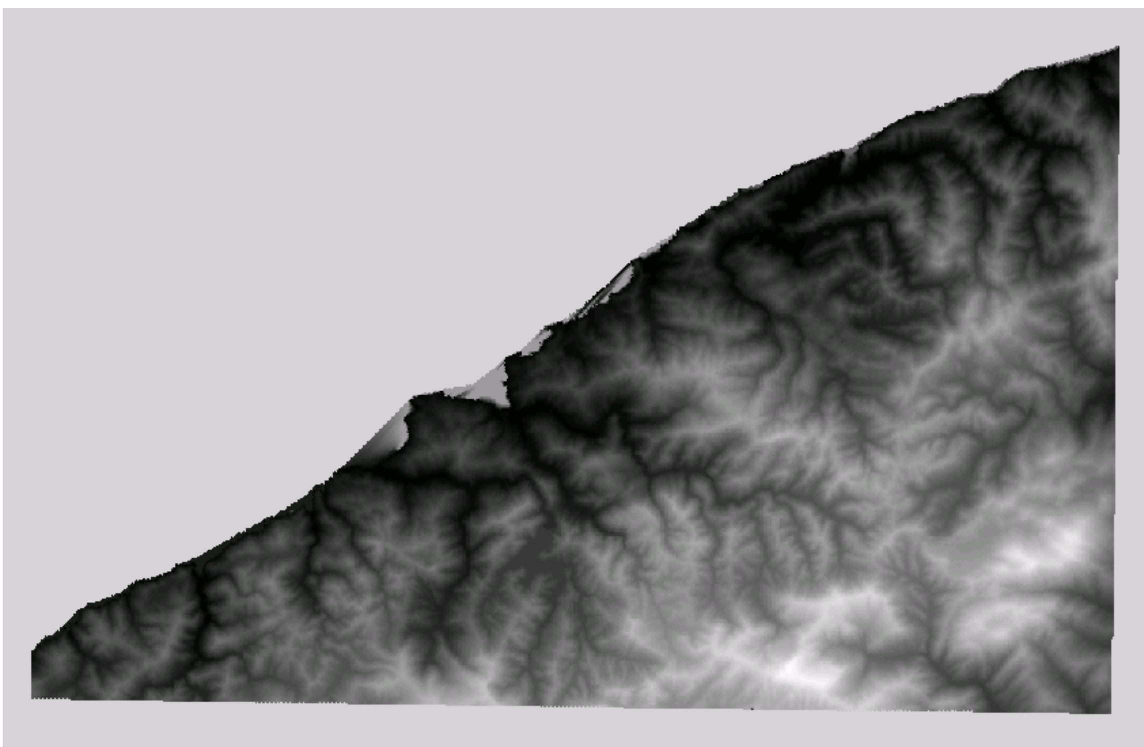

Figure 5.9: DEM25000

5.7.2 New Reference DEM - from large scale photogrammetric mapping (DEM2005)

The new reference digital elevation model of the test field Zonguldak was produced in 2005 based on a photogrammetric flight project of the Zonguldak Municipality. It is named in this thesis as DEM2005. It has 10m grid spacing.

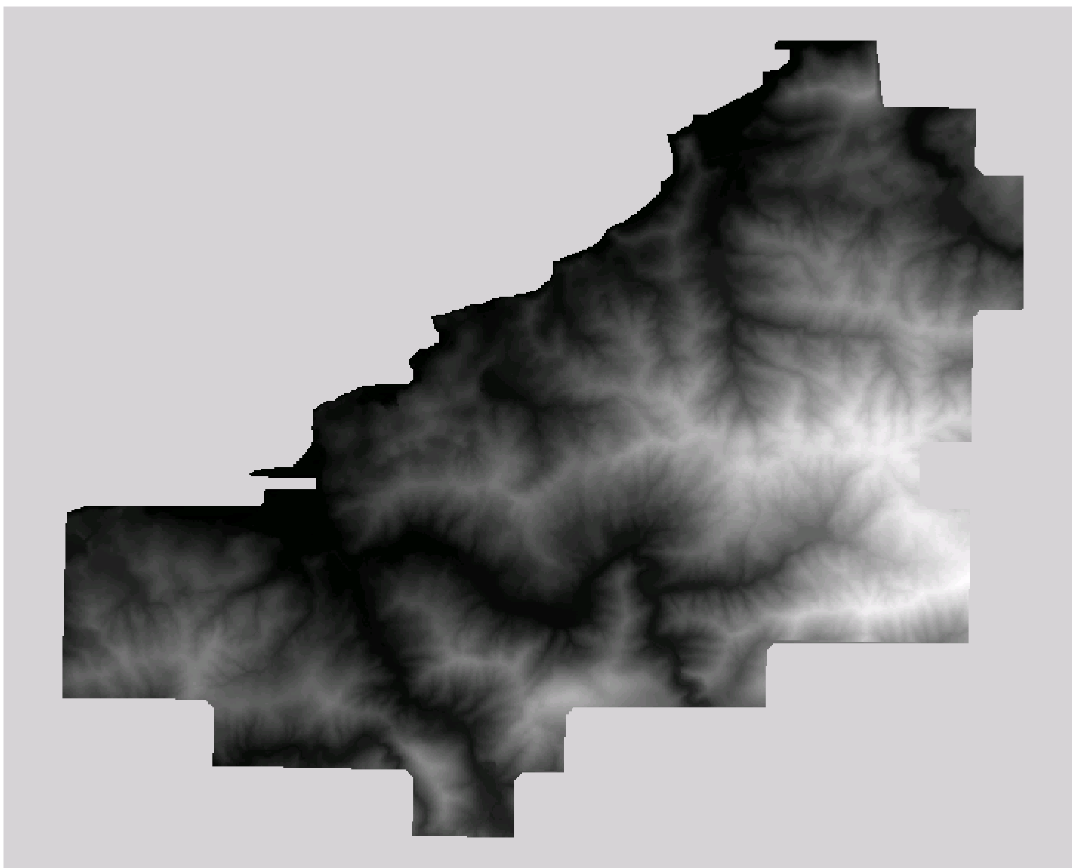

Figure 5.10: DEM2005

6. RESULTS

6.1. Shifting of DEMs

As first step with program DEMSHIFT - developed by K. Jacobsen, Institute of Photogrammetry and Geoinformation, University of Hannover, Germany- the reference DEMs and SRTM C-band and X-band DEMs of test field were shifted separately to the same data base – see table 6.1. *11 iterations* and as *maximal accepted DZ 50.00m* was selected. Because of large shift values the radius of convergence for the shift adjustment was exceeded. By this reason at first an approximate shift like described in 5.3 has been used. At first shift values were approximately 50m and pre-corrected with program MANI. After this the final shift has been adjusted by DEMSHIFT.

Reference DEM	Input DEM	Original RMSZ	Manual shift before start of DEMSHIFT		RMSZ after manua l shift	Shift by DEMSHIFT		RMSZ
			X	Y		X	Y	
DEM 25000	c-band	33.53	0	0	----	-75.66	- 110.51	11.08
DEM 25000	x-band	27.28	0	0	----	50.73	197.07	10.66
DEM 2005	c-band	53.11	130.65	1549.79	6.14	-0.06	-0.21	6.08
DEM 2005	x-band	26.44	-4.427	1852.80	6.71	-3.53	-3.33	6.61

Table 6.1: Shifts of the DEMs after initial shift with MANI

In Table 6.1, it can be seen that after shifting of SRTM C-band and X-band DSMs the height discrepancies against the DEM2005 are smaller than against the DEM25000.

6.2 Analysis of DEMs

The shifted SRTM C-band and X-band height models were checked against the reference height models separately for open and forest areas with program DEMANAL. For DEMANAL the maximal accepted DZ was selected with 50m, the maximal accepted tangent of terrain inclination was selected with 2.00 and as number of iterations 2 were chosen. In the second iteration, shift and vertical scale were respected. These settings were made depending upon the characteristic of the test field.

For the separation of the open and forest areas, a classification layer was used with the grey value 0 for the open areas and 255 for the forest areas.

❖ Analysis of SRTM X-band

- X-band DSM against DEM2005 for open areas (without forest)

Table 6.2 shows the results of SRTM X-band against DEM2005 for open areas area.

reference DEM	X-band		open area
	1st iteration	2nd iteration	
	SZ=A+B*tan(slope)	SZ=A+B*tan(slope)	
DEM2005 open areas	4.55+10.577*tan(slope)	4.01+7.937*tan(slope)	74.76%

Table 6.2 SRTM X-band DSM against DEM2005 for open areas

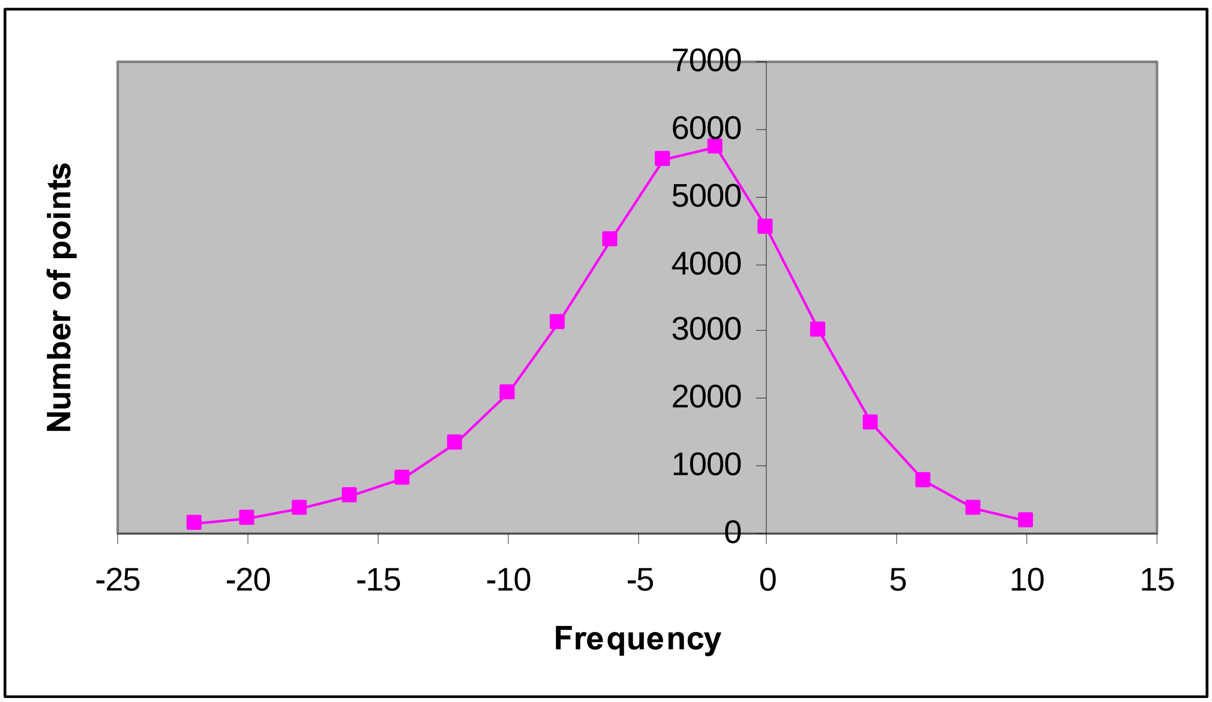

Figure 6.1: Frequency distribution of DZ in the first iteration of DEMANAL SRTM X-band against DEM2005 for open areas

Figure 6.2: X-band DSM against DEM 2005 for open areas
Light grey: open areas, dark grey: forest, black: no data, white spots: excluded points

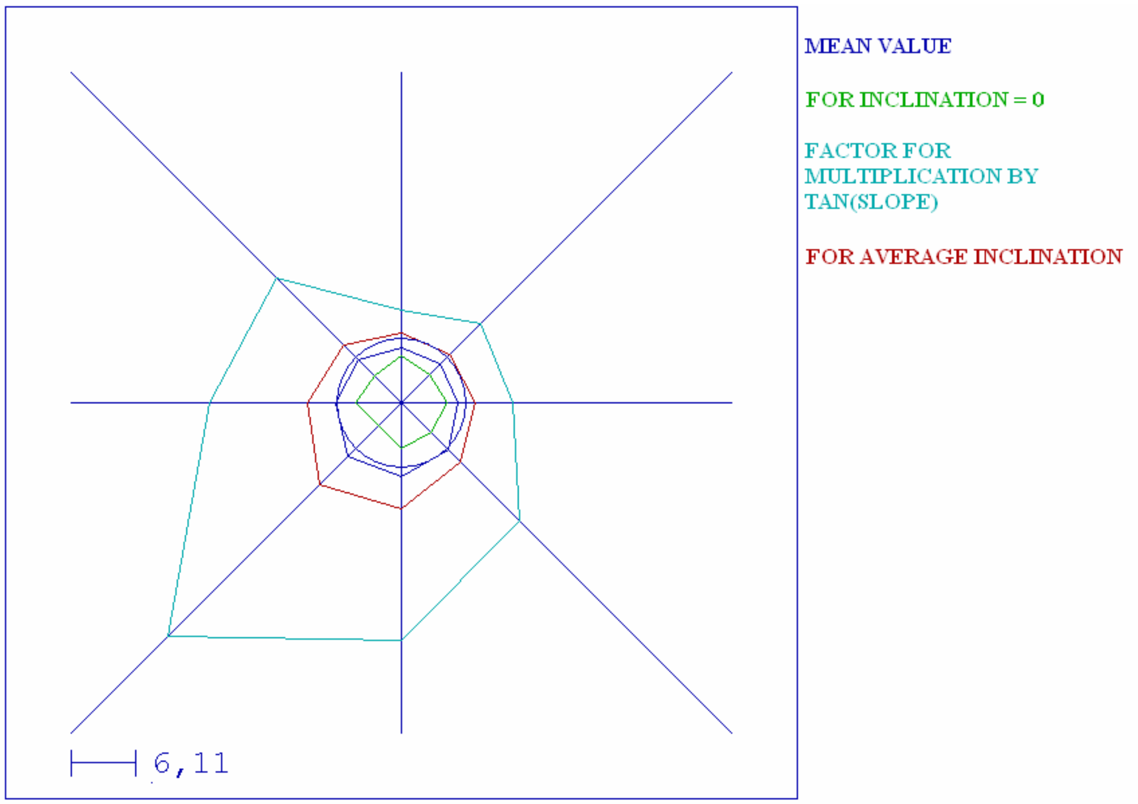

Figure 6.3: RMSE of X-band DSM against DEM 2005 for open areas as a function of the terrain inclination direction (aspects)

- X-band DSM against DEM2005 for forest areas

reference DEM	X-band		Forest areas
	1^{st}.iteration	2^{nd}.iteration	
	SZ=A+B*tan(slope)	SZ=A+B*tan(slope)	
DEM2005 forest	5.73+13.050*tan(slope)	4.47+10.775*tan(slope)	25.24%

Table 6.3: SRTM X-band DSM against DEM2005 in forest areas

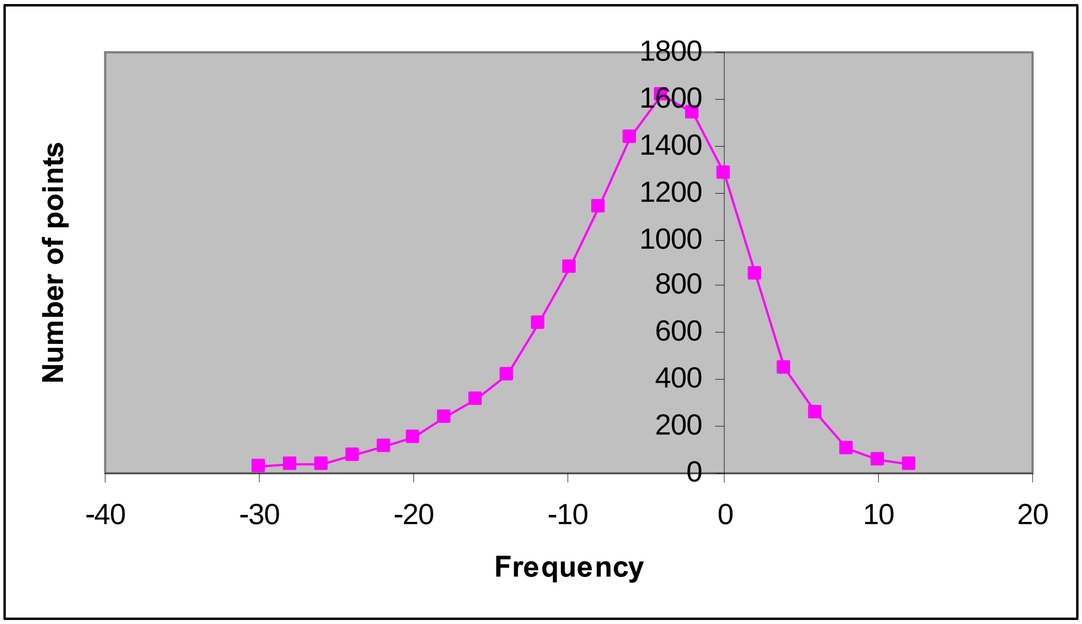

Figure 6.4: Frequency distribution of DZ in the first iteration of DEMANAL SRTM X-band against DEM2005 for forest areas

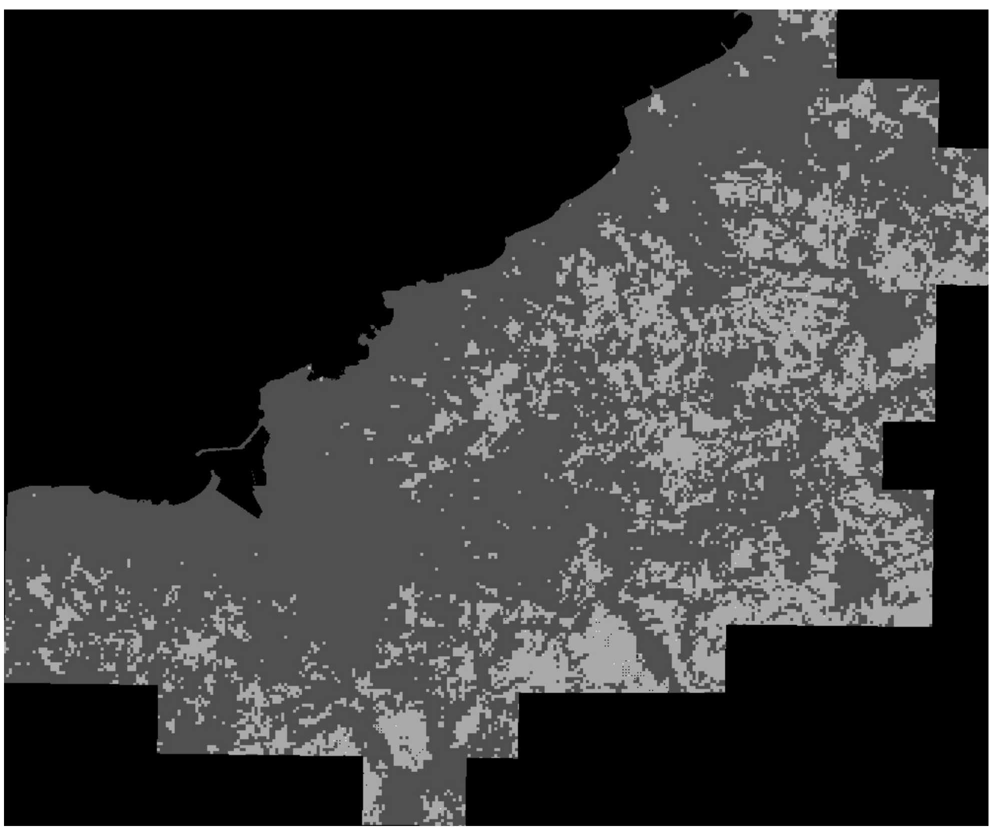

Figure 6.5: X-band DSM against DEM 2005 for forest areas
Light grey: forest, dark grey: open areas, black: no data, white spots: excluded points

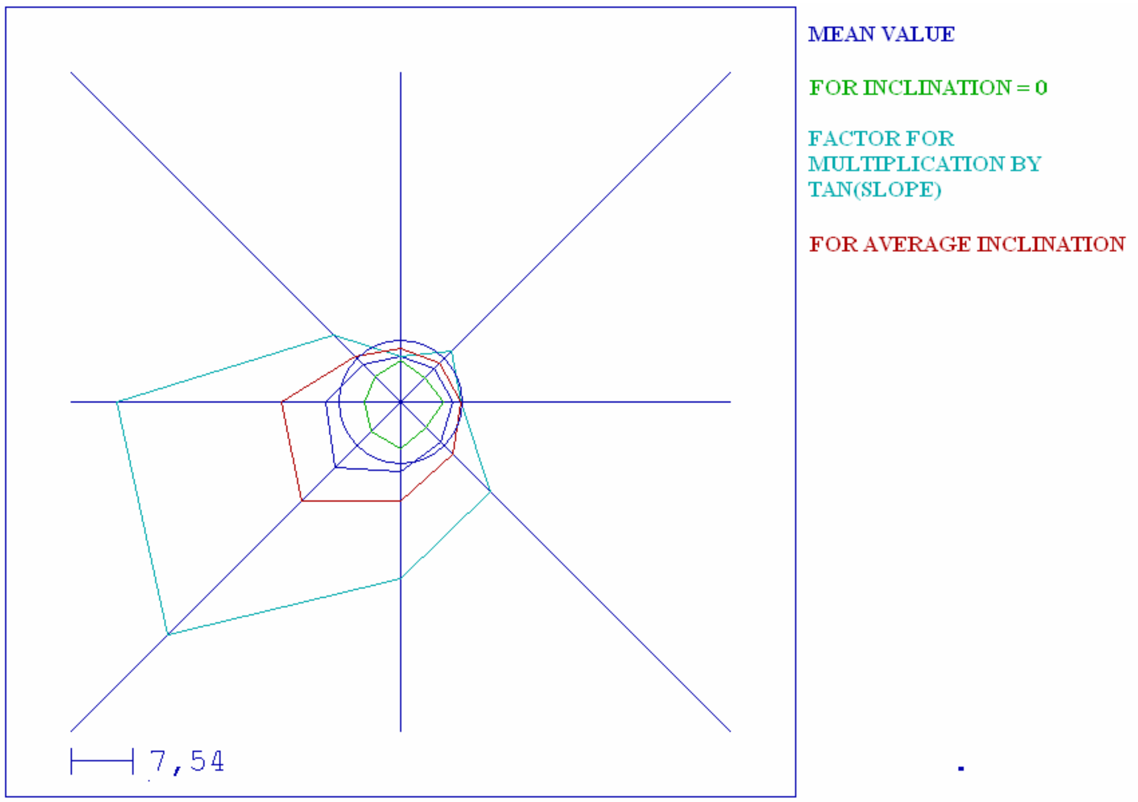

Figure 6.6: RMSE of X-band DSM against DEM 2005 for forest areas as a function of the terrain inclination direction

- SRTM X-band DSM against DEM25000 for open areas

reference DEM	X-band		open areas
	1st iteration	2nd iteration	
	SZ=A+B*tan(slope)	SZ=A+B*tan(slope)	
DEM25000 open areas	10.35+8.974*tan(slope)	9.74+8.014*tan(slope)	55.63%

Table 6.4: SRTM X-band DSM against DEM25000 for open areas

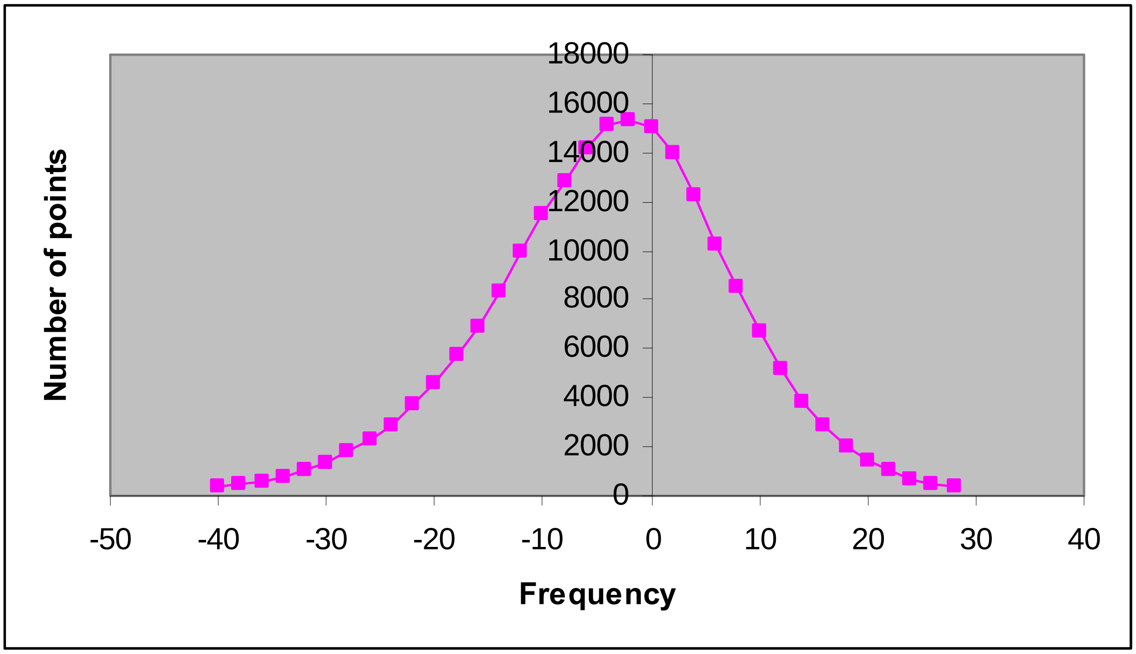

Figure 6.7: Frequency distribution of DZ in the first iteration of DEMANAL
SRTM X-band against DEM25000 for open areas

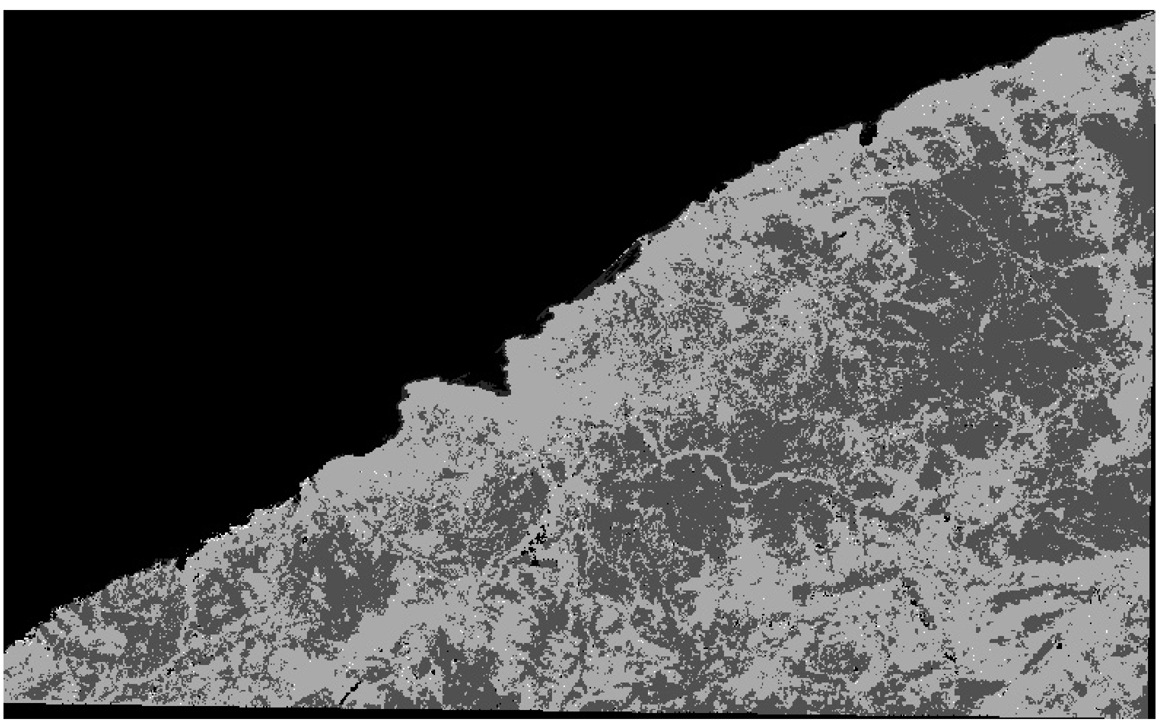

Figure 6.8: X-band DSM against DEM25000 for open areas
Light grey: open areas, dark grey: forest, black: no data, white spots: excluded points

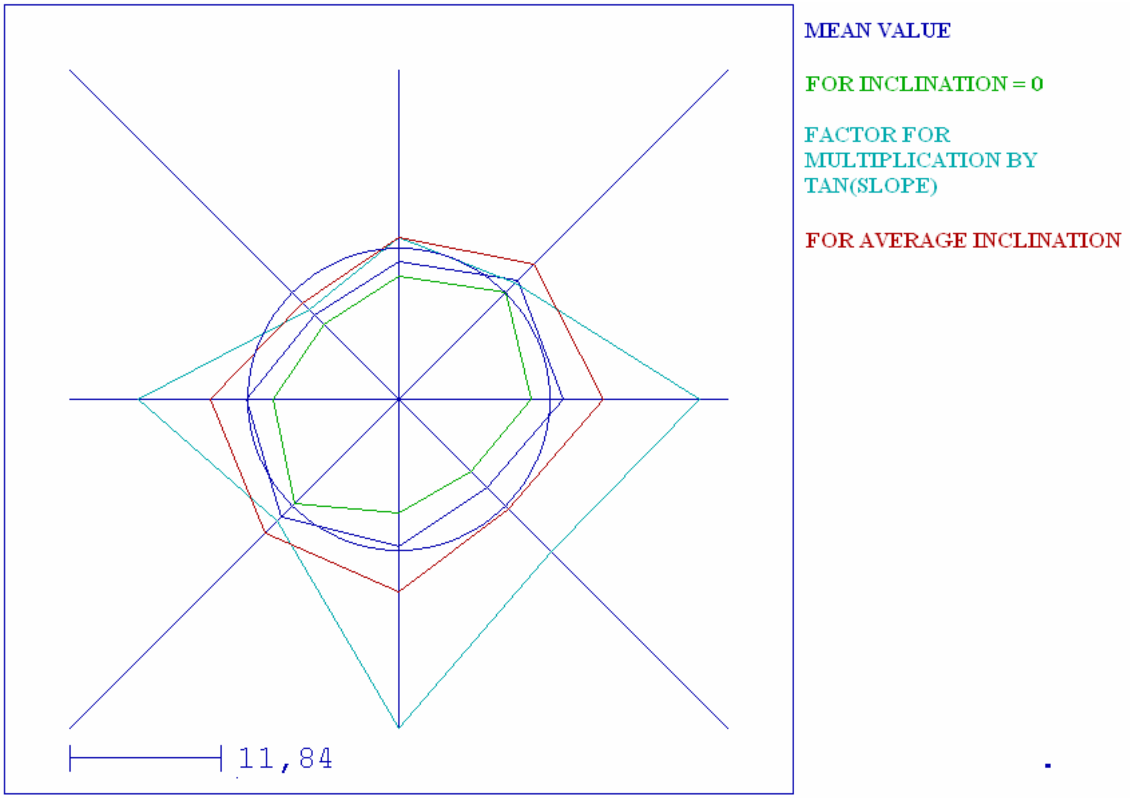

Figure 6.9: RMSE of X-band DSM against DEM25000 for open areas as a function of the terrain inclination direction

- SRTM X-band DSM against DEM25000 for forest areas

reference DEM	X-band		forest area
	1st.iteration	2nd.iteration	
	SZ=A+B*tan(slope)	SZ=A+B*tan(slope)	
DEM25000 forest	13.30+8.888*tan(slope)	11.19+8.191*tan(slope)	44.37%

Table 6.5: SRTM X-band DSM against DEM25000 for forest areas

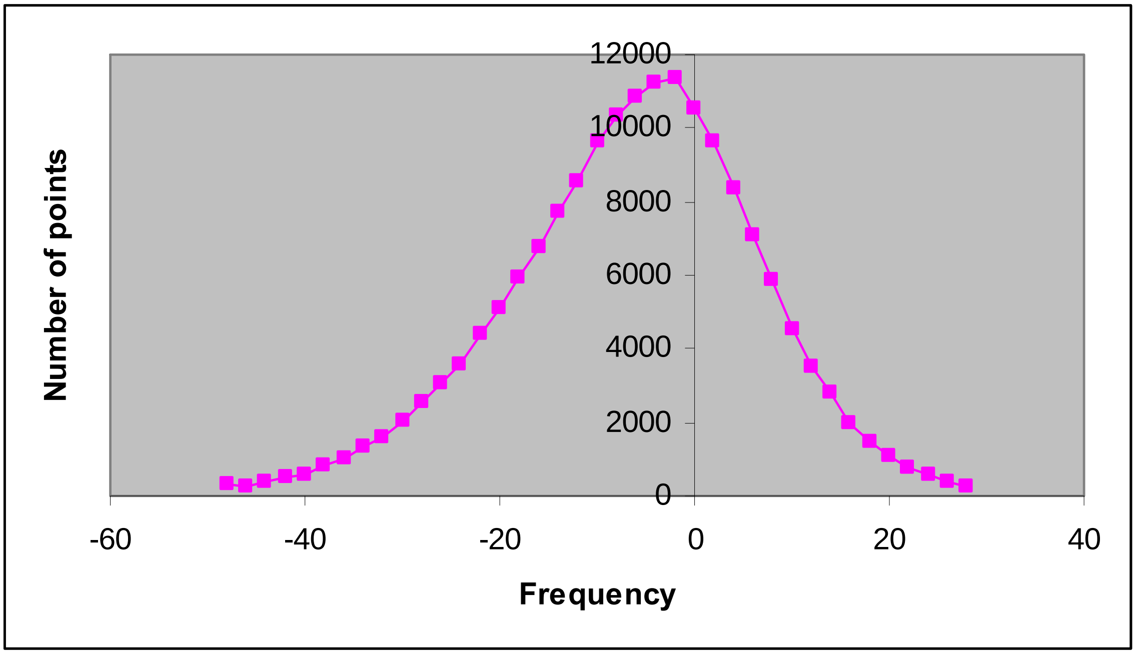

Figure 6.10: Frequency distribution of DZ in the first iteration of DEMANAL SRTM X-band against DEM25000 for forest areas

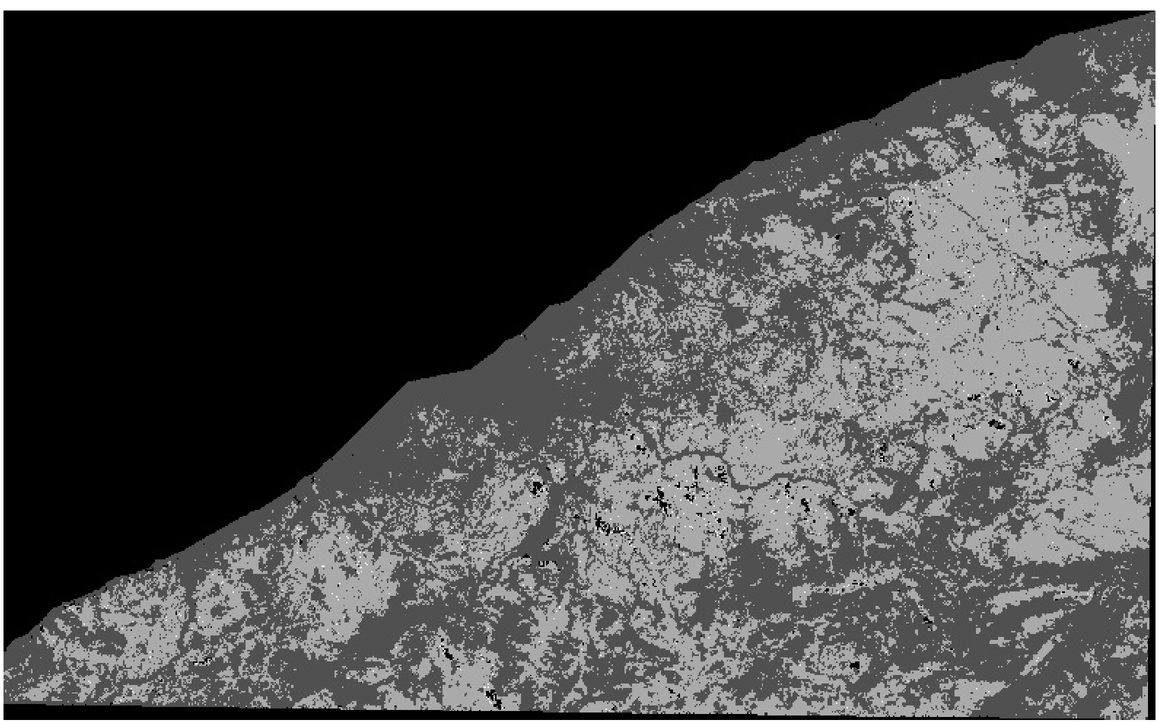

Figure 6.11: X-band DSM against DEM25000 for forest areas
Light grey: forest, dark grey: open area, black: no data, white spots: excluded points

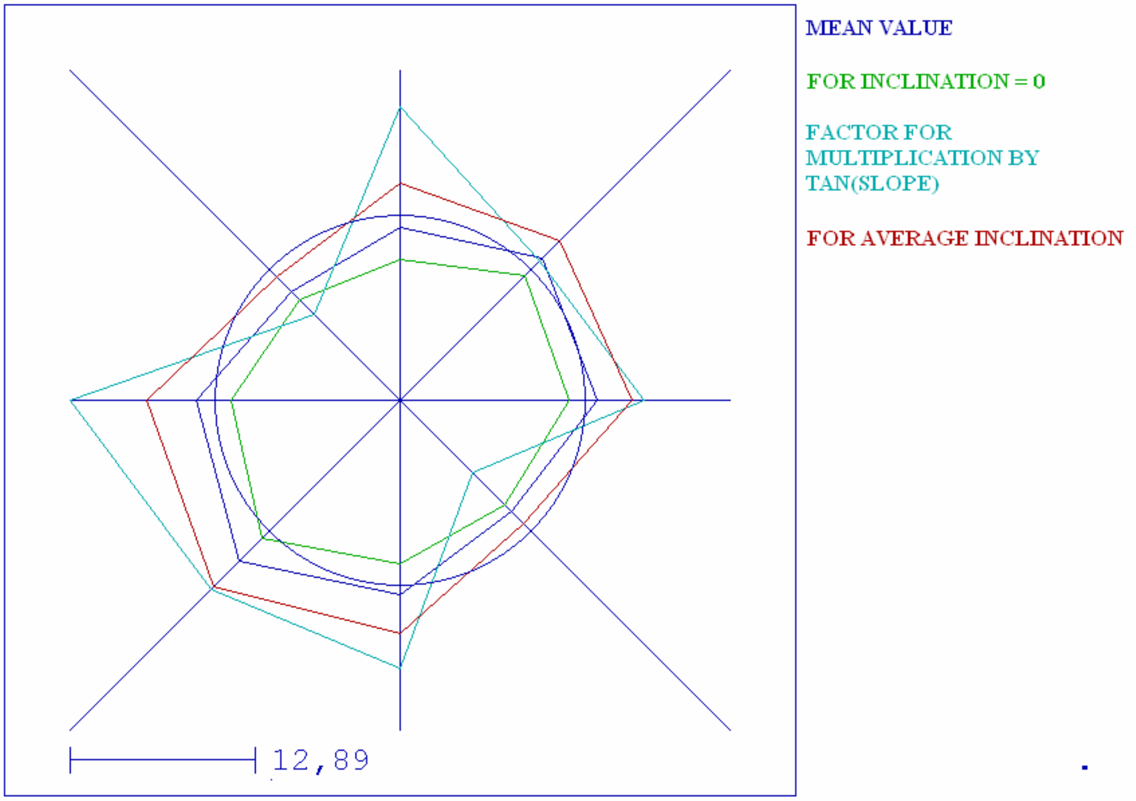

Figure 6.12: RMSE of X-band DSM against DEM25000 for forest areas as a function of the terrain inclination direction

❖ Analysis of SRTM C-band

- SRTM C-band DSM against DEM2005 for open areas

reference DEM	C-band		open area
	1st iteration	2nd iteration	
	SZ=A+B*tan(slope)	SZ=A+B*tan(slope)	
DEM 2005 open area	5.92+5.725*tan(slope)	4.35+6.698*tan(slope)	77.02%

Table 6.6: SRTM C-band DSM against DEM2005 for open areas

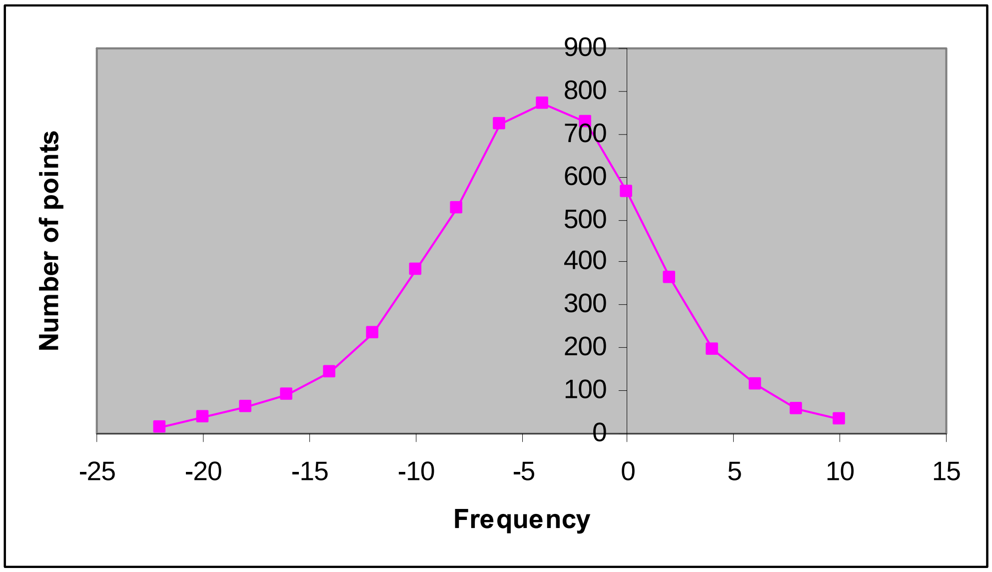

Figure 6.13: Frequency distribution of DZ in the first iteration of DEMANAL SRTM C-band against DEM2005 for open areas

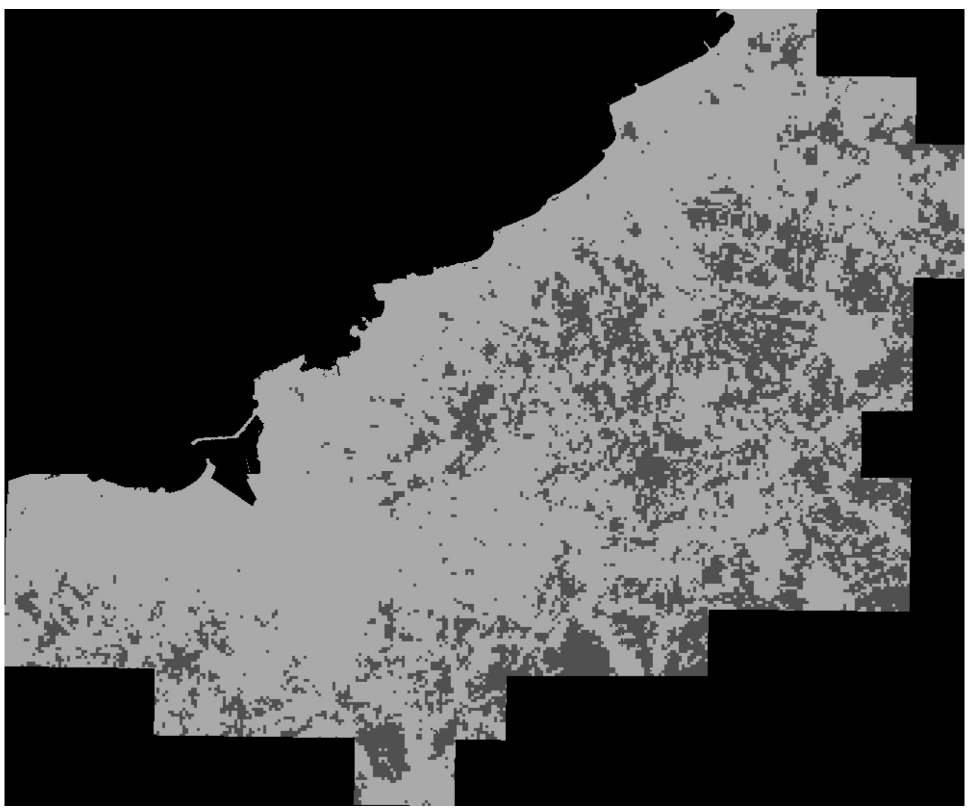

Figure 6.14: C-band DSM against DEM 2005 for open areas
Light grey: open areas, dark grey: forest, black: no data, white spots: excluded points

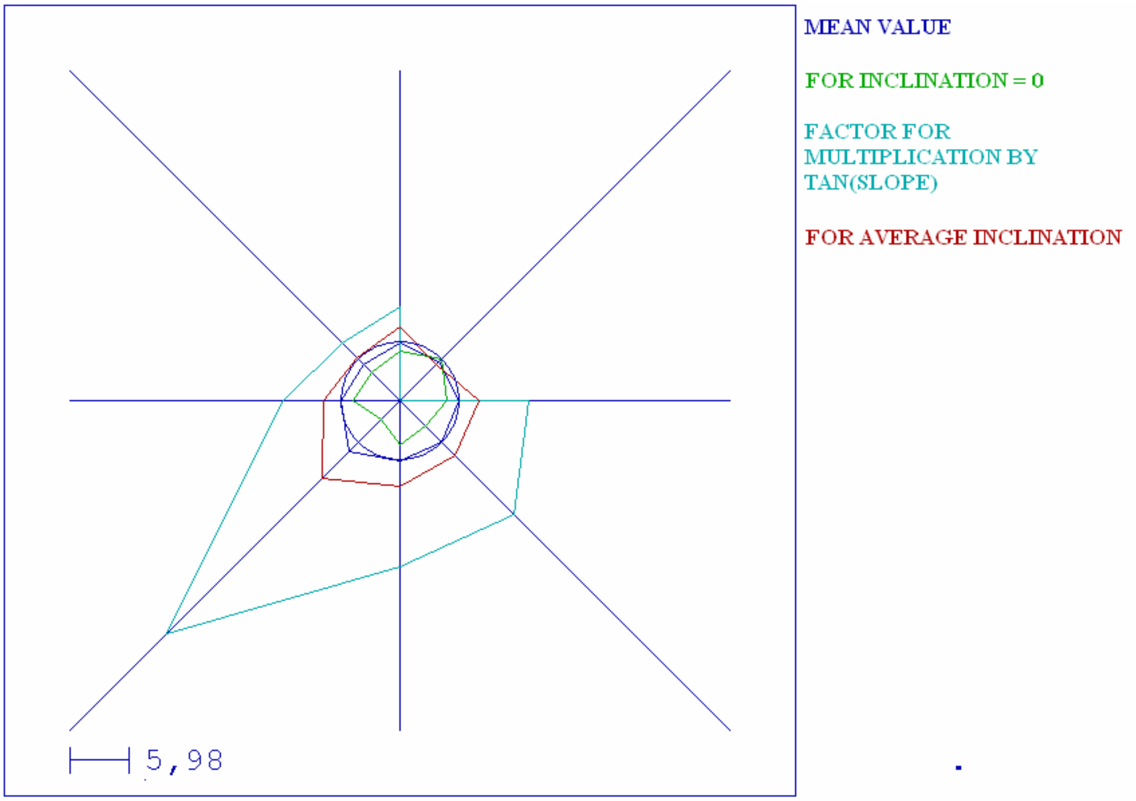

Figure 6.15: RMSE of C-band DSM against DEM2005 for open areas as a function of the terrain inclination direction

- SRTM C-band DSM against DEM2005 for forest areas

reference DEM	X-band		forest areas
	1stiteration	2nditeration	
	SZ=A+B*tan(slope)	SZ=A+B*tan(slope)	
DEM2005 forest	6.32+6.512*tan(slope)	5.74+2.621*tan(slope)	22.98%

Table 6.7: SRTM C-band DSM against DEM2005 for forest areas

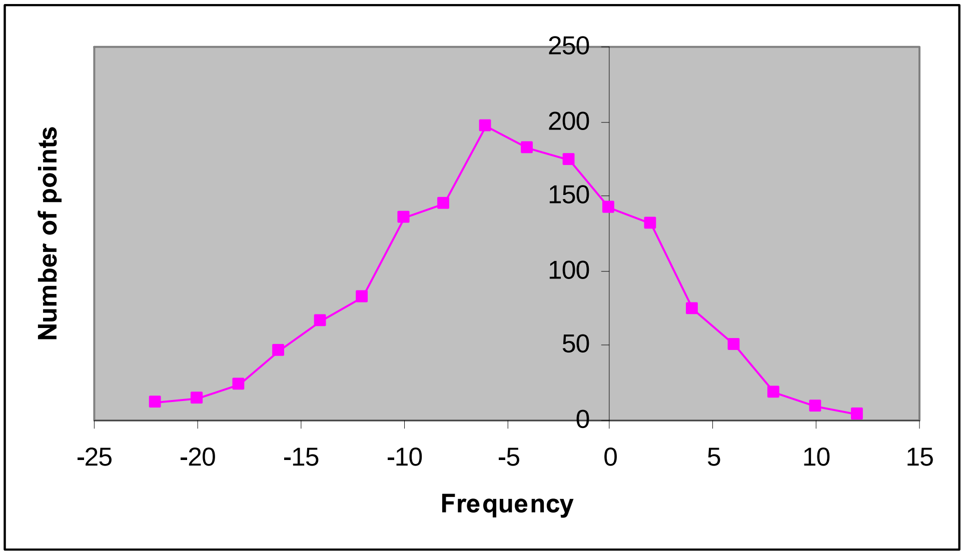

Figure 6.16: Frequency distribution of DZ in the first iteration of DEMANAL SRTM C-band against DEM2005 for forest areas

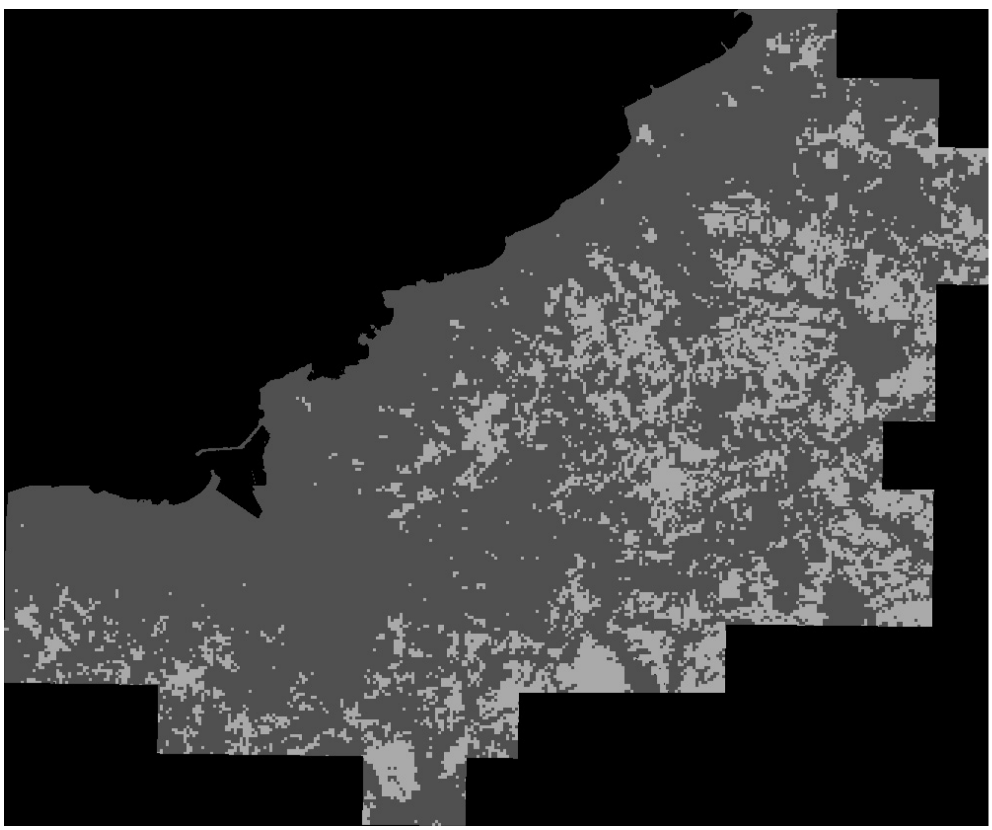

Figure 6.17: C-band DSM against DEM2005 for forest areas
Light grey: forest, dark grey: open areas, black: no data, white spots: excluded points

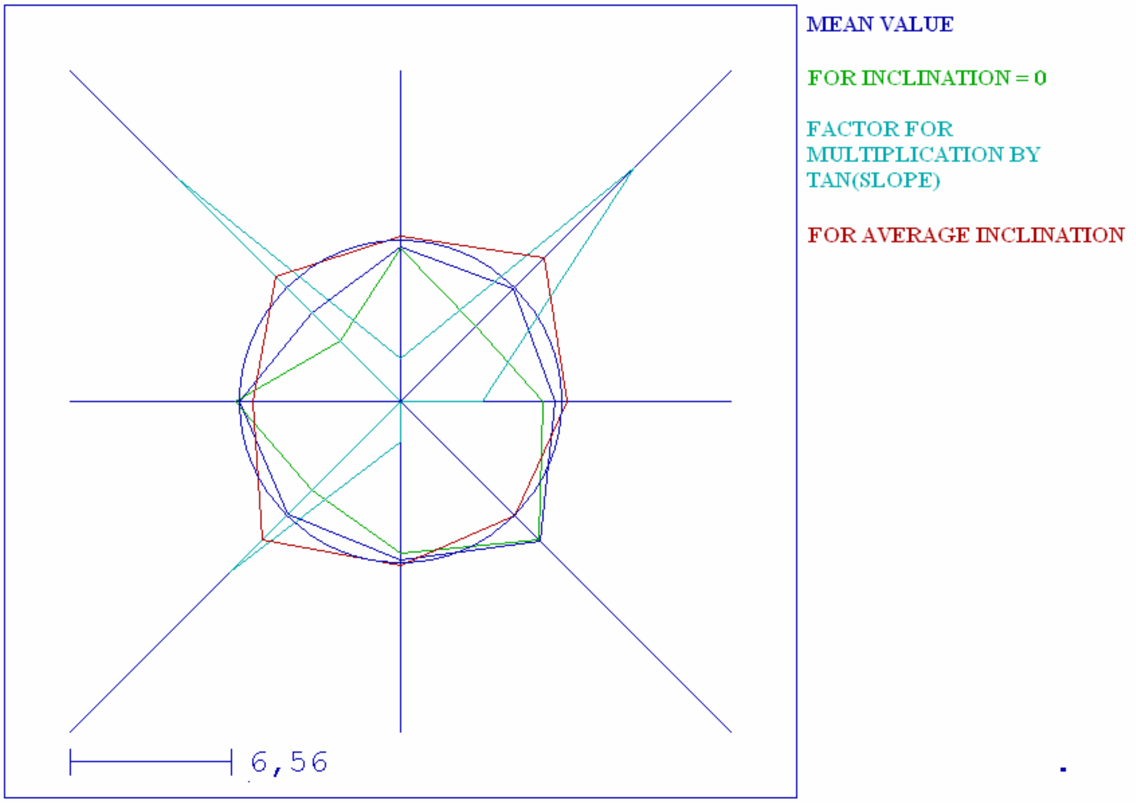

Figure 6.18: RMSE of SRTM C-band DSM against DEM2005 for forest areas as a function of the terrain inclination direction

- SRTM C-band DSM against DEM25000 for open areas

reference DEM	X-band		open area
	1st iteration	2nd iteration	
	SZ=A+B*tan(slope)	SZ=A+B*tan(slope)	
DEM25000 open areas	8.43+5.968*tan(slope)	7.81+5.906*tan(slope)	56.67%

Table 6.8: C-band DSM against DEM25000 for open areas

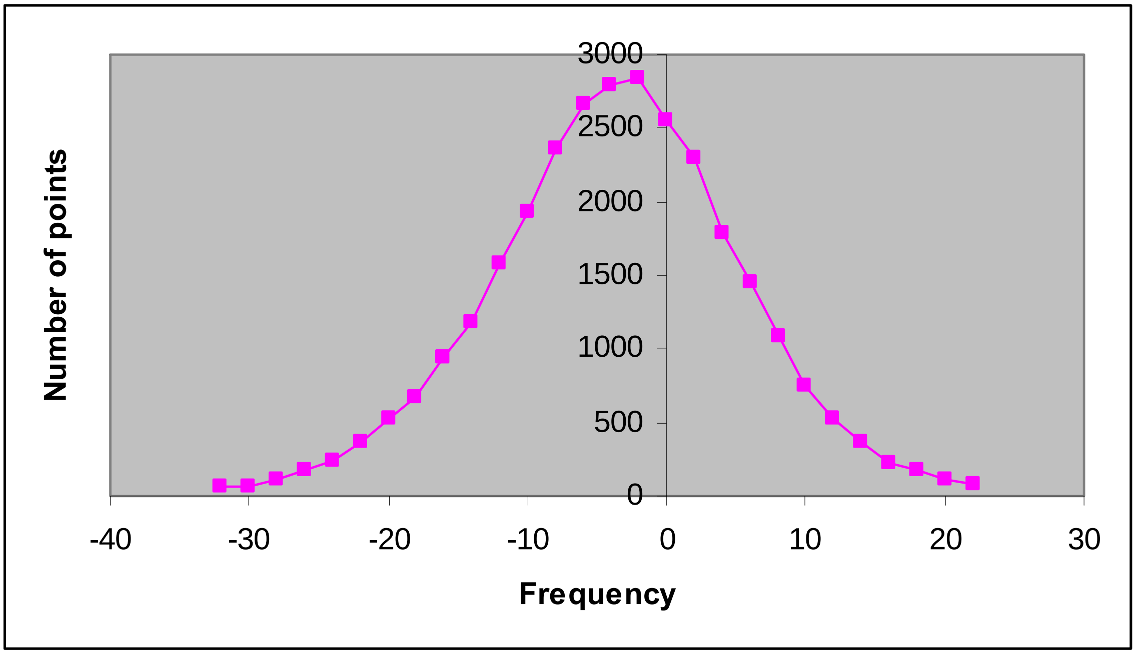

Figure 6.19: Frequency distribution of DZ in the first iteration of DEMANAL
SRTM C-band against DEM25000 for open areas

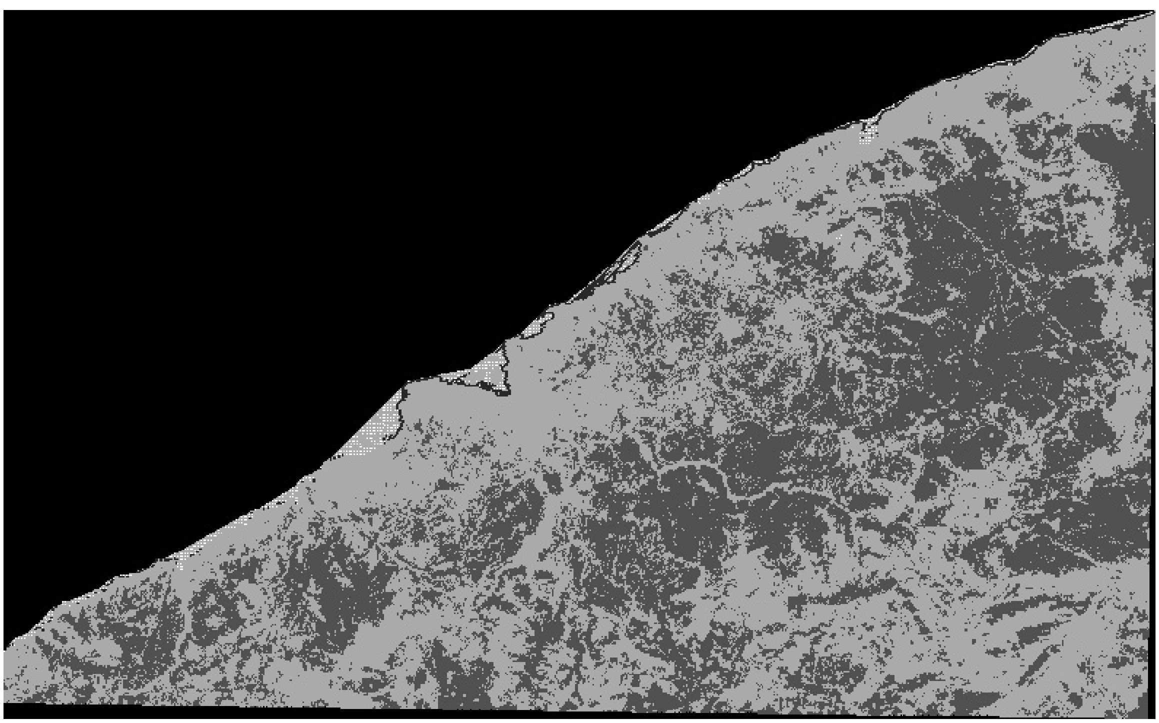

Figure 6.20: C-band DSM against DEM25000 for open areas
Light grey: open areas, dark grey: forest, black: no data, white spots: excluded points

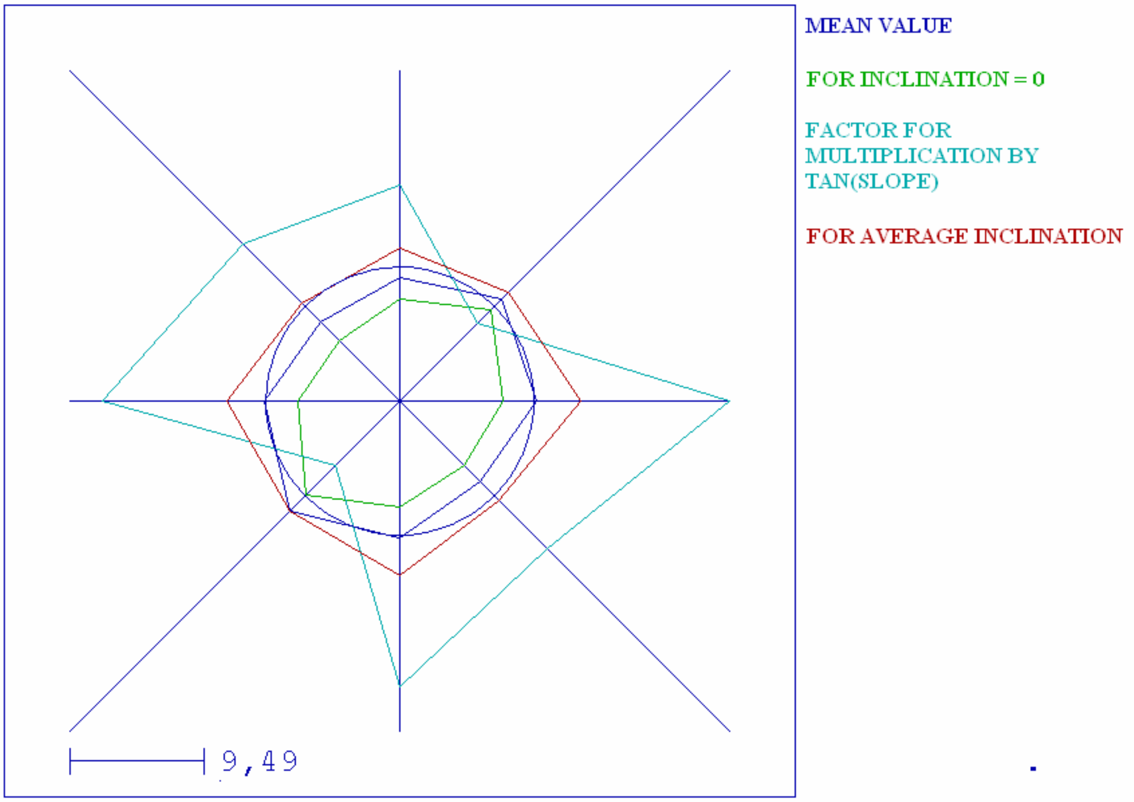

Figure 6.21: RMSE of C-band DSM against DEM25000 for open areas as a function of the terrain inclination direction

- SRTM C-band DSM against DEM25000 for forest areas

reference DEM	X-band		forest areas
	1st iteration	2nd iteration	
	SZ=A+B*tan(slope)	SZ=A+B*tan(slope)	
DEM25000 forest	10.65+7.117*tan(slope)	8.82+6.070*tan(slope)	43.33%

Table 6.9: SRTM C-band DSM against DEM25000 for forest areas

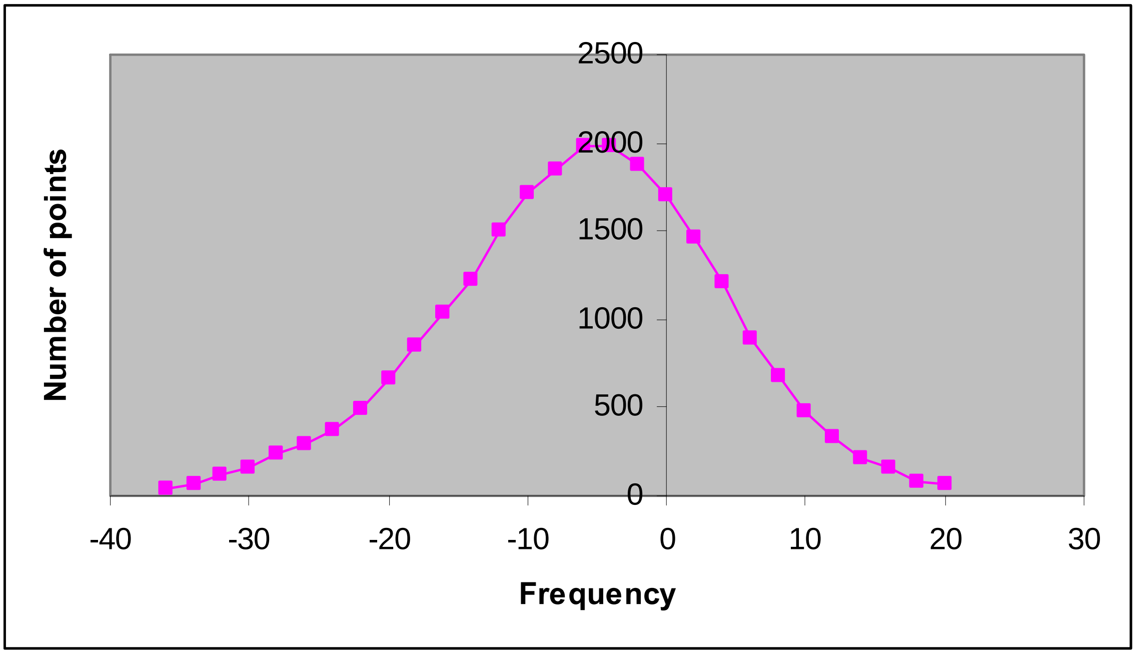

Figure 6.22: Frequency distribution of DZ in the first iteration of DEMANAL
SRTM C-band against DEM25000 for forest areas

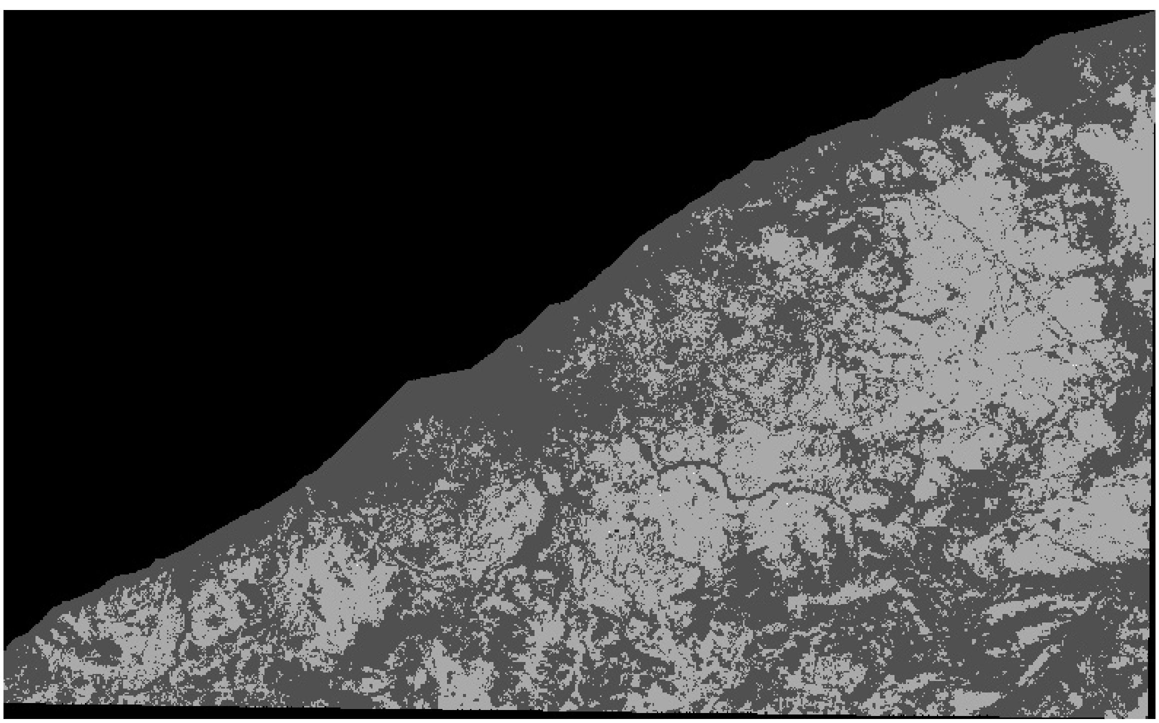

Figure 6.23: C-band DSM against DEM25000 for forest areas
Light grey: forest, dark grey: open area, black: no data, white spots: excluded points

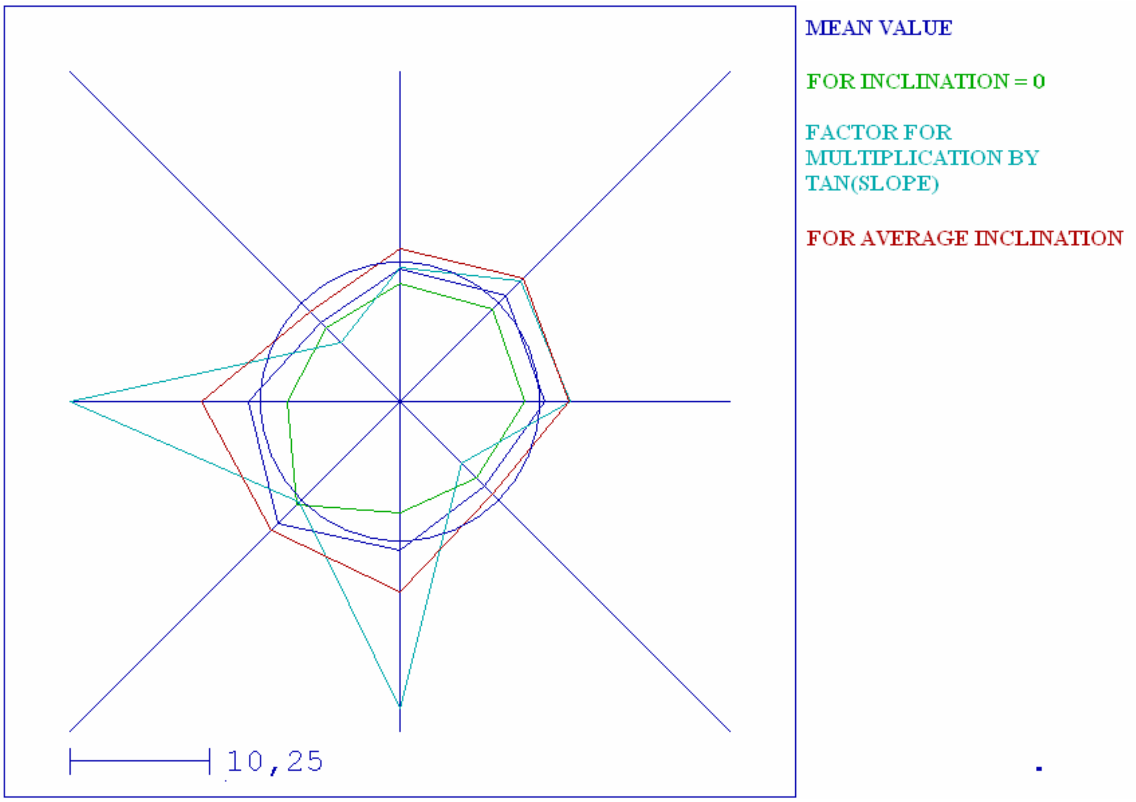

Figure 6.24: RMSE of C-band DSM against DEM25000 for forest areas as a function of the terrain inclination direction

reference DEM	X-band		C-band	
	1st iteration	2nd iteration	1st iteration	2nd iteration
	SZ=A+B* tan(α)	SZ=A+B* tan(α)	SZ=A+B* tan(α)	SZ=A+B* tan(α)
DEM2005 open area	4.55+10.577*tan(α) 74.76%	4.01+7.937* tan(α) 74.76%	5.92+5.725* tan(α) 77.02%	4.35+6.698* tan(α) 77.02%
DEM2005 forest	5.73+13.050* tan(α) 25.24%	4.47+10.775* tan(α) 25.24%	6.32+6.512* tan(α) 22.98%	5.74+2.621* tan(α) 22.98%
DEM25000 open area	10.35+8.974* tan(α) 55.63%	9.74+8.014* tan(α) 55.63%	8.43+5.968* tan(α) 56.67%	7.81+5.906* tan(α) 56.67%
DEM25000 forest	13.30+8.888* tan(α) 44.37%	11.19+8.191* tan(α) 44.37%	10.65+7.117* tan(α) 43.33%	8.82+6.070* tan(α) 43.33%

Table 6.10: Results of analysis with program DEMANAL for SRTM X-band and C-band DSMs (SZ) α = slope

Compared DEM	X-band			C-band		
	1st iteration			1st iteration		
	RMSZ	bias	without bias	RMSZ	bias	without bias
DEM2005 open area	7.35	-3.99	6.18	7.43	-4.44	5.96
DEM2005 forest	9.33	-5.43	7.58	8.21	-4.88	6.60
DEM25000 open area	12.62	-3.82	12.03	10.18	-3.56	9.53
DEM25000 forest	14.53	-6.30	13.09	11.98	-6.20	10.25

Table 6.11: Results of analysis with program DEMANAL for SRTM X-band and C-band DSMs (RMSZ, bias)

As summary of table 6.10 and 6.11, we see followings:

- SRTM X-band height model for open and flat area has 4.0m up to 4.5m root mean square differences against the DEM2005; this is better than for the SRTM C-band DSM with 4.3m up to 5.9m. Also in forest areas the X-band results are better than the C-band results.
- Factors for multiplication by tan(slope) values are smaller on the SRTM C-band DSM because of average of different view directions.
- The root mean square discrepancies against the DEM25000 are quite larger, indicating accuracy of the DEM25000 in the range of 6m-8m, including also the

effect of the interpolation over 40m spacing for the DEM25000 against 10m spacing for the DEM2005. The spacing effect on the bilinear interpolation can be seen at the results of program ZANAL (see table 6.16 and 6.17)

6.3 Analysis of SRTM X-band separately for 3 sub-areas

The accuracy assessment of SRTM X-band DSM has been made also separately for three sub-areas, separated with the window function of program BLCON belonging to program system BLUH. The sub-area 1 (figure 6.25) has been taken by the SRTM from the descending orbit, sub-area 2 from the ascending orbit and sub-area 2 from ascending and descending orbit. That means the sub-area 3 is based on the mean results of 2 observations, indicating a higher accuracy shown also by the height error map – an estimation of the height accuracy – belonging to the SRTM-X-band data set (see figure 5.8). The three parts of SRTM X-band DSM are shown in figure 6.25.

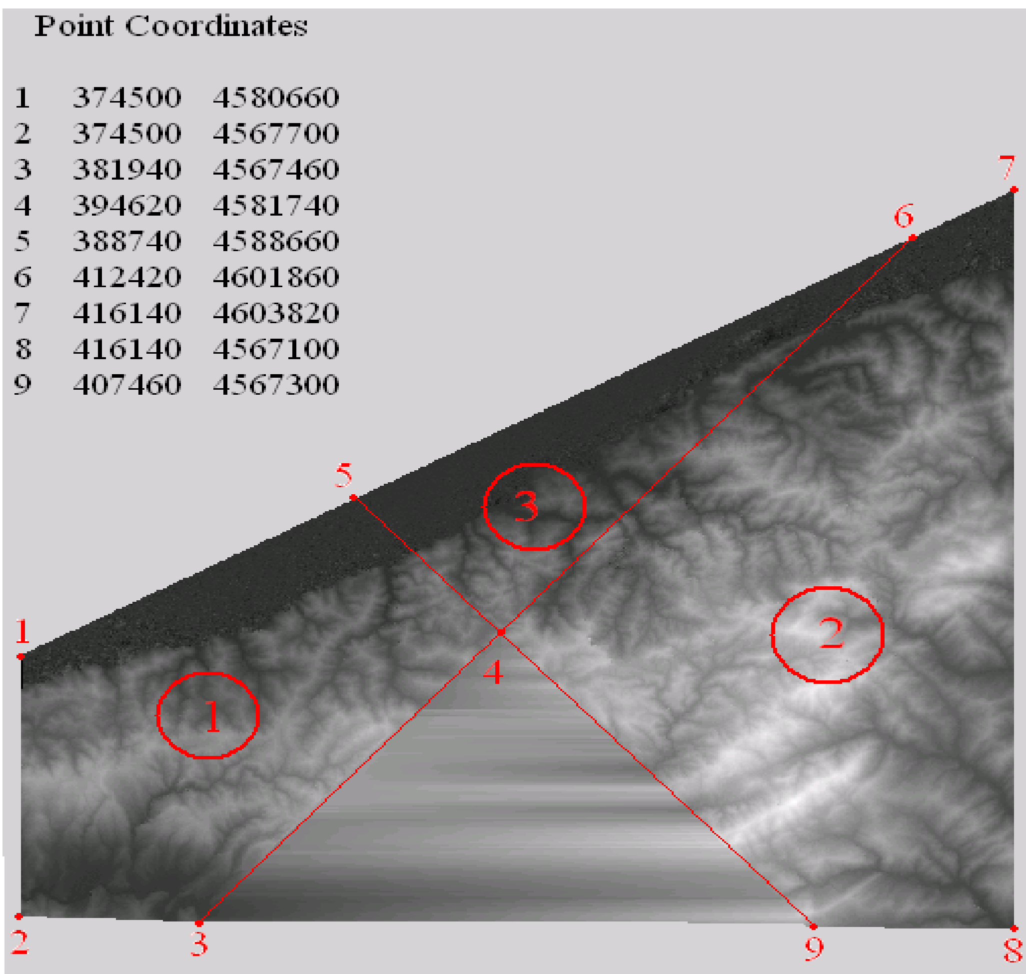

Figure 6.25: Sub-areas of SRTM X-band DSM

The SRTM X-band DSM has been divided into 3 sub-DSMs except no-data part seen as a smooth triangle area without any detail in lower part of figure 6.25. The limits of these 3 sub-areas are shown below:

- Sub-area 1

Sub-area 1 is limited by points 1, 2, 3, 4, 5

1	374500	4580660
2	374500	4567700
3	381940	4567460
4	394620	4581740
5	388740	4588660

- sub-area 2

Sub-area 2 is limited by points 4, 6, 7, 8, 9

4	394620	4581740
6	412420	4601860
7	416140	4603820
8	416140	4567100
9	407460	4567300

- sub-area 3

Sub-area 3 is limited by points 4, 5, 6

4	394620	4581740
5	388740	4588660
6	412420	4601860

In the third sub-area the estimated height accuracies in the Height Error Map are dominating approximately 4.8m. Only in small areas, represented with green points, it is reaching 8.8m (see figure 5.8).

Reference DEM	X-band		
	sub-area 1	sub-area 2	sub-area 3
	SZ=A+B*tan(slope)	SZ=A+B* tan(slope)	SZ=A+B* tan(slope)
DEM2005 open area	------	5.41+12.318* tan(slope) 4.98+9.295* tan(slope)	4.70+6.918* tan(slope) 4.05+6.040* tan(slope)
DEM2005 forest	------	7.29+14.710* tan(slope) 5.47+13.060* tan(slope)	5.63+8.909* tan(slope) 5.08+6.530* tan(slope)
DEM25000 open area	7.37+15.769* tan(slope) 7.13+16.003* tan(slope)	10.49+8.784* tan(slope) 9.75+7.827* tan(slope)	7.93+10.725* tan(slope) 7.48+9.201* tan(slope)
DEM25000 forest	9.16+11.318* tan(slope) 9.09+10.683* tan(slope)	12.89+10.230* tan(slope) 10.39+9.589* tan(slope)	11.63+7.941* tan(slope) 10.60+7.417* tan(slope)

Table 6.12: Results of the separate analysis of the sub-areas - SRTM X-band DSM
Upper line: 1st iteration, lower line: 2nd iteration of program DEMANAL

Reference DEM	X-band					
	1st iteration					
	sub-area 2			sub-area 3		
	RMSZ	bias	without bias	RMSZ	bias	without bias
DEM2005 open area	9.29	-4.99	7.83	6.47	-3.18	5.63
DEM2005 forest	10.68	-6.13	8.74	7.69	-4.01	6.56
DEM25000 open area	12.68	-4.52	11.85	10.49	-3.20	9.99
DEM25000 forest	14.47	-7.11	12.60	12.46	-4.48	11.63

Table 6.13: Results of the separate analysis of the sub-areas - SRTM X-band DSM

Better results of the mean values of the ascending and descending orbit (sub-area 3) can be seen against the values just based on a single observation (sub-area 2) in relation to the more precise reference DEM2005. This also can be seen in relation to the not so accurate reference DEM25000 – here the sub-area 1 shows better results for the flat areas, but not for the inclined parts. This may be caused by the different terrain characteristics in sub-area 1 and in general it is hidden behind the lower accuracy of the reference DEM25000. Also the dependency on the slope (table 6.12) in sub-area 3 is smaller because of double observation.

6.4 Influence of DEM-Interpolation

The preceding results are showing the discrepancies of the original DEM-points, which have been compared with the reference height models. In DEMANAL the height value corresponding to the point location in the file which shall be analyzed is computed by bilinear interpolation of the grided reference DEM. Under operational conditions also the SRTM-height models have to be interpolated for achieving the height values at the required positions. The interpolation always is causing a loss of accuracy depending upon the spacing and the terrain roughness. The accuracy loss of the interpolation of course should be larger for the C-band DSM having an original spacing of 3arcsec than for the X-band DSM having only a spacing of 1 arcsec. By this reason height models with constant spacing have been generated with interpolation in triangles in program LISA. This was based on the original data shifted to the height reference with program DEMSHIFT. The interpolated height models with a spacing of 15m for the X-band DSM and 40m for the C-band DSM have been analyzed again to get some information about the loss of accuracy caused by interpolation.

Reference DEM	DSM	1st iteration	RMSZ	RMSZ without bias	Relation of accuracy – for flat areas	Relation of RMSZ
DEM2005 open areas	X-band	$5.59+14.161*\tan(\alpha)$	9.26	8.23	(5.59/4.55) **1.23**	(9.26/7.35) **1.25**
DEM2005 forest	X-band	$6.78+15.552*\tan(\alpha)$	11.09	9.74	(6.78/5.73) **1.18**	(11.09/9.33) **1.18**
DEM2005 open areas	C-band	$10.58+16.903*\tan(\alpha)$	14.67	13.73	(10.58/5.92) **1.79**	(14.67/7.43) **1.97**
DEM2005 forest	C-band	$12.20+16.049*\tan(\alpha)$	16.32	15.49	(12.20/6.32) **1.93**	(16.32/8.21) **1.98**

Table 6.14: Accuracy of interpolated X-band DSM and C-band DSM (against DEM2005) and relation to the accuracy of the not interpolated height points (see also table 6.10)
α = slope

- The influence of the interpolation can be seen by comparison of tables 6.10 and 6.14.
- Especially the C-band data are strongly influenced by the interpolation because of 92m point spacing. Interpolation is made point by point and C-band has large spacing between points.
- The X-band data are not so much influenced by the interpolation because of the smaller point spacing of 30m.

The loss of accuracy by interpolation can be analyzed also with program ZANAL. It allows the interpolation over a multiplication of the spacing and a comparison of the interpolated value against the corresponding original height value.

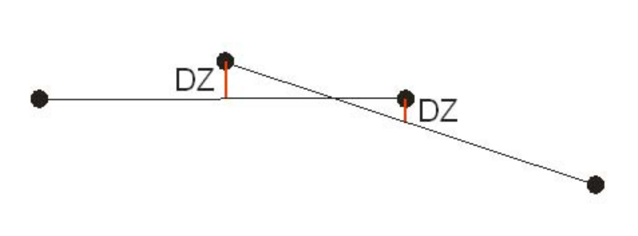

Figure 6.26:
Analysis of influence of interpolation by ZANAL as example of interpolation over the double spacing

An estimation of the loss of accuracy by interpolation is possible based on the hypothesis that the loss of accuracy is depending upon the square of the spacing.

In ZANAL the DEM which shall be analyzed can be divided into windows. The number of windows can be selected as 2*2, 4*4, 6*6 etc.

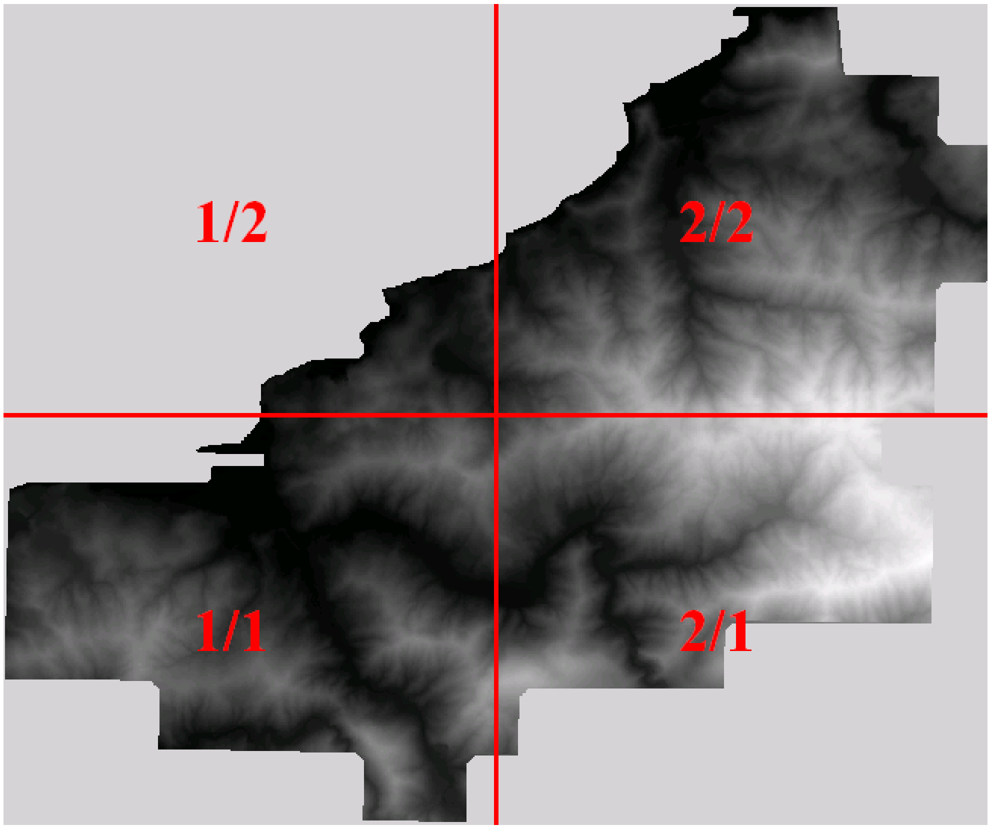

Figure 6.27: DEM2005 with 2*2 windows in ZANAL

Window	RMS	linear mean
1/1	1.29	.91
1/2	1.34	.81
2/1	1.46	1.05
2/2	1.40	1.00

Table 6.15: Bilinear interpolation results of DEM2005 in ZANAL (windows 2*2)

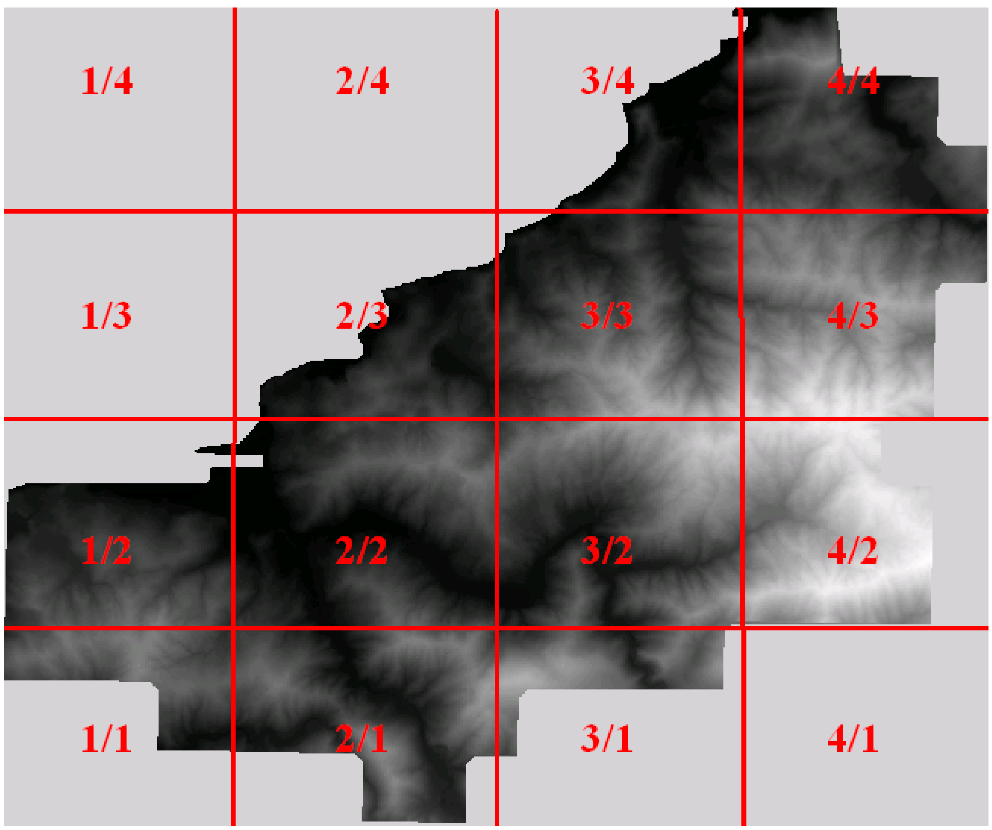

Figure 6.28: DEM2005 with 4*4 windows in ZANAL

Window	RMS	linear mean
1/1	1.31	.95
1/2	1.26	.85
1/3	.00 (sea)	.00 (sea)
1/4	.00 (sea)	.00 (sea)
2/1	1.43	1.04
2/2	1.16	.82
2/3	1.34	.80

2/4	.00 (sea)	.00 (sea)
3/1	1.43	.91
3/2	1.44	1.06
3/3	1.42	1.03
3/4	1.35	.85
4/1	1.74	1.19
4/2	1.49	1.10
4/3	1.57	1.18
4/4	1.19	.83

Table 6.16: Bilinear interpolation results in ZANAL of DEM2005 (windows 4*4)

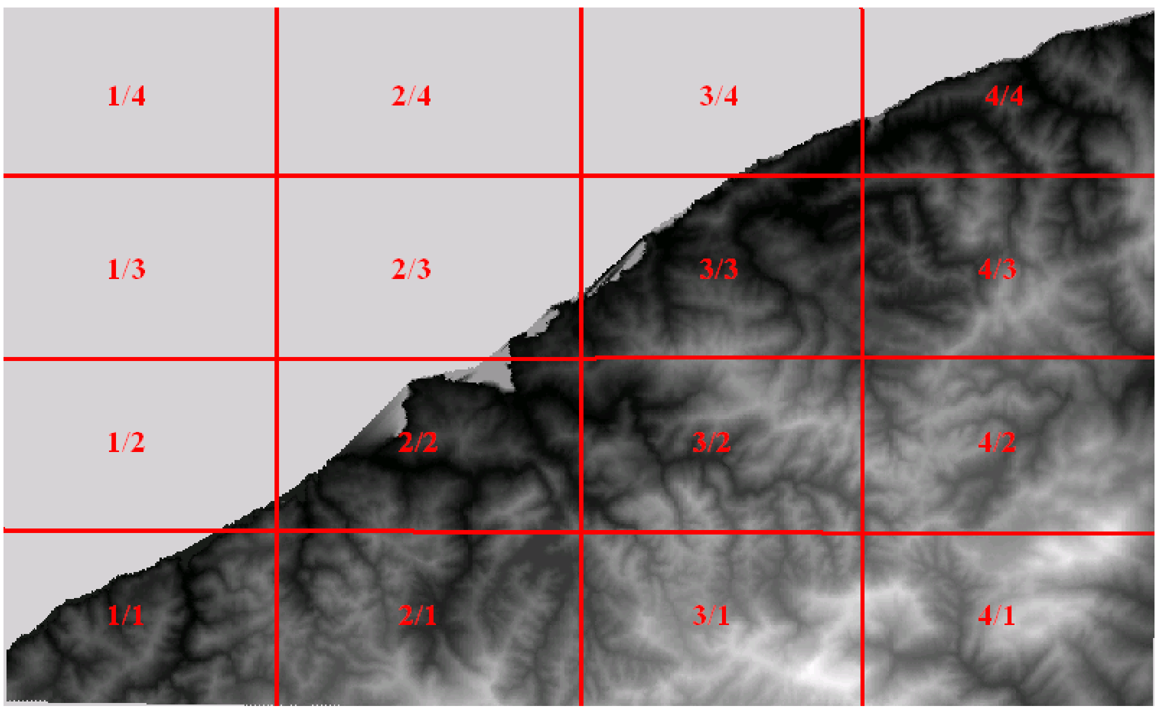

Figure 6.29: DEM25000 with 4*4 windows in ZANAL

Window	**RMS**	**linear mean**
1/1	9.42	6.87
1/2	16.27	9.57
1/3	.00 (sea)	.00 (sea)
1/4	.00 (sea)	.00 (sea)
2/1	8.45	6.54

2/2	7.53	5.02
2/3	6.17	3.58
2/4	.00 (sea)	.00 (sea)
3/1	8.09	6.06
3/2	8.66	6.74
3/3	20.49	7.71
3/4	23.38	9.74
4/1	6.96	5.35
4/2	6.81	5.25
4/3	7.41	5.81
4/4	18.33	8.32

Table 6.17: Bilinear interpolation results in ZANAL of DEM25000 (windows 4*4)

The DEM25000 has 40m point spacing while the DEM2005 has 10m point spacing that's why in DEM2005 interpolation is made 20m by 20m and in DEM25000 80m by 80m. The bilinear interpolation results of ZANAL for these DEMs can be different up to 2^4= 16 times. That means the results for DEM2005 can be smaller 16 times against DEM25000.

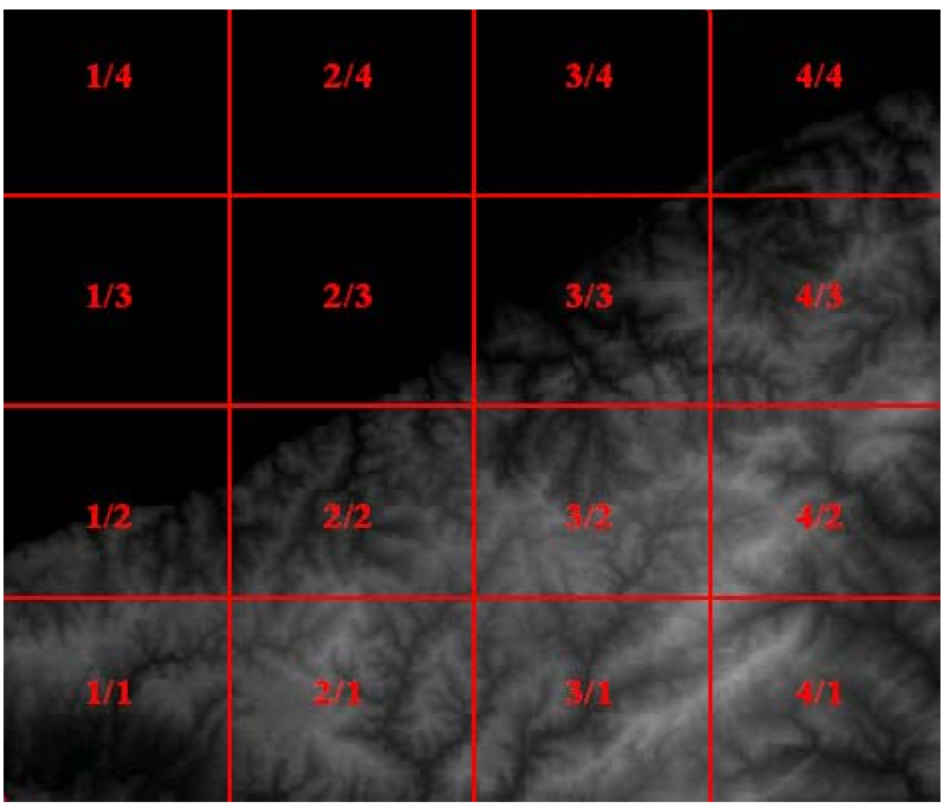

Figure 6.30: SRTM C-band DSM with 4*4 windows in ZANAL

Figure 6.30 is only a part of SRTM C-band DSM because this DSM was exceeding the capacity of program ZANAL.

Window	**RMS**	**linear mean**
1/1	10.65	7.20
1/2	9.28	4.70
1/3	.46	.31
1/4	.33	.19
2/1	13.21	9.46
2/2	12.72	8.87
2/3	4.12	1.14
2/4	.50	.34
3/1	12.56	9.06
3/2	12.60	9.03
3/3	11.62	7.25
3/4	2.10	.57
4/1	11.91	8.52
4/2	12.59	9.12
4/3	12.98	9.39
4/4	8.82	4.25

Table 6.18: Bilinear interpolation results of ZANAL for SRTM C-band DSM (windows 4*4)

Because of 80m point spacing the results of bilinear interpolation for SRTM C-band DSM in ZANAL are larger than for DEM2005.

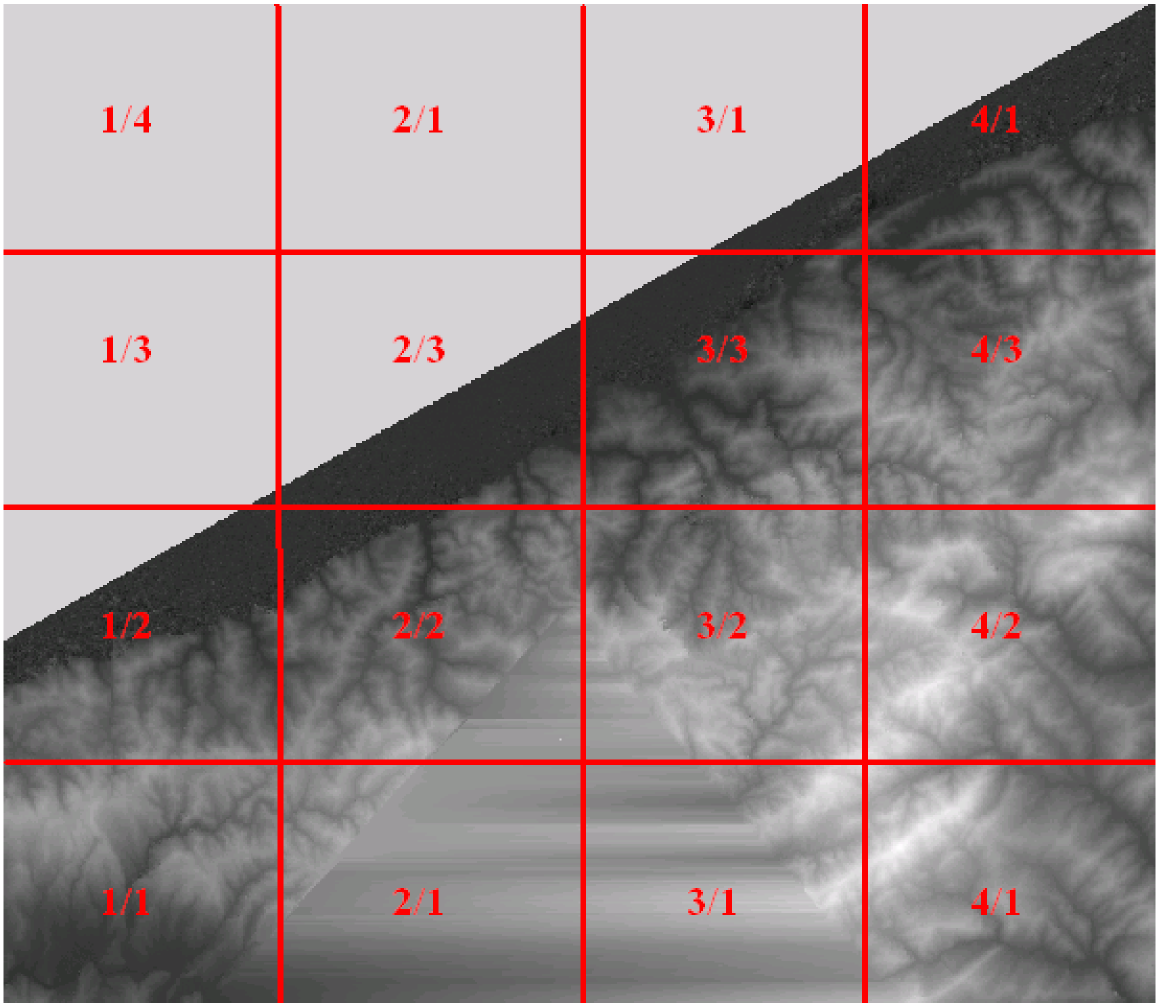

Figure 6.31: SRTM X-band DSM with 4*4 windows in ZANAL

Window	RMS	linear mean
1/1	7.64	5.25
1/2	17.05	10.84
1/3	12.31	9.08
1/4	.00(sea)	.00(sea)
2/1	5.50	3.52
2/2	10.91	7.09
2/3	13.07	8.93
2/4	.00(sea)	.00(sea)
3/1	7.55	5.46
3/2	9.20	6.64
3/3	11.20	7.65
3/4	14.80	10.07

4/1	7.72	5.69
4/2	8.59	6.37
4/3	8.80	6.63
4/4	16.56	11.11

Table 6.19: Bilinear interpolation results of ZANAL for SRTM X-band DSM (windows 4*4)

Because of 30m point spacing the results of bilinear interpolation for SRTM X-band DSM are closer to DEM25000.

In program ZANAL a strong influence of the bilinear interpolation is shown because test field Zonguldak has very rough terrain.

6.5 Morphologic Information

The morphologic details of a DEM can be checked by the shape of contour lines.

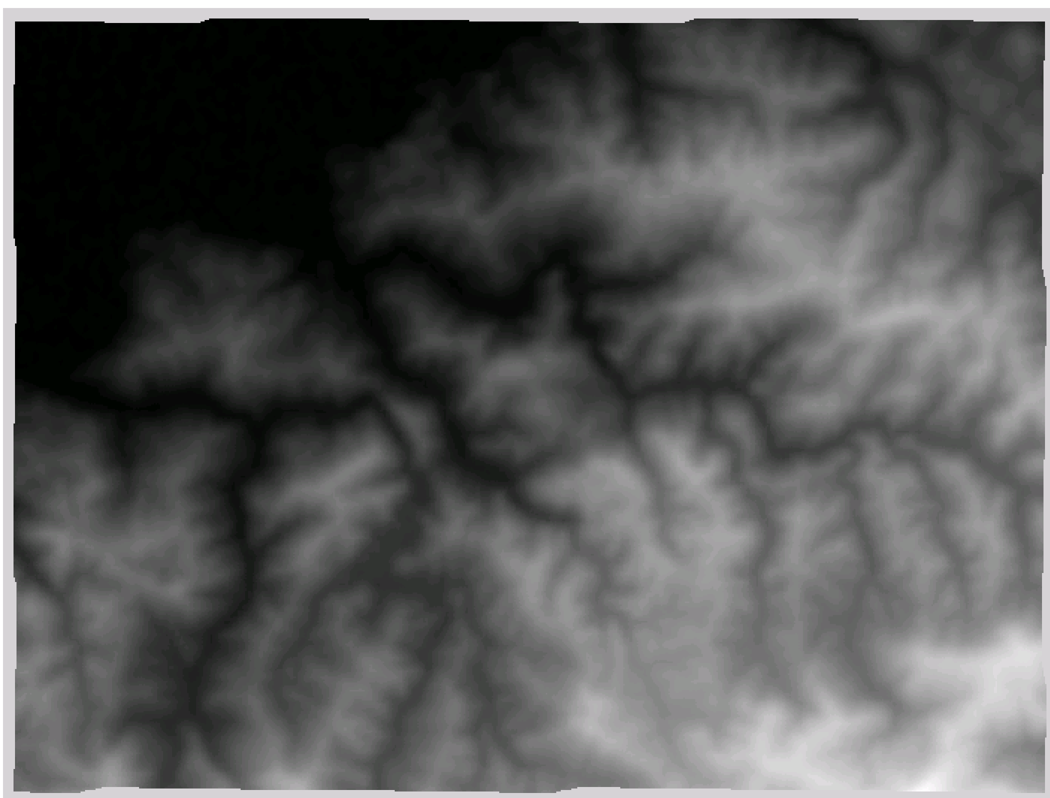

Figure 6.32: Centre of Zonguldak from SRTM C-band DSM

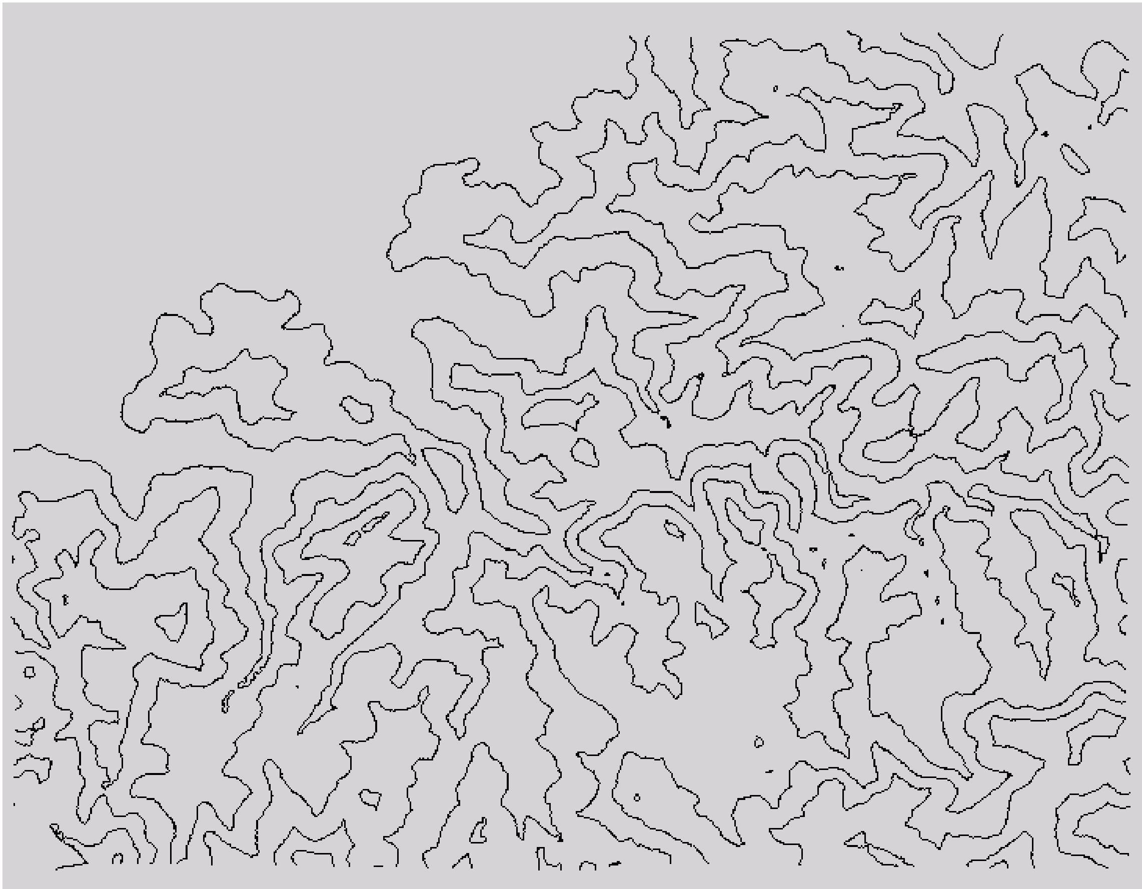

Figure 6.33: Contour-lines of Zonguldak city based on SRTM C-band DSM

The SRTM C-band DSM having a spacing of 3 arcsec does not include the same amount of morphologic details like the SRTM X-band DSM having 1 arcsec spacing (figure 6.34).

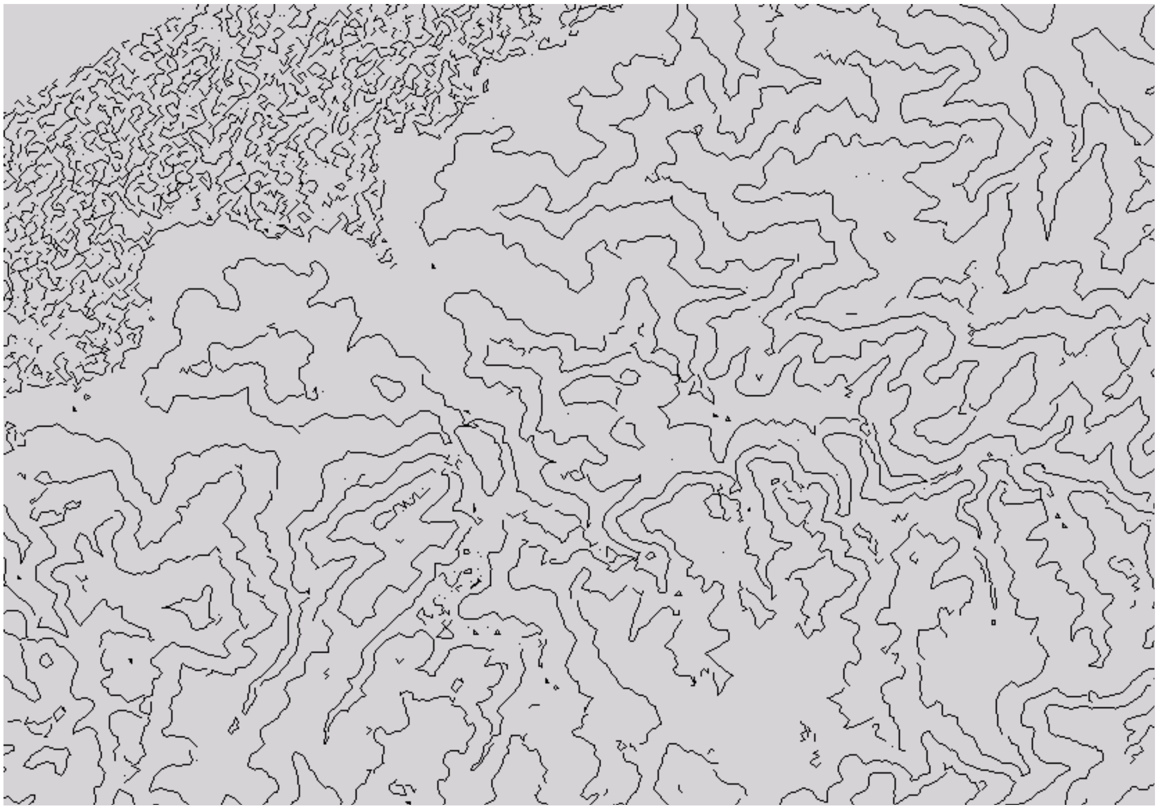

Figure 6.34: Contour-lines of Zonguldak city based on SRTM X-band DSM

6.6 Differential DEMs

Differences of digital elevation models can be generated by program LISA. Figure 6.35 and 6.36 shows the colour coded differential DEM of the SRTM C-band DSM against the reference DEM2005 generated by LISA and grey coded differential DEM generated by DEMANAL using maximal accepted DZ 30m for better visualization with scale effect. The structure of Zonguldak's terrain is very rough and because of large point spacing in SRTM C-band DSM some areas are not optimal in differential DEMs and these areas can be seen with light colour in figure 6.35 and with dark colour in figure 6.36.

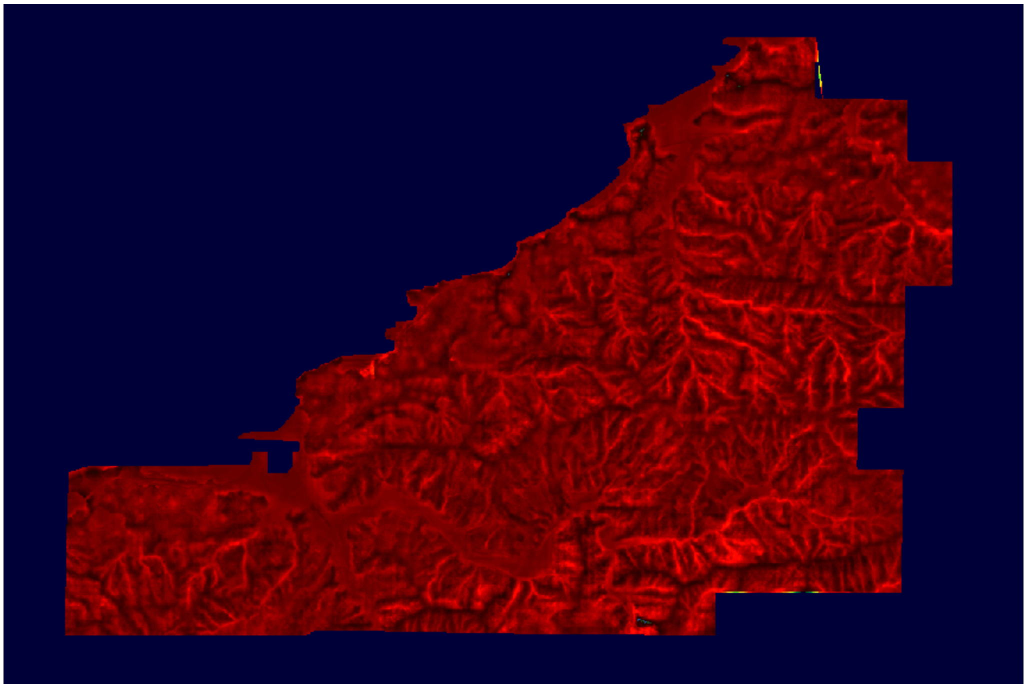

Figure 6.35: Differential DEM between SRTM C-band DSM and DEM2005 (by LISA)

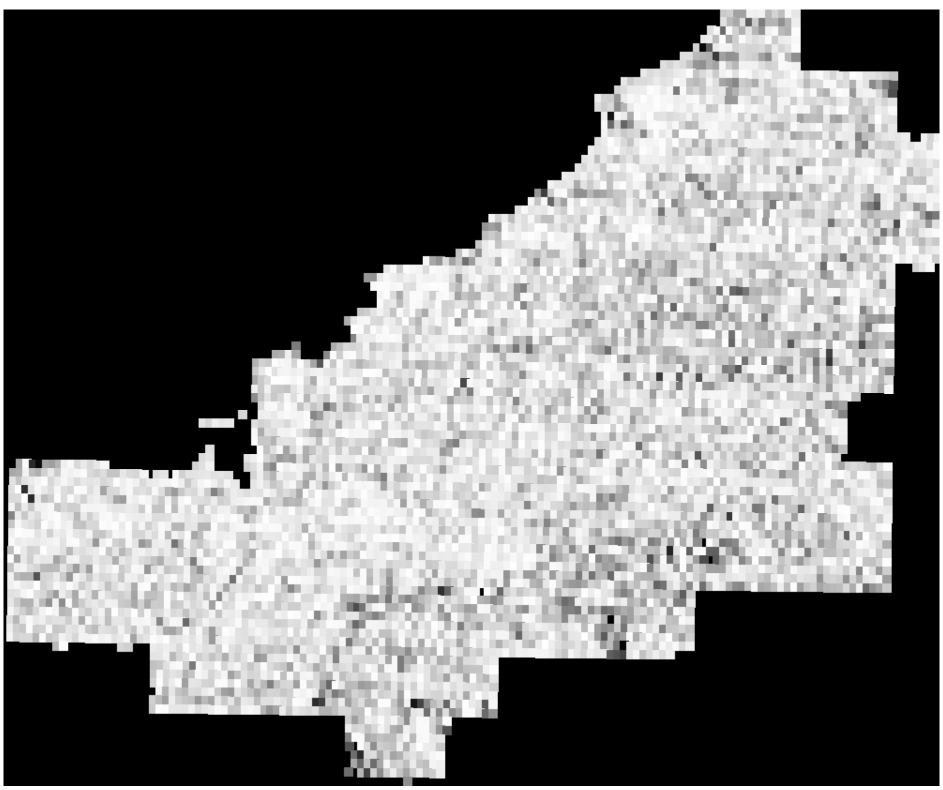

Figure 6.36: Differential DEM between SRTM C-band DSM and DEM2005 (by DEMANAL)

At the figure 6.36, forest areas and very steep areas are darker (= larger discrepancies). More bright parts (=smaller discrepancies) are located in the flat areas. Figure 6.37 shows the histogram of the differences computed by DEMANAL. This corresponds to the frequency distribution of the differences shown in figure 6.7 and 6.10 together because the graphical presentation shown in figure 6.36 has not been selected for open and forest areas.

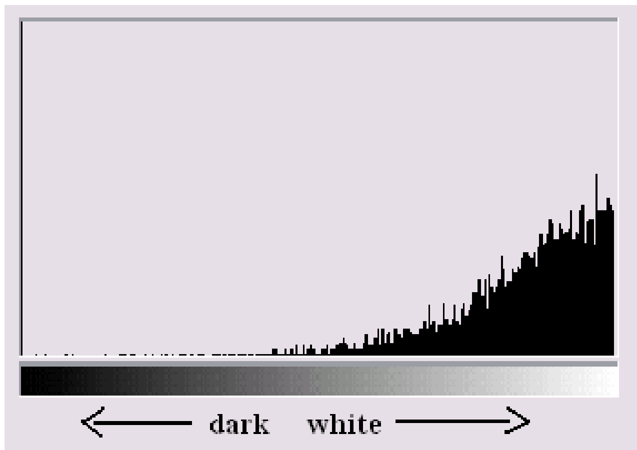

Figure 6.37: Histogram of height differences

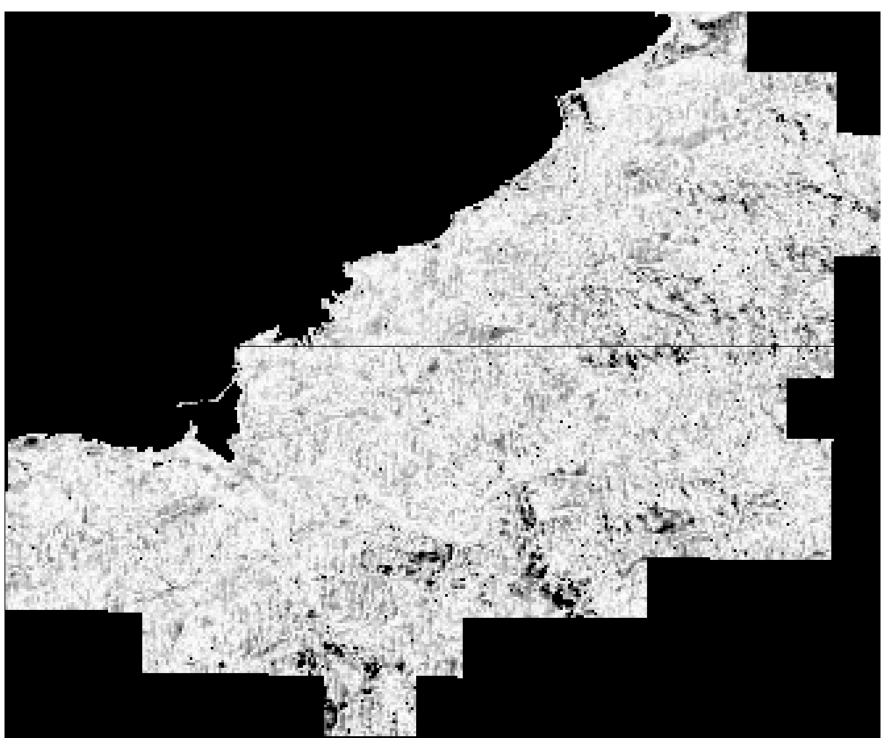

Figure 6.38: Differential DEM between SRTM X-band DSM and DEM2005
(by DEMANAL)

The differential DEM SRTM X-band DSM against DEM2005 shows more details because of 1 arcsec point spacing.

CONCLUSION

The analysed SRTM X-band and C-band DSMs in the area of Zonguldak do have accuracy similar to other not so mountainous areas. In general the accuracy has to be expressed as a function of terrain inclination and it is not the same for forest and open areas. The height discrepancies against the reference height models are not exactly normal distributed; some remaining effects of buildings and vegetation can be seen at the frequency distribution of the differences. So for open areas without influence of vegetation and buildings the accuracy will be better. The X-band DSM shows accuracy depending upon the aspects, for the C-band data this cannot be seen because of the averaging of the height models based on different orbits.

The height points of the C-band and the X-band DSM are in the same accuracy range. An improvement of the quality is possible by means of control areas allowing the determination of the bias. The difference in spacing can be seen by the interpolation in the very mountainous area of Zonguldak. This is causing a loss of accuracy by the factor of 2.0 for the C-band data. The smaller spacing of the X-band data is only leading to a loss of accuracy by interpolation in the range of 20%. In not so mountainous areas the loss of accuracy by interpolation will be significantly smaller. In general both SRTM height models can be used for several applications. They do have the advantage of being homogenous in all covered areas.

If reference digital elevation models of the test area are compared, it is obvious that the reference digital elevation model generated in 2005 by large scale photogrammetry has better accuracy. It is 4-6m more accurate than the digital elevation model based on contour lines of 1: 25000 scale topographic maps.

ACKNOWLEDGEMENTS

I would like to thank Dr. –Ing. Karsten Jacobsen from the Institute of Photogrammetry and Geoinformation (IPI), University of Hannover, Germany and acknowledge for help and advices. I would also like to thank Assoc. Prof. Dr. Gürcan Büyüksalih from the Department of Geodesy and Photogrammetry, Faculty of Engineering, Zonguldak Karaelmas University, Turkey and I would like to thank International Affairs of Zonguldak Karaelmas University, Turkey for the support during the project period and all their efforts for me.

REFERENCES

books / doctor thesis	
Hanssen, R. F., 2000:	Radar Interferometry, Data Interpretation and Error Analysis, Delft University of Technology, Delft 2000, ISBN 0-7923-6945-9
Leberl, F. W., 1989:	Radargrammetric Image Processing, Boulder Colorado 1989, ISBN 0-89006-273-0
Li, Z., Zhu Q., Gold C., 2005:	Digital Terrain Modeling: Principles and Methodology, ISBN 0-415-32462-9
Santitamnont, P., 1998:	Interferometric SAR Processing for Topographic Mapping, Hannover 1998, ISSN 0174-1454
papers	
Bamler, R. 1999:	The SRTM Mission: A World Wide 30m Resolution DEM from SAR Interferometry in 11 Days, Photogrammetric Week, Wichmann Verlag, Heidelberg 1999
Büyüksalih, G., Marangoz A., Jacobsen, K., 2005	Generation and Analysis of Height Models Based on Satellite Information, Hannover Workshop, Hannover 2005
Hounam, D., Werner, M., 1999:	The Shuttle Topography Mission (SRTM), Research Index, DLR, 1999
Jacobsen, K., 2002:	Comparison of High Resolution Mapping from Space, INCA workshop, Ahmedabad 2002
Jacobsen, K., 2004:	Analysis of Digital Elevation Models based on Space Information: EARSeL Symposium. Dubrovnik, 2004
Jacobsen, K., 2005 a:	Analyses of SRTM Elevation Models, EARSEL 3D- RS Workshop, Porto 2005
Jacobsen, K., 2005 b:	DEMs Based on Space Images Versus SRTM Height Models, ASPRS Annual Conference, Baltimore 2005
Koch, A., Lohmann, P., 2000:	Quality Assessment and Validation of Digital Surface Models Derived from the Shuttle Radar Topography Mission (SRTM), IAPRS, Vol. XXXIII, Amsterdam 2000
Koch, A., Heipke, C. 2001:	Quality Assessment of Digital Surface Models Derived From the Shuttle Radar Topography Mission (SRTM), IEEE 2001 International Geoscience and Remote Sensing Symposium, University of New South Wales, Sydney (Australia)
Koch, A., Heipke, C., Lohmann, P., 2002:	Analysis of SRTM DTM - Methodology and practical results, IntArchPhRS, Com.IV, Ottawa, Vol.XXXIV Part 4
Rosen, P.,Eineder, M., Rabus, B.,Gurrola, E., Hensley, S., Knopfle, W., Breit, H., Roth, A., Werner, M., 2001	SRTM-Mission-Cross Comparison of X and C Band Data Properties,IGARSS Sydney, Australia 2001

Sefercik, U., Jacobsen, K., 2006:	Analysis of SRTM Height Models, Turkish-German Geodetic Days, Berlin 2006
Werner, M., 2001	Status of the SRTM data processing: when will the world-wide 30m DTM data be available?, Photogrammetric Week, Stuttgart 2001

internet sites

http://pollux.nss.nima.mil/NAV_PUBS/ RNM/310ch1.pdf October, 2005
http://www.dlr.de/ December, 2005
http://www.landinfo.com/products_dems.htm November, 2005
http://www2.jpl.nasa.gov/srtm/ December, 2005
http://www.digital-elevation.com/gallery.htm October, 2005
http://www.dlr.de/srtm/neu/neu_en.htm December, 2005
http://www.vterrain.org/Elevation/dem.html October, 2005
http://www.cgrit.it/tecnologie/lsa.html November, 2005
http://www.usgs.gov/ November, 2005
http://edc.usgs.gov/guides/dem.html November, 2005
http://www.ngdc.noaa.gov/mgg/topo/img/ December, 2005

LIST OF FIGURES

LIST OF TABLES